Atenuação de múltiplas por empilhamento Kirchhoff em afastamento comum

Cláudio Guerra, Eduardo Filpo* e Martin Tygel†*
* PETROBRAS S/A, Brasil
† UNICAMP, Brasil

Abstract

We present some results of a new multiple attenuation method designed for application on general finite-offset data, in particular to common-offset (CO) data. The method extends the recently developed Multiple Suppresion by Kirchhoff Stacking (MSKS) method, introduced in Filpo and Tygel (1999), that applies to zero-offset (ZO) or stacked data. The proposed method consists of transforming the CO data into the ZO domain, simulate the multiples in this new domain, transform them back to the CO domain and finally subract the simulated CO multiples from the corresponding ones observed in the input data, after the application of an amplitude adjustment filter. One of the main difficulties of eliminating multiples is not to alter the amplitudes of concurrent primaries. In that sense, the proposed method achieves quite satisfactory results.

Introdução

Recentemente, Filpo e Tygel (1999) introduziram o método *Multiple Suppresion by Kirchhoff Stacking (MSKS ZO)* para a situação *zero offset* (ZO). O *MSKS ZO* apresenta excelentes resultados quando aplicado em dados empilhados com afastamentos curtos (*near*) ou ainda com todos os afastamentos. Em muitos casos, para estudos de *amplitude versus offset* (AVO), realizar a atenuação de múltiplas somente no *near* é suficiente pois nos dados de afastamento longo (*far*) elas se apresentam já bastante atenuadas devido ao seu empilhamento fora de fase. Porém, quando esse não é o caso, a presença de múltiplas pode dificultar a obtenção de resultados confiáveis. Neste trabalho, apresentamos um método de atenuação de múltiplas (Guerra, 1999) para dados em configurações gerais de afastamentos finitos, em particular para a configuração de afastamento comum (CO). O novo método, a seguir designado por MSKS CO, expande a aplicabilidade do *MSKS ZO* de Filpo e Tygel (op cit). O método se baseia nos princípios e resultados da chamada *Abordagem Unificada de Imageamento Sísmico de Reflexão*, inroduzida em Hubral et. al (1996) e Tygel, et al. (1996), bem como no trabalho de Santos et al. (1997) sobre a continuação de afastamentos. Basicamente, o método proposto consiste em (a) transformar os dados em afastamento comum (CO) em seus correspondentes em afastamento nulo (ZO) através da migração para afastamento nulo (MZO); (b) simular cinematicamente as múltiplas ZO; (c) transformar as múltiplas ZO para a configuração CO através da operação inversa do MZO; (d) aplicar um filtro para ajuste das amplitudes das múltiplas CO com relação às correspondentes observadas e (e) subtrair as múltiplas ajustadas daquelas nos dados de entrada. Um dos maiores desafios na tarefa de eliminar múltiplas consiste, além da eliminação propriamente dita, em não alterar as amplitudes das primárias concorrentes. Nesse sentido, o método proposto alcança resultados bastante satisfatórios.

MSKS Zero Offset

O *MSKS ZO* envolve a simulação cinemática das múltiplas ZO em uma seção que seja uma boa aproximação de dados ZO (seção de *near trace* e/ou seção empilhada corrigidas de NMO/DMO), seguida de ajuste de amplitudes das múltiplas simuladas através de um filtro adaptador para subtração nos dados de entrada. A geração de múltiplas ZO é realizada pela aplicação em cascata de operadores de migração e demigração. Esta técnica é *denominada abordagem unificada de imageamento sísmico* e está descrita em Hubral et al., (1996) e Tygel et al., (1996). Conforme a Figura 1, considere uma malha de pontos, $N_m=(x_m,t_m)$, nos quais devem-se posicionar as amplitudes da seção de múltiplas a ser construída. Os pontos na malha ZO de entrada são designados por $N_p(x_p,t_p)$. Para cada ponto N_m, o método envolve a soma dos dados de entrada ao longo de uma curva específica, $t_p = T_{MSKS}(x_p, N_m)$, cujo resultado será colocado no ponto N_m. Essa curva é determinada através de uma migração deste ponto, em configuração de múltipla ZO, seguida de uma demigração, em configuração de primária ZO. No caso de a curva de empilhamento ser tangente a uma reflexão primária da seção de entrada (o que acontece quando o ponto N_m se situa efetivamente sobre a múltipla desta primária), um valor significativo será posicionado em N_m. Realizando esse procedimento para todos os pontos da malha, obtém-se a simulação da múltipla representada pela sua curva de tempo de trânsito de reflexão, $t_m = T_m(x_m)$ e respectivas amplitudes.

MSKS Common Offset

Santos et al. (1997) descreveram as rotinas de continuação de afastamentos (*OCO*), também a partir da abordagem unificada de imageamento sísmico. Duas particularizações do *OCO* são o *MZO*

(*Migration to Zero Offset*) e sua operação inversa *IMZO*. Através do MZO, obtém-se dados ZO a partir de dados CO. O IMZO realiza a transformação inversa. O *MSKS Common Offset* (*MSKS CO*) se propõe a expandir o *MSKS ZO*. Para tanto, são utilizados os algoritmos da continuação de afastamentos (*OCO*) e do próprio *MSKS ZO*. Resumidamente, o método reside em: a) transformar seções CO em ZO via *MZO*; b) simular as múltiplas ZO com o *MSKS ZO*; c) transformar as seções de múltipla ZO em suas correspondentes CO através do *IMZO*; d) subtrair dos dados CO originais a múltipla simulada CO após o ajuste das amplitudes por um filtro adaptador. A geometria das transformações do método está esboçada na Figura 2. Com uma configuração de medição CO, suponhamos que foram registradas a reflexão primária, $T_{pCO}(x_p)$ e a múltipla, $T_{mCO}(x_m)$. O *MZO* leva esses eventos para $T_{pZO}(x_p^0)$ e $T_{mZO}(x_m^0)$, respectivamente, na configuração de medição ZO. Simulam-se as múltiplas ZO empilhando-se as amplitudes ao longo da curva $T_{MSKS}(x_p^0, N_m)$ para todos os pontos N_m na seção de múltipla a ser construída. Por fim, realiza-se o *IMZO*, que transforma a múltipla ZO simulada, $T_{mZO}(x_m^0)$, em sua correspondente CO, $T_{mCO}(x_m)$. A cinemática da múltipla CO simulada, $T_{mCO}(x_m)$, se aproxima assintoticamente da múltipla CO registrada, $T_{mCO}(x_m)$. A seção que contém essa múltipla em afastamento comum terá suas amplitudes ajustadas por meio do filtro adaptador antes de ser subtraída da seção de entrada para a atenuação da múltipla.

Na Figura 3 está mostrada a comparação de dados em afastamento comum (1200m) antes e depois do *MSKS CO*. A Figura 4 é uma visão detalhada da Figura 3. Pode-se observar a boa performance do método. A Figura 5 apresenta o resultado do *MSKS CO* na forma de dados *far offset* empilhados com ângulos de incidência entre 20 – 40°. Na porção assinalada com uma seta pode-se observar a quase total eliminação da múltipla. Note que nos dados de entrada, a ocorrência da múltipla poderia gerar um alto valor na seção de fator de fluido (visto que nos *nears* ela não está presente) podendo mascarar este atributo em anomalias que porventura ocorressem nos dados.

Conclusões

Foram apresentados resultados práticos do *MSKS CO*. Atualmanete, a implantação do método envolve 3 integrais tipo Kirchhoff (*MZO*, *MSKS* e *IMZO*). Essas integrais são realizadas ao longo de operadores cujas aberturas são pequenas, de forma que o *MSKS CO* não consome muito tempo de CPU. Porém, a despeito de sua rapidez computacional, está sendo estudada a geração da múltipla CO a partir de dados de entrada CO por meio de apenas uma integral.

Referências

Filpo, E. e Tygel, M., Deep-water multiple suppresion in the near-offset range, The Leading Edge, 1999, 18, 81-84.

Guerra, C. , Eliminação de reflexões múltiplas por empilhamento tipo Kirchhoff em configuração de afastamento comum. Dissertação de mestrado. UNICAMP, 1999.

Hubral, P., Schleicher, J., e Tygel, M., An unified approach to 3-D seismic reflection imaging, Part I: Basic concepts: Geophysics, 1996, 61, 742-758.

Santos, L.T., Schleicher, J. e Tygel, M. , 2.5-D true amplitude offset continuation: Journal of Seismic Exploration, 1997, 6, 103 – 116.

Tygel, M., Schleicher, J., e Hubral, P., An unified approach to 3-D seismic reflection imaging, Part II: Theory: Geophysics, 1996, 61, 759-775.

Agradecimentos

Agradecemos à PETROBRAS pela autorização para publicação do presente trabalho.

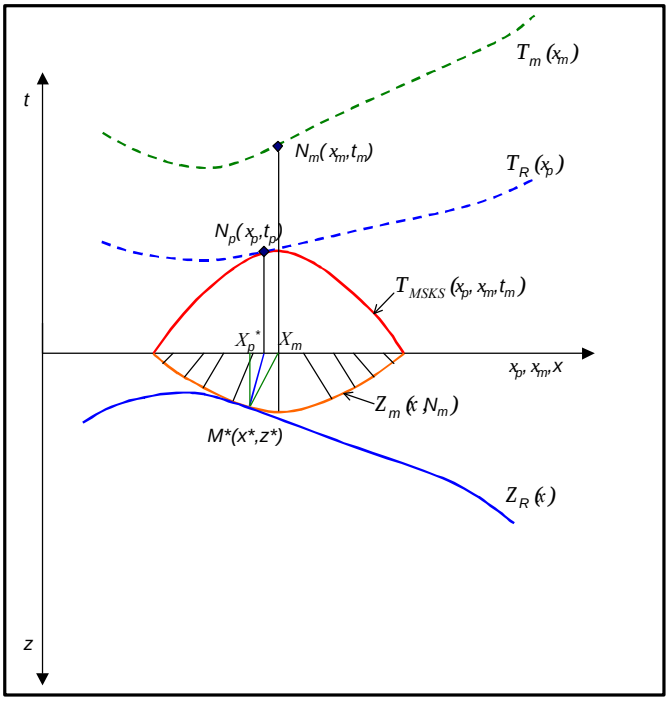

Figura 1 - Construção da curva de empilhamento do MSKS. A imagem migrada do ponto N_m é a curva isócrona $Z_m(x,N_m)$. Tratada como um refletor, a isócrona é demigrada na configuração de primária ZO (raios normais à isócrona), dando origem, em tempo, à curva $T_{MSKS}(x_p, x_m, t_m)$ que é a curva de empilhamento procurada. Caso a isócrona seja tangente a um refletor em profundidade, a curva de empilhamento será tangente à curva de reflexão em tempo. Na figura estão também representados o refletor, $Z_R(x)$, sua curva de tempo de reflexão, $T_R(x_p)$ e a curva de reflexão da múltipla, $T_m(x_m)$.

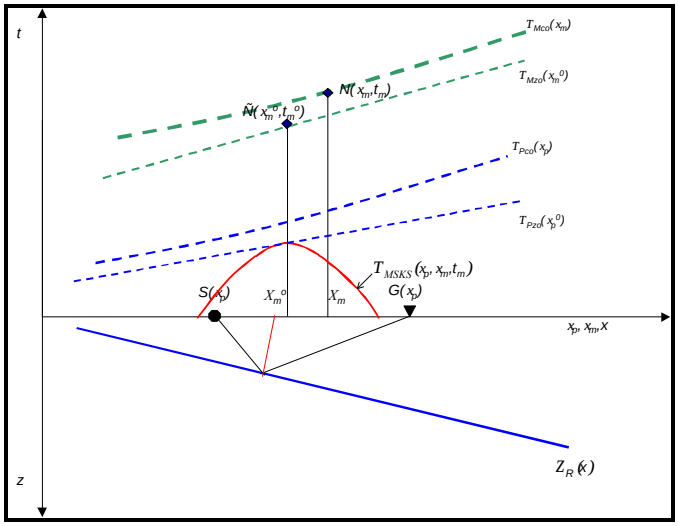

Figura 2 – Geometria do método de eliminação de múltiplas em afastamento comum.

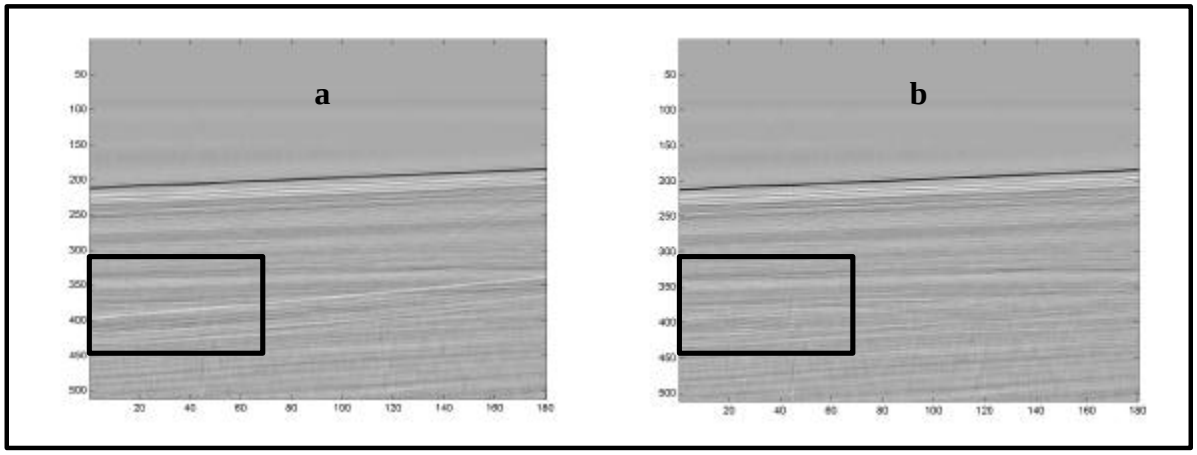

Figura 3 – Comparação da aplicação do método em dados em afastamento comum (1200m). a) dados de entrada; b) dados após o *MSKS CO*.

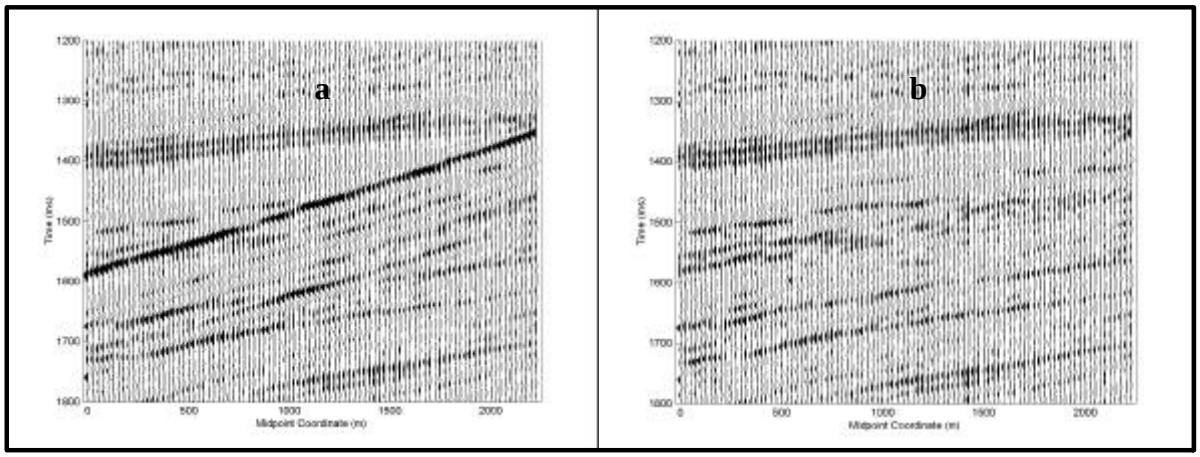

Figura 4 – Detalhe da figura anterior.

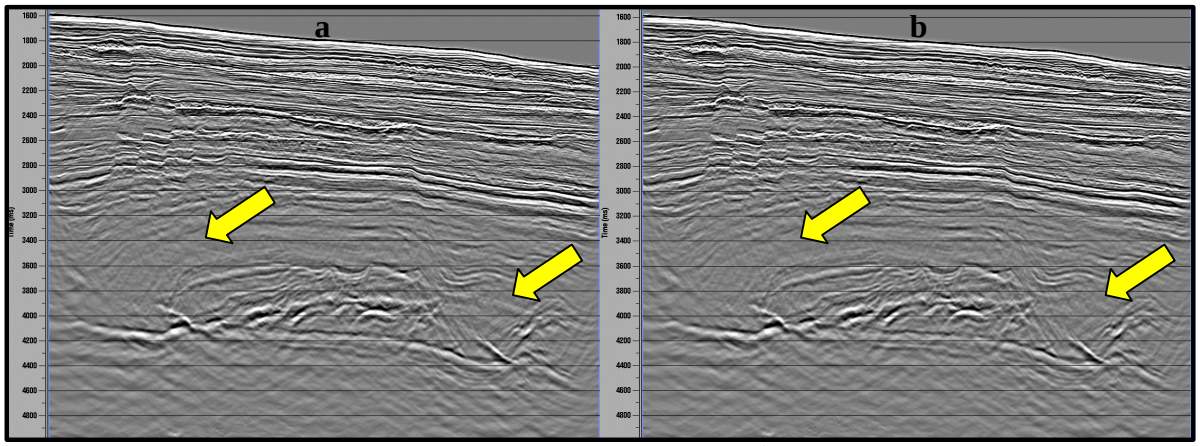

Figura 5 – Comparação da aplicação do método em dados *far* (20 – 40°). a) dados de entrada; b) dados após o *MSKS CO*.

Basis for Non-stationary Suppression of Multiples by KBC

Lourenildo W. B. Leite and Marcus P. C. Rocha
UFPa - Curso de Pós–graduação em Geofísica. lwbleite@ufpa.br. mrocha@ufpa.br.

Abstract
We present here some theoretical basis for multiple attenuation of seismic time sections (1D and 2D) based on the theory of Kalman-Bucy. The KB theory was extended by Crump (KBC) to seismic deconvolution, and by Mendel for generating seismograms. This subject continues as an interesting research topic, and we study it as an alternative to complement the classical Wiener-Hopf-Levinson theory for prediction (WHLP). It is rather intriguing the a priori condition of stationarity in the design of these operators.

Introduction
The mathematical and physical representation of a model by state variable is non unique. The present method is flexible to permit the solution of different problems, and we aim here to obtain a prediction operator for multiple deconvolution based on the Kalman-Bucy (KBCP) theory. The input has a message, $m(k)$, under convolution, and an additive noise component, $n(k)$, in the form: $g(k) = s(k) * r(k) + n(k)$, where $r(k)$ is the reflectivity series, and $s(k)$ is the primary pulse.

Crump (1974) represents the state variable, $x(t)$, as being the reflectivity coefficients, $x(t) = r(t)$. In this case the process is recursive for the generation of the state vector, expressed by:

$$r(k) = \sum_{i=1}^{L} b_i^C(k) r(k-i) + u(k-1), \quad \text{(system)},$$

$$y(k) = s(k) * r(k) + w(k), \quad \text{(output)},$$

where $u(k)$ and $w(k)$ are theoretically considered as a white stochastic process. Mendel et al. (1979) represents the state variable, $x(t)$, as being the seismic trace, $x(t) = g(t)$, to generate seismograms.

The present construction of 1D KBC operator is partly made by analogy with the Wiener-Hopf-Levinson´s (WHLP) prediction operators.

Method
We introduce here a form on how to relate the KBC methods to multiple suppression on a reflection seismic trace, taking the WHLP for analogy. Defining $g(t)$ as the state vector in the form:

$$g(k) = \sum_{i=1}^{L} b_i(k) g(k-i) + u(k-1), \quad \text{(system)}$$

$$y(k) = g(k) + w(k). \quad \text{(output)}$$

This equation projects the seismic trace forward through an weighted average of previous values, and this permits, in principle, to build a vector $b_i(k)$ to establish such a relationship for $g(k)$.

The coefficients of the WHLP operator are obtained through the autocorrelation, while the present KBCP case are obtained through the vector $b_i(k)$.

The equation in matricial expanded form is:

$$\begin{bmatrix} g_1 \\ g_2 \\ g_3 \\ \vdots \\ g_N \end{bmatrix} = \begin{bmatrix} 0 & \cdots & 0 & 0 & b_0(0) \\ 0 & \cdots & 0 & b_0(1) & b_1(1) \\ 0 & \cdots & b_0(2) & b_1(2) & b_2(2) \\ \vdots & \vdots & \vdots & \vdots & \vdots \\ b_0(N-1) & \cdots & b_{L-2}(N-1) & b_{L-1}(N-1) & b_L(N-1) \end{bmatrix} \begin{bmatrix} g_{N-1} \\ \vdots \\ g_2 \\ g_1 \\ g_0 \end{bmatrix} + \begin{bmatrix} u_0 \\ u_1 \\ u_2 \\ \vdots \\ u_N \end{bmatrix}.$$

And in compact form: $\underline{a} = \underline{\underline{B}}\ \underline{b}$. We have that: $L = \sum_{i=1}^{P} T_i$, $(P = 1, 2, \ldots\ k = 1, 2, 3, \ldots, N)$, where L is the length of the operator $b_i(k)$, N is the length of the input, and P represents the periodicity of the events to be attenuated.

The desired solution for $\underline{\underline{B}}$ from the matricial equation, having a special structure, is of difficult solution. A first natural form to resolve it is by a try-and-error method that makes it dependent on a parameter β, and follows a resumed description:

For $k = 1$: $b_0(0) = g_1 / g_0$.

For $k = 2$: $b_1(1) = \beta\, b_0(0)$,

$b_0(1) = \{g_2 - [b_1(1) g_0]\} / g_1$.

For $k = 3$: $b_1(2) = \beta\, b_0(1)$, $b_2(2) = \beta\, b_1(1)$,

$b_0(2) = \{g_3 - [b_1(2) g_1 + b_2(2) g_0]\} / g_2$.

For $k = N$:

$$b_1(N-1) = \beta b_0(N-2) \quad b_2(N-1) = \beta b_1(N-2) \ldots b_{N-1}(N-1) = \beta b_{N-2}(N-2)$$

$$b_0(N-1) = \frac{g_N - [b_1(N-1) g_{N-2} + b_2(N-1) g_{N-3} + \cdots + b_{L-1}(N-1) g_1 + b_L(N-1) g_0]}{g_{N-1}}$$

During the computational experiments $0 < \beta < 1$, and it was made constant for a single trace . The $b_i(k)$ functions, determined by recursive process, and are shown in Figure 1.

The 1D KBCP operator has a construction similar to the WHLP, and takes the form (see Figure 2):

$$h_k(i) = [1,0,0,\ldots,0, b_{T_1}(k), 0,0,\ldots,0, b_{T_2}(k), \ldots]$$

For multi-channel (2D case), the prediction time distance is off-set time dependent, $T = T(x,t)$, and we adopted a deterministic travel-time law to measure $T(x,t)$, as given by:

$$t(x) = \left[t_0^2 + (x/\bar{v})^2 \right]^{1/2}; \bar{v}^2 = \sum_{i=1}^{N+M} v_i^2 t_i \Big/ \sum_{i=1}^{N+M} t_i,$$

where $\bar{v}$ is the root-mean-square velocity accounting for the multiples, with N the number of trespassed layers, and M the number of repeated layers. (Taner & Koehler, 1969). The 2D KBCP operator with a construction similar to the WHLP, takes the form (see Figure 3):

$$h_{jk}(i) = [1,0,0,\ldots,0,b_{T_1(x)}(k),0,0,\ldots,0,b_{T_2(x)}(k),\ldots]$$

Figure 4 is the model to generate the seismograms, and Figure 5 is an example of 1D KBCP deconvolution.

From the matricial equation $\underline{a} = \underline{\underline{B}}\ \underline{b}$, we obtain that: $\underline{\underline{B}} = (\underline{a}\underline{b}^T)(\underline{b}\underline{b}^T)^{-1}$. From the table below, the elements of matrix $\underline{\underline{B}}$ does not have yet the desired structure to recover the values of $b_i(k)$ for the solution for the KBCP operator. This matrix must still be triangularized to a special form.

Table 1 – Values of $\underline{a}$, $\underline{b}$ e $\underline{\underline{B}}$, for N=6.

$\underline{a}$	$\underline{\underline{B}}$						$\underline{b}$
0.10	1.29	1.32	-1.62	-2.71	1.05	5.06	0.08
0.13	0.76	3.66	-2.62	-1.97	0.39	3.58	0.11
0.13	0.45	3.87	-2.65	-2.10	0.42	3.83	0.43
0.11	0.36	-0.48	0.31	-3.38	0.93	7.13	0.13
0.08	-0.25	1.45	-0.99	-1.47	0.4	3.54	0.11
0.05	0.32	-0.17	-0.22	-1.19	0.46	2.82	0.05

Conclusions

The results obtained are nice, and the KBCP method shows to be more flexible for operation than the WHLP, if it can be optimized for routine.

Theories for the present proposed study seem to be scarce for the authors. Other results of the present method are presented in Rocha & Leite (2001).

Acknowledgments

The authors are grateful to project sponsors FINEP/CTPETRO and PRH-ANP/MME/MCT-UFPa, Brazil.

Bibliography

Crump, N. (1974). *A Kalman filter approach to the deconvolution of seismic signals*. Geophysics, v. 39, n. 1, p. 1-13.

Mendel, M. J., Nahi, E. N. & Chan, M. (1979) *Synthetic seismograms using the state-space approach*. Geophysics, v. 44, n 5, p. 880-695.

Rocha, M. P. C. & Leite, L. W. B. (2001). *Results of Suppression of Multiples the KBC Method*. Submitted to VII CISBGf. Salvador, Bahia.

Taner, M. T. & Koehler, F. (1969). *Velocity spectra-digital computer derivation and application of velocity functions*. Geophysics, 34, 859-881.

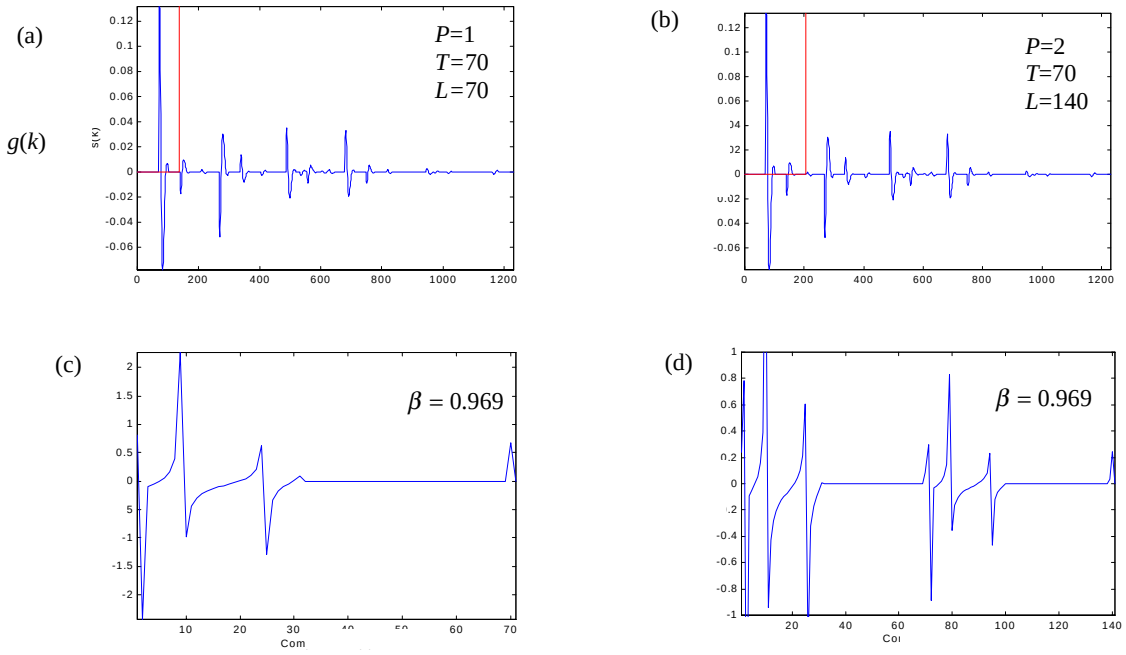

Figure 1. Examples of the function $b_i(k)$ for different values of periodicity P, and of length L. (a) and (b) show the window (size L) over the trace. (c) and (d) show the respective $b_i(k)$ for the windows.

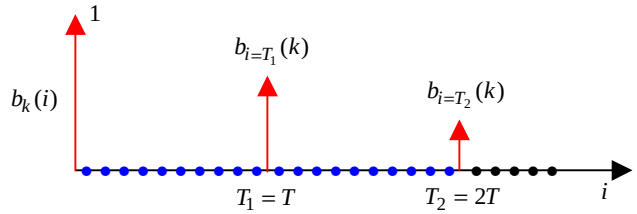

Figure 2. Structure of the $b_i(k)$ KBCP operator for analogy with the WHLP. 1D case. T is constant.

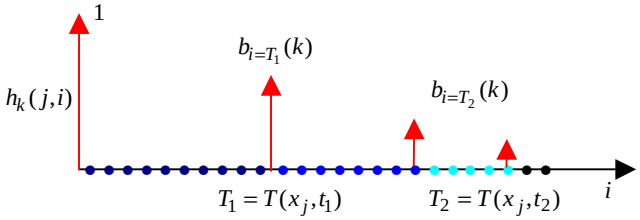

Figure 3. Structure of the $b_{ij}(k)$ KBCP operator for analogy with the WHLP. 2D case. $T=T(x, t)$ is variable.

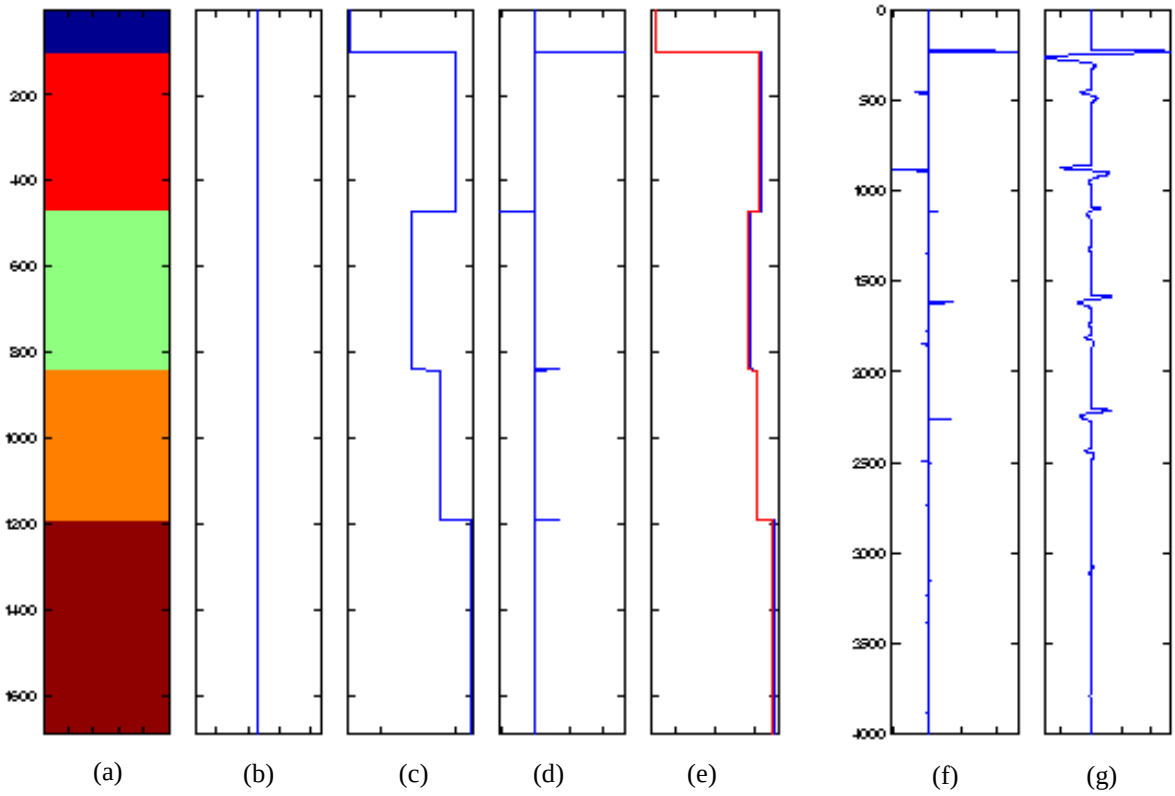

Figure 4. Model of 4 layers over a half space for operator analysis. (a) Geological section. (b) Density log. (c) Velocity log. (d) Distribution of reflection coefficients. (e) RMS log and Average Velocities. (f) Reflectivity. (g) Seismic trace obtained by convolution between the medium impulse response calculated by the Goupillaud solution (f) with an effective source pulse (Berlage function).

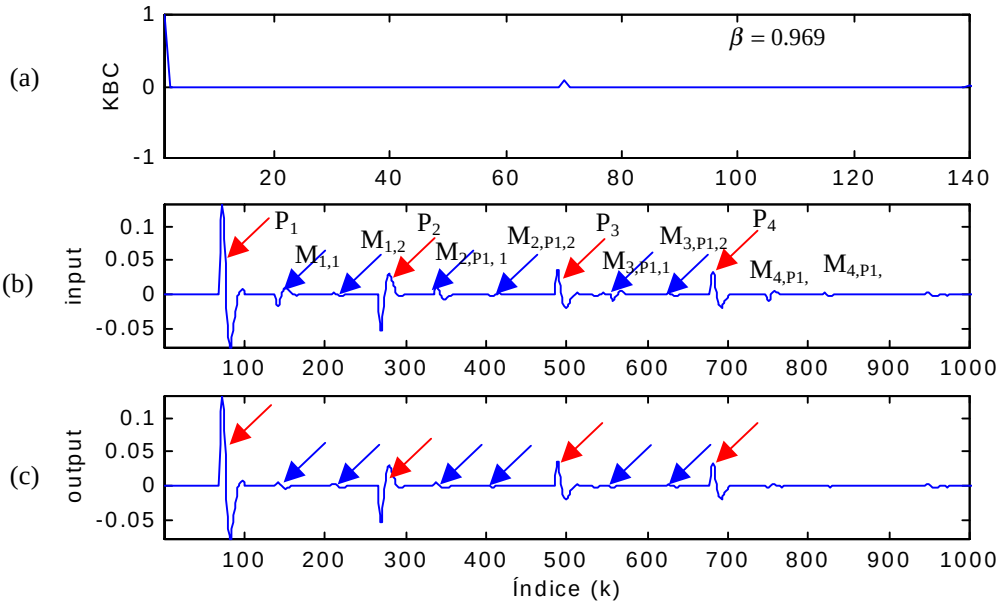

Figure 5. Red arrows indicate the primaries, and blue arrows the multiples. (a) The KBCP operator. (b) Input trace. (c) Output of the KBCP. Try-and-error method. The results are clear and good as characterized by the attenuation of the events pointed by the blue arrows.

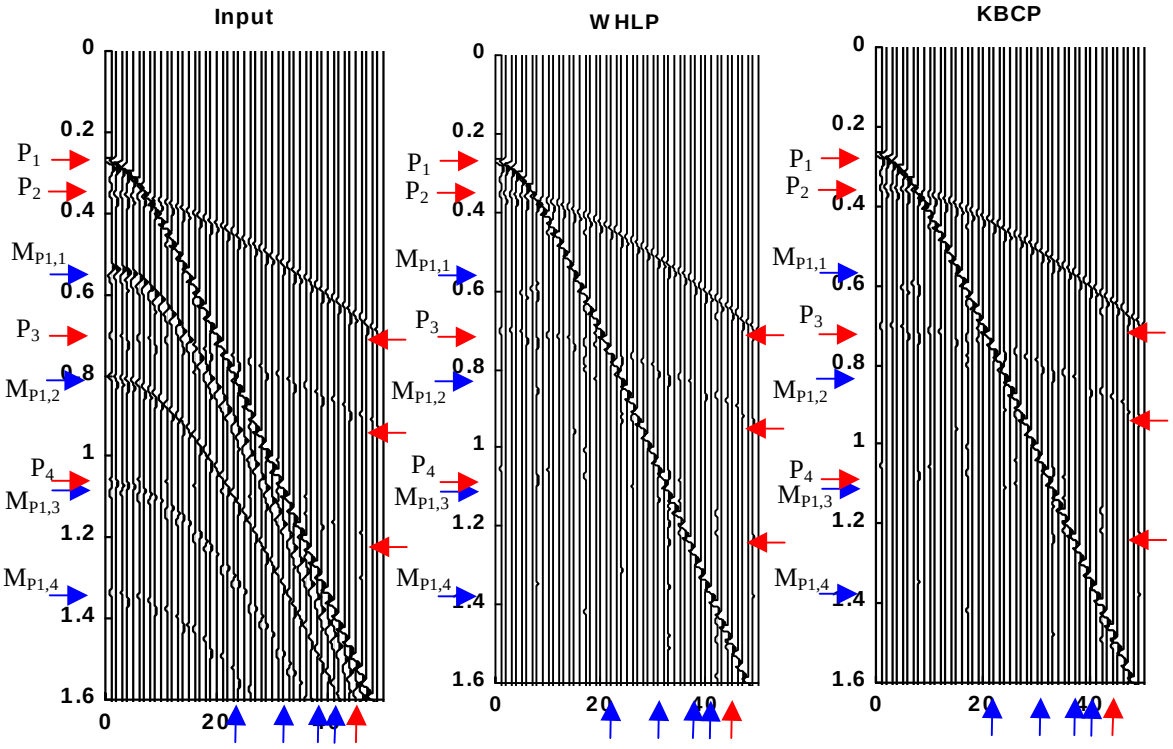

Figure 6. Synthetic time section for the model (4 layers over a half-space). Symmetric multiples. Red arrows are primaries, and blue arrows are multiples. (a) Input showing several multiples of two types. (b) WHLP correspondent output for comparison. (c) KBCP output. β = 0,9820. Nice outputs without (or weak) multiples left as shown by the blue arrows. There are no refraction events.

Basis for Moving Pass-windows for Multiple Suppression

Lourenildo W. B. Leite and Fábio J. C. Alves
UFPa - Curso de Pós–graduação em Geofísica. *lwbleite@ufpa.br*. *fjca@ufpa.br*.

Abstract
This work discusses the basis of a proposed pass-window for selecting events interpreted on a seismic trace, and on its autocorrelation function. The method is a modification of the WHLP filter for the suppression of multiples. The solution is justified by the description of the effective-pulse as composed by a series of multiples to be deconvolved, starting with single-channel, and then extrapolated to multi-channel by a deterministic law.

Introduction
Suppression of symmetric and asymmetric multiples in reflection seismic processing is already classical, and it remains as an interesting problem to be resolved. The desired solution depends on the type and amount of a priori information available, and on the ability to insert them in the governing equations.
The problem under investigation is a deviation from the Wiener-Hopf-Levinson´s prediction (WHLP) applied to multiple suppression. The study is supported on the basic philosophy that the WHL´s theory offers the possibility for adding information to the design of specific operators (time-variant and time-invariant).

Governing equations
A natural model is of stationarity. The filter, $h(t)$, outputs by convolution, it is time-invariant, and constrained to satisfy a desired output, $d(t)$, through the Wiener-Hopf-Levinson equation. The criteria is the minimization of the variance between the desired, $d(k)$, and the real outputs, $\hat{g}(k)$, $I(h_i) = E\{[\sum_{k=1}^{N} \hat{g}(k) - d(k)]^2\}$, and it results in the governing equation: $\sum_{k=1}^{N} h(k)\phi_{gg}(l-k) = \phi_{dg}(l)$.
The input has a message, $m(k)$, and an additive noise component, $n(k)$, and it is expressed by the form: $g(k) = m(k) + n(k) = s(k) * \varepsilon(k) + n(k)$, where $\varepsilon(k)$ is the reflectivity series, and $s(k)$ is the primary source-pulse. The desired output is the message, $d(k) = m(k+T)$, where T is the prediction distance, and at this point the operator is time-invariant and single-channel. The correlations are: $\phi_{gg}(k) = \phi_{mm}(k) + \phi_{nn}(k)$, $\phi_{dg}(k) = \phi_{mm}(k+T)$, $\phi_{nn}(k) = \sigma_m^2\,\delta(k)$. The signal/noise ratio is not known in practical problems, and this control is through the constant whitening parameter σ_v^2.

Method
The open general WHLP equation in parametric form shows its composition subject to analysis. Submitted to a window, $w(k)$, it is organized in 1D as:

$$\sum_{k=1}^{N} h(k)[\phi_{ss}(k) + \sigma_v^2\,\delta(k)] = \phi_{gg}(l+T)\,.$$

The autocorrelation function of the seismic trace, $\phi_{gg}(k)$, can be expressed in terms of its contributions, and on the relation among them. One of these is the reflectivity function that can be simple when the distribution of $\varepsilon(k)$ is pure random, what means that $\phi_{\varepsilon\varepsilon}(k)$ is a white series, and that theoretically multiples are absent (Silvia & Robinson, 1979). Even in this simplified situation $\phi_{gg}(k)$ has diversified forms.
The dependence of the autocorrelation on the seismic trace can be analyzed starting from the construction of $g(k)$, and justified as the result of the convolution between the primary source-pulse, $s(k)$, and the reflectivity, $\varepsilon(k)$, with an additive random noise component. The general expression for $\phi_{gg}(l) = E\{g(k)\,g(k-l)\}$ is given by: $\phi_{gg}(k) = \phi_{\varepsilon\varepsilon}(k) * \phi_{ss}(k)$, where the crossed terms with the noise component are considered non-correlated. For the special condition of $\phi_{\varepsilon\varepsilon}(k)$ as white series, this makes $\phi_{\varepsilon\varepsilon}(k) = \sigma_\varepsilon^2\,\delta(k)$, and $\phi_{gg}(k)$ results in a simple scaled form as $\phi_{gg}(k) = \sigma_\varepsilon^2\,\phi_{ss}(k)$. (Gosh, 1998).
Some characteristics of $\phi_{gg}(k)$ can be further analyzed through $\phi_{ss}(k)$. As an example intentionally simple is the case of one simple multiple, not accounted for in $\varepsilon(n)$, represented by a delayed pulse by T units, with the effective source-pulse, $f(k)$, constructed by: $f(k) = s(k) - r\,s(k-T)$, where T= (layer thickness)/(layer velocity), and r is the reflection coefficient between the layer and the lower half-space. A next case is that of two simple multiples with different time distances (T_i and T_j), and described by: $f(k) = s(k) - r_i s(k-T_i) - r_j s(k-T_j)$.

A generalization is given by $f(k)=\sum_{i=0}^{I} r_i\, s(k-T_i)$, and it results in an autocorrelation of the form:

$$\phi_{gg}(k) \approx \phi_{ff}(k) = \sum_{i=0}^{I}\sum_{l=0}^{I} r_i r_l \phi_{ss}(k-T_i+T_l).$$

The first term of the series is $\sigma_r^2 \phi_{ss}(k)$, where the variance, $\sigma_r^2 = \sum_{i=0}^{I} r_i^2$, modifies the desired segment $\phi_{ss}(k)$, and the deconvolutional operator has a factor that scales $\varepsilon(n)$. From this equation we can not make many conclusions, and computational experiments is an efficient way for practicality. For selection of $\phi_{ss}(k)$, it is necessary that the lengths of the source-pulse, and of the temporal pass-window to be shorter than the first multiple. Besides, deconvolution with elongated operators can destroy the information; operator with length T_i includes the suppression of the multiple of period T_i, and the operator with length $T_i + T_j$ deconvolves the multiples T_i and T_j. The operator may not distinguish a desired multiple from a non desired multiple. These simple models are examples based on the structure of the autocorrelation. The distances between maxima of $\phi_{gg}(k)$ allow, in principle, the measurement of important parameters (T_i and T_j) for the model.

The application of a window on the autocorrelation $\phi_{gg}(k)$ has the form $\phi_{gg}^{W}(s) = \phi_{gg}(k) W(k)$. Continuing with the simple model, and equating the parts together, the operation is now described by:

$$\sum_{k=1}^{N} h(k)\phi_{gg}(n-k) \approx \sum_{i=0}^{I}\sum_{j=0}^{I} W(k_1-k_2)\phi_{ss}(n-T_i+T_j).$$

$W(k) = W(k_2-k_1) = 1$, for k_2 and k_1 the corners of the rectangular pass-window to the autocorrelation function for selecting the event to be suppressed on the input trace.

For the multi-channel (2D case), the operator is $h = h(x,t)$, and the WHLP equation is modified to:

$$\sum_{k=1}^{N} h_2(k,x)\phi_{gg}[l-k;x] = W(l_2-l_1;x)\phi_{gg}[l+T(x)],$$

with the prediction distance now off-set(x)-time(t) dependent, $T = T(x,t)$. We adopted the law as:

$$t(x) = \left[t_0^2 + (x/\bar{v})^2\right]^{1/2};\ \bar{v}^2 = \sum_{i=1}^{N+M} v_i^2 t_i \Big/ \sum_{i=1}^{N+M} t_i,$$

where $\bar{v}$ is the root-mean-square velocity accounting for the multiples, with N the number of trespassed layers, and M the number of repeated layers. (Taner & Koehler, 1969).

Results and Conclusions

Applications and results of moving pass-windows are in Alves & Leite (2001). The figures show examples of window strategies, and results for the model formed by one layer over a half-space. Figure 1 explores the time section, and trace autocorrelations. Figure 2 are details of the process for the first trace of Figure 1, showing the trace (input), the autocorrelation and the pass-window, the prediction-error operator, and the deconvolved trace (output) with good results due to the existing periodicity. Figure 3 gives the upper and lower limits for the 2D moving pass-windows for the time section; the blue lines are for the first multiple, the red lines for the second multiple, and the yellow for the third multiple. For each window, the first event is considered as the primary and the multiple as the secondary. The pass-window limits are defined on the basis of the difference of arrival between multiples, in order to keep the periodicity. Figure 4 gives geometrical details of the mathematical algorithm proposed for the moving pass-window, that in this case are for the first and for the second multiple suppression. Figure 5 gives details of the autocorrelation, of the crosscorrelation and of the prediction-error operator for the trace of Figure 4. Figure 6 gives the output for a zero off-set section, and for common-source section. Results of the modified WHLP is good for the zero-offset section due to the strong periodicity of the events. In the case of common-source the proposed algorithm makes it possible to apply the theory for creating a periodicity by introducing a deterministic law. This law being tested, it can eventually be used for other purposes of processing.

Acknowledgments

The authors are to grateful to the project sponsors FINEP and PRH-ANP/MME/MCT-UFPa, Brazil.

Bibliography

Gosh, S. K. (1998). *Ergodicity of stationary white Gaussian processes*. Geophysics, 63, 6, 2091-2092.

Silvia, M.T. & Robinson, E.A. (1979). *Deconvolution of Geophysical Time Series in the Exploration of Oil and Natural Gas.* Elsevier Sc. Publ. Co. Amsterdam, Netherlands.

Alves, F. J. C. & Leite, L. W. B. (2001). *Results of a proposed WHL operator for multiple suppression.* Submitted to VII CISBGF. Salvador, Bahia.

Taner, M. T. & Koehler, F. (1969). *Velocity spectra-digital computer derivation and application of velocity functions.* Geophysics, 34, 859-881.

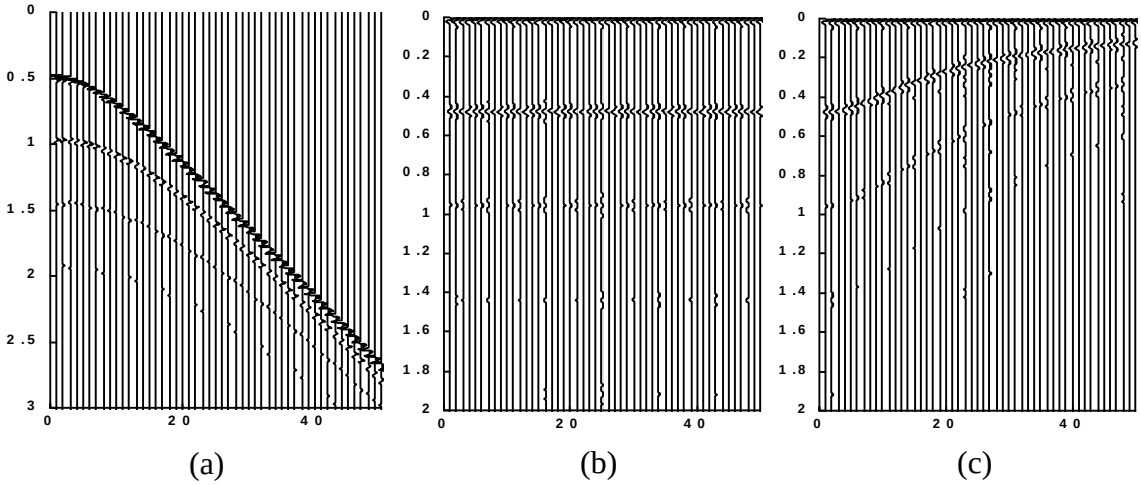

Figure 1. (a) Seismic time section of common-source. (b) Autocorrelation of zero-offset section. (c) Autocorrelation of time section (a). The forward model is formed by one layer over a half-space.

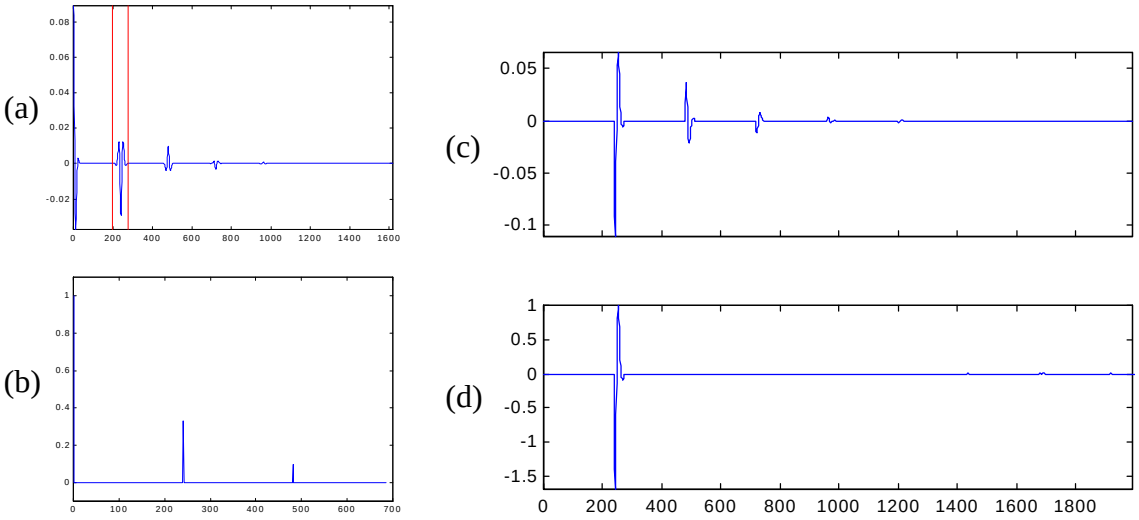

Figure 2. (a) First trace of the autocorrelation of Figure 1c, and limits of the pass-window. (b) Prediction-error operator. (c) First trace from Figure 1a. (d) Deconvolved trace where we observe the suppression of the multiples.

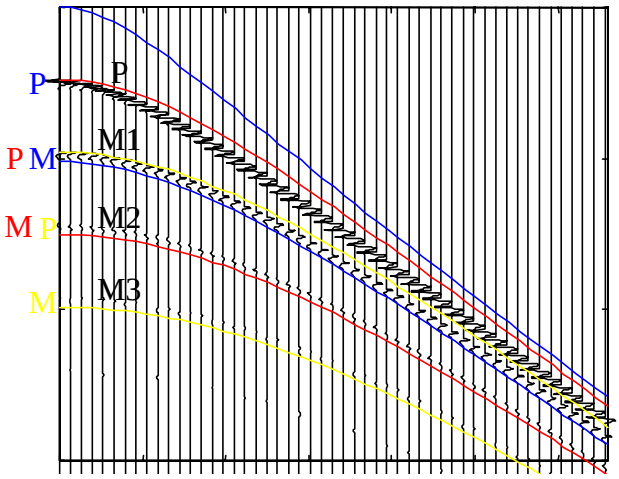

Figure 3. Seismic section giving information of primaries (P) and multiples (M1, M2 and M3). The blue lines are the upper and lower limits of the pass-window for suppression of multiple M1. The red lines are the upper and lower limits of the pass-window for suppression of multiple M2. The yellow lines are the upper and lower limits for suppression of multiple M3. For each window, the first event becomes the primary (P, P and P) and the second event is considered the multiple for theoretical consistency (M, M and M).

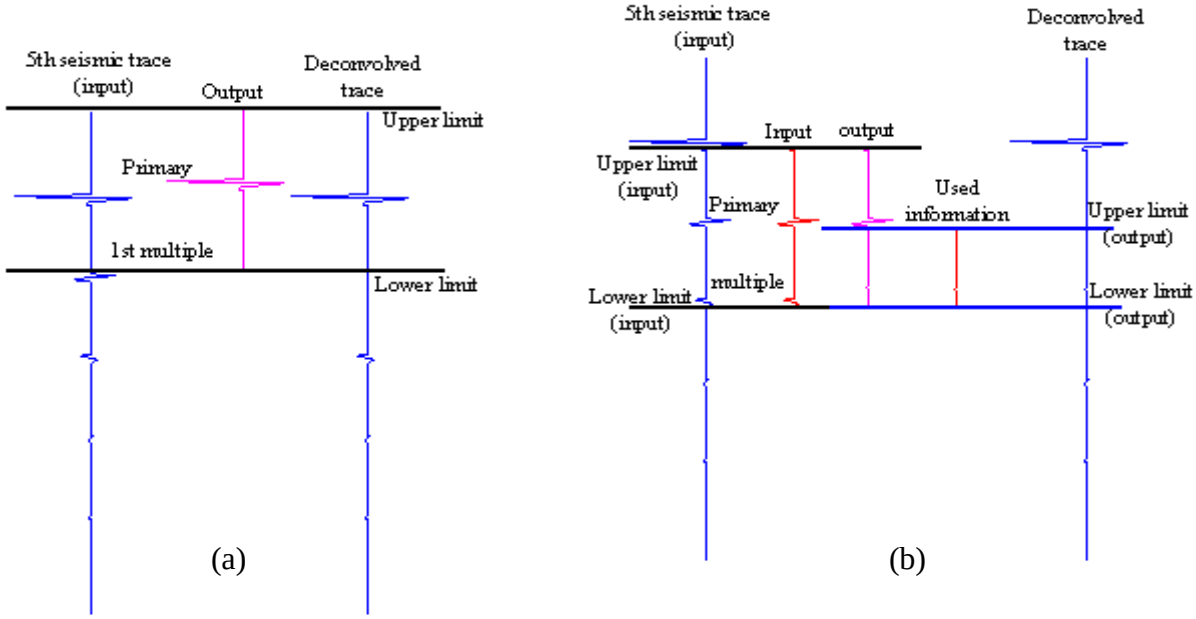

Figure 4. Examples of application of the pass-window. (a) Geometry for the suppression of first multiple of the 5th trace of the time section of Figure 1a. (b) Geometry for the suppression of the second multiple of the 5th trace of the time section of Figure 1. The complete pass-windows are drawn in Figure 3.

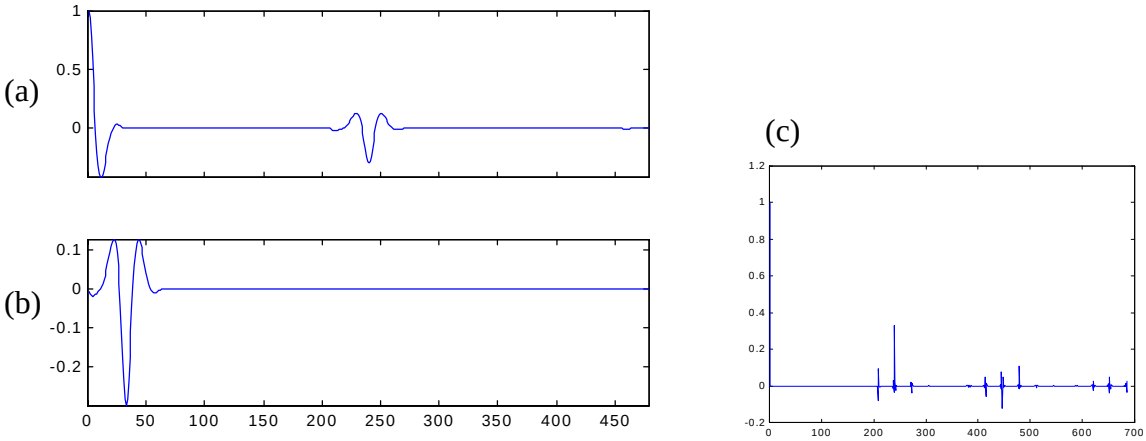

Figure 5. (a) Autocorrelation of the time window of Figure 4b. (b) Crosscorrelation (input and shifted input) for calculating the prediction operator. (c) Prediction-error operator showing oscillations.

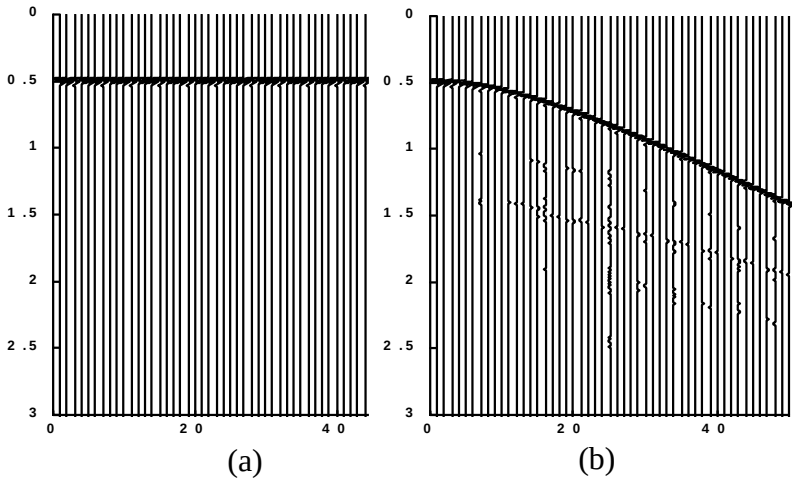

Figure 6. Deconvolved sections. (a) Zero-offset, as in Figure 1b. (b) Common-source, as in Figure 1c.

Deconvolução preditiva multicanal no domínio tau-p e interpolação de traços sísmicos na atenuação de múltiplas

Aury Cândido Bezerra e Milton J. Porsani

PETROBRAS/CPGG-UFBA

Abstract

Sea-floor multiple suppresion is treated here using multichannel predictive deconvolution. The reason for applying predictive deconvolution in the tau-p domain is that the multiple seemed quite periodic in this domain. During the transformation to the tau-p domain, the data showed noise due to the poor spatial sampling of the original data. Interpolation methods have been used to diminish the spatial alias efects, improving the quality of the imaging methods. We have used the interpolation method proposed by Porsani (1999). The results obtained with this method before the tau-p transform reduced very significantly the spatial alias effect and multichannel predictive deconvolution applied on common p panels shows to be more effective.

Introdução

Numa seção sísmica estão presentes energias primárias e múltiplas. Sendo primária a energia que foi registrada tendo sofrido apenas uma reflexão ascendente. Por sua vez, as múltiplas sofrem pelo menos duas reflexões ascendentes e uma descendente antes de serem registradas. As técnicas de imageamento sísmico têm importância fundamental na descoberta e no desenvolvimento de campos de petróleo, entre estas está a migração. No entanto os métodos de migração requerem a ausência de reflexões múltiplas, já que os operadores de migração não as distinguem das primárias, podendo introduzir refletores falsos nos dados migrados, prejudicando sobremaneira a imagem a ser interpretada. Apresenta-se aqui um método de atenuação de múltiplas que usa a deconvolução preditiva multicanal no domínio tau-p. O uso de dados adquiridos com grande intervalo entre as estações receptoras introduz efeitos de falseamento durante a transformação para o domínio tau-p. A interpolação dos traços sísmicos no domínio CMP é utilizada aqui como solução para os problemas de falseamento. Porsani (1999) demonstrou que é possível obter a interpolação dos traços com a solução de apenas um sistema de equações, através do uso de um filtro de predição intermediária. Este filtro trabalha nas amostras pares predizendo as ímpares resultando na otimização do algoritmo de Spitz (1991), cujo método de interpolação trabalha no domínio da frequência (f-x), baseando-se no fato de que eventos lineares presentes em uma seção composta de traços igualmente espaçados podem ser interpolados de forma exata, independente de seus mergulhos. A possibilidade de predição de eventos no domínio f-x permite que a interpolação de cada traço seja obtida como resposta de um sistema linear associado ao operador preditivo de erro. O algoritmo de Spitz necessita da solução de dois sistemas de equações lineares para cada frequência.

Filtragem Multicanal

Um filtro multicanal age sobre vários traços sísmicos simultaneamente. Para fins de ilustração deixemos o filtro ter 3 coeficientes/canal e atuar sobre 2 canais. Utilizando representação matricial podemos escrever,

$$\begin{bmatrix} \tilde{z}_0 \\ \tilde{z}_1 \\ \tilde{z}_2 \\ \vdots \\ \tilde{z}_m \\ \vdots \\ \vdots \end{bmatrix} = \begin{bmatrix} x_0 & y_0 & 0 & 0 & 0 & 0 \\ x_1 & y_1 & x_0 & y_0 & 0 & 0 \\ x_2 & y_2 & x_1 & y_1 & x_0 & y_0 \\ \vdots & \vdots & \vdots & \vdots & \vdots & \vdots \\ x_m & y_m & \vdots & \vdots & \vdots & \vdots \\ 0 & 0 & x_m & y_m & \vdots & \vdots \\ 0 & 0 & 0 & 0 & x_m & y_m \end{bmatrix} \begin{bmatrix} a_1 \\ b_1 \\ a_2 \\ b_2 \\ a_3 \\ b_3 \end{bmatrix} \quad (1)$$

A expressão para o erro entre valores observados, z_t e calculados $\tilde{z}_t$, pode ser representada como segue,

$$e_t = z_t - \tilde{z}_t = \sum_{k=1}^{3} x_{t-k+1} a_k + \sum_{k=1}^{3} y_{t-k+1} b_k \, .$$

Minimizando a forma quadrática $Q(\mathbf{a}, \mathbf{b}) = \sum e_t$ com relação aos parâmetros $\{a_j, b_j\}$ obtém-se o sistema de equações normais, com matriz dos coeficientes com estrutura bloco-Toeplitz (Lima, 1999) cuja solução pode ser obtida com a recursão de Levinson multicanal. Deixando $z_t = x_{t+L}$, teremos o filtro multicanal com predição L.

Interpolação de traços sísmicos

Considerando uma seção no domínio t-x com 2N-1 traços equi-espaçados formada por L eventos lineares invariantes traço a traço e com mergulhos distintos. Aplicando-se a transformada de Fourier de cada traço obtém-se a seção de dados complexos no domínio f-x, tendo $\mathbf{g(f)} = (g_1(f), \quad g_2(f), ..., \quad g_N(f))^T$ como o dado de entrada no domínio f-x. Neste domínio cada componente de traço pode ser escrita como:

$$g_k(f) = \sum_{j=1}^{L} a_j(f) {Z_j}^{k-1}(f) \qquad (2)$$

onde $a_j(f)$ é a transformada de Fourier do pulso sísmico correspondente ao evento j e, $Z_j(f) = exp(i2\pi f p_j)$ é o deslocamento de fase correspondente ao deslocamento no tempo p_j entre traços adjacentes no evento j.
Considerando-se apenas 3 eventos lineares, L= 3, e considerando 3 traços ímpares consecutivos, a equação (1) pode ser escrita como o sistema linear de equações,

$$\begin{bmatrix} g_k \\ g_{k+\frac{1}{2}} \\ g_{K+1} \end{bmatrix} = \begin{bmatrix} 1 & 1 & 1 \\ Z_1^{\frac{1}{2}} & Z_2^{\frac{1}{2}} & Z_3^{\frac{1}{2}} \\ Z_1 & Z_2 & Z_3 \end{bmatrix} \begin{bmatrix} a_1 Z_1^{k-1} \\ a_2 Z_2^{k-1} \\ a_3 Z_3^{k-1} \end{bmatrix} \qquad (3)$$

suprimindo assim para simplificação a dependência da frequência. Na matriz 3 X 3 de Van Der Monde as colunas são linearmente independentes, o que a caracteriza como de posto 3. Como consequência, qualquer outra componente espaçada de Δ x, pode ser obtida como combinação linear a partir dos dados espaçados de $2\Delta x$,

$$\begin{bmatrix} p_3 & p_2 & p_1 \end{bmatrix} \begin{bmatrix} g_k \\ g_{k+\frac{1}{2}} \\ g_{k+1} \end{bmatrix} = g_{k+\frac{3}{2}} \qquad (4)$$

Interpolação mediante convolução

No ítem anterior mostrou-se com base na equação (2), que qualquer coeficiente pode ser obtido através da combinação linear de outros. Então podemos escrever,

$$\begin{bmatrix} q_3 & q_2 & q_1 \end{bmatrix} \begin{bmatrix} g_K \\ g_{k+1} \\ g_{k+2} \end{bmatrix} = g_{k+\frac{5}{2}} \qquad (5)$$

onde $\mathbf{q}(f) = (q_3 \quad q_2 \quad q_1)^T$ representa o filtro de meia predição, cujas componentes satisfazem o seguinte sistema de equações ,

$$\begin{bmatrix} 1 & {}^iZ_1 & {}^iZ_1{}^2 \\ 1 & {}^iZ_2 & {}^iZ_2{}^2 \\ 1 & {}^iZ_3 & {}^iZ_3{}^2 \end{bmatrix} \begin{bmatrix} q_3 \\ q_2 \\ q_1 \end{bmatrix} = \begin{bmatrix} {}^iZ_1{}^{\frac{5}{2}} \\ {}^iZ_2{}^{\frac{5}{2}} \\ {}^iZ_3{}^{\frac{5}{2}} \end{bmatrix} \qquad (6)$$

O filtro ${}^i\mathbf{q}(f) = ({}^iq_3 \quad {}^iq_2 \quad {}^iq_1)^T$ trabalha sobre os dados de entrada espaçados de 2Δx para predizer dados espaçados de Δx. Consequentemente, a cada freqüência, os valores interpoladas dos traços podem ser estimados diretamente através da convolução do filtro de meia predição com o dado de entrada (Porsani, 1999).

Implementação prática do algoritmo

- Transformada de Fourier direta de T-X para F-X, dos traços de entrada, utilizando algoritmo FFT com 2nft pontos (nft=número de pontos utilizado na transformada de Fourier);
- Cálculo do filtro de predição intermediária para cada frequência dentro da banda do sinal;
- Redução do eixo de frequência preservando apenas os componentes ímpares;
- Cálculo dos coeficientes associados aos traços interpolados através da convolução do operador de predição intermediária com os coeficientes do dados de entrada, para cada frequência
- Transformada de Fourier inversa com nft pontos para obter os traços interpolados no domínio T-X.

Aplicação aos dados da Noruega

A falta de periodicidade das múltiplas nos traços mais afastados se constitui num grande problema para a DP monocanal, ou multicanal quando aplicada sobre traços de uma família CMP (Lima, 1999). No domínio do p comum contorna-se o problema da periodicidade. Durante a transformação das famílias CMPs de 24 traços, para o domínio $\tau - p$ observou-se fortes efeitos numéricos devidos principalmente ao forte falseamento espacial das reflexões. Com o objetivo de amenizar tais efeitos, observado no dado transformado para o domínio $\tau - p$, foi realizada uma interpolação dos traços sísmicos das famílias CMPs, utilizando o algoritmo proposto por Porsani (1999). As Figuras 1 e 2 ilustram, respectivamente, uma família CMP original e o resultado da interpolação de primeira ordem (um

traço interpolado entre dois adjacentes da seção original). Após a interpolação foi efetuada a transformação dos CMPs para o domínio $\tau - p$, conforme ilustrado na Figura 3.
A Figura 4a mostra a seção empilhada original, ou seja, sem deconvolução.
A organização dos traços em painéis de p-comum forneceu o domínio próprio para aplicação da DP multicanal, uma vez que nesse domínio as reflexões múltiplas são periódicas. Nos exemplos seguintes de DP multicanal foram utilizados 3 canais formado por traços adjacentes de painéis p-comum (Lima e Porsani, 2000). Após a DP os dados foram reorganizados em famílias CMPs sendo aplicada a transformação $\tau - p$ de volta para o domínio $t - x$.
A Figura 4b mostra a seção empilhada após a DP multicanal no domínio p-comum.
A Figura 4c mostra a seção empilhada utilizando-se os CMPs interpolados, ou seja, seguindo-se as sequência de processamento:

- Interpolação de primeira ordem dos CMPs,
- Transformação τ-p dos CMPs interpolados,
- Organização dos traços em painéis de p-comum,
- DP multicanal no domínio p-comum,
- Reorganização dos dados para o domínio τ-p ,
- Transformação *tau*-p inversa para o domínio CMP,
- Empilhamento.

No empilhamento tomou-se o cuidado de sortear apenas os traços ímpares, tendo-se utilizado apenas os 24 traços por CMP, como no dado original.

Conclusões

Sabendo-se que o efeito de falseamento espacial está diretamente relacionado ao espaçamento entre as estações receptoras (Robinson, 1967), utilizamos a interpolação de traços sísmicos para reduzir os efeitos do falseamento espacial na transformação dos CMPs para o domínio τ-p. Os CMPs interpolados foram organizados em painéis de p-comum e estes foram submetidos à DP multicanal do tipo Wiener-Levinson. Os filtros preditivos multicanais levam em conta a coerência lateral dos eventos refletidos presente nos canais adjacentes e faz o método de DP ser mais eficaz na remoção de eventos múltiplos. O tempo requerido na DP multicanal é diretamente proporcional ao número de canais utilizados. Aumentando-se o número de canais também aumentamos a robustez da DP, entretanto a partir de 7 canais a DP multicanal torna-se instável, com a necessidade de uma maior percentagem de luz branca, o que inibe a efetividade do filtro (Lima, 1999).O procedimento combinado, qual seja, interpolação e transformada τ-p aliada à organização dos dados em painéis p-comum, faz o método de DP multicanal bastante efetivo para a atenuação das múltiplas, conforme ilustram os bons resultados obtidos com os dados da Noruega.

Agradecimentos

Aury Cândido Bezerra agradece à PETROBRAS a oportunidade de realizar o mestrado em geofísica no CPGG-UFBA.

Referências

Lima A. de P., 1999, Deconvolução de Reflexões Múltiplas nos domínios t-x e τ - p com filtros multicanais. Dissertação de mestrado, CPGG-UFBA.

Lima A. de P., e Porsani, M. J., 2000, Deconvolução de Reflexões Múltiplas e 'peg-legs'utilizando filtragem Wiener-Levinson Multicanal. VII Simpósio de Geofísica da PETROBRAS, Salvador, Ba.

Porsani M., 1999, Seismic trace interpolation using half-step prediction filters, Geophysics, 64(5): 1461-1467.

Robinson, E. A., 1967, Multichannel time series analysis with digital computer programs, San Francisco, Holden-Day.

Spitz, S., 1991, Seismic trace interpolation, Geophysics, 50: 785-794.

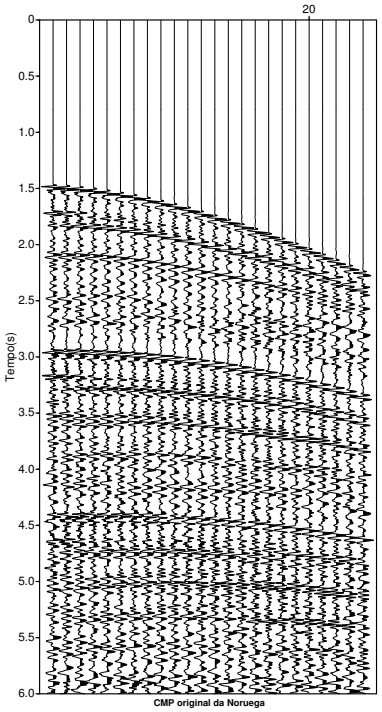

Figura 1: CMP original

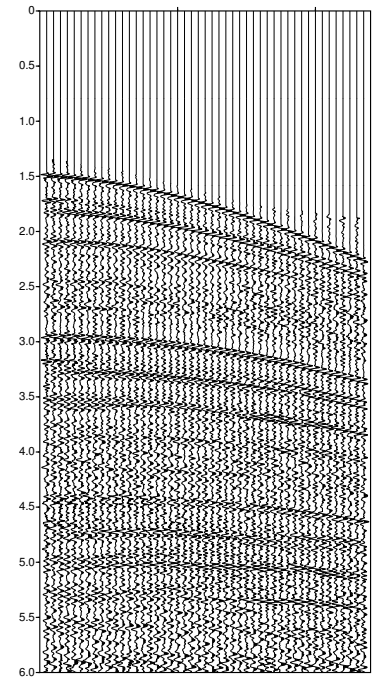

Figura 2: CMP da Noruega pós-interpolação de ordem 1

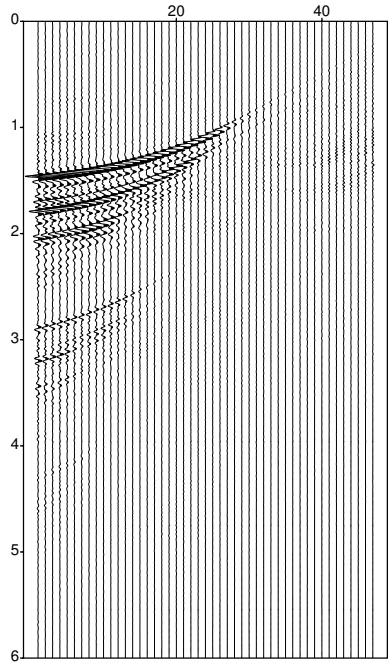

Figura 3: Painel τ-p do CMP da Noruega pós-interpolação

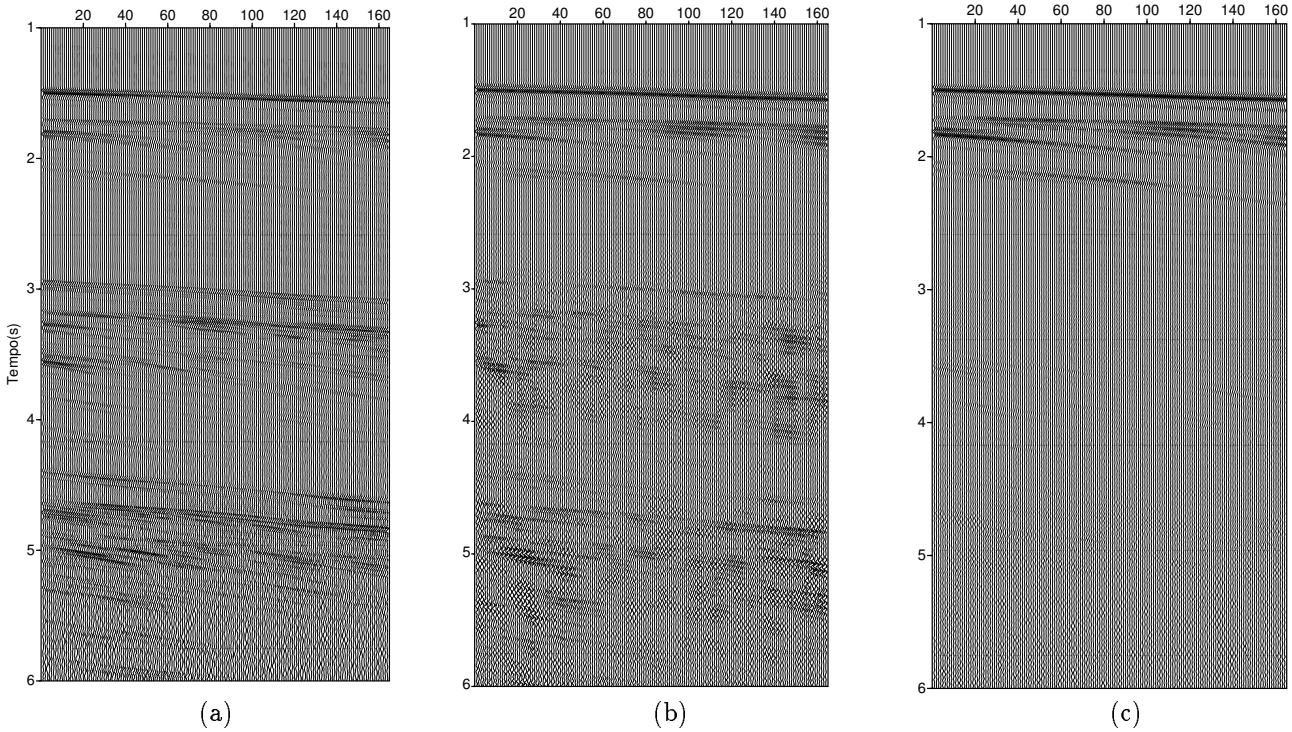

Figura 4: a) Seção original da Noruega, b) Seção após DP multicanal no domínio do p-comum, c) Seção após DP multicanal no domínio do p-comum após interpolação

Empilhamento SRC Considerando Múltiplas Reflexões

*Maciel, R. *; Cruz, J. C. R. **; Garabito, G. ** , UFPa,Brasil.*
** maciel_rosangela@yahoo.com.br,**jcarlos, german@ufpa.br*

Abstract

In seismic exploration the multiple reflections are dealt with as a noise to be compressed in the seismograms, in order to enhance de primary reflections. In this paper we simulate zero-offset intra-bed multiple reflection by using the new staking method called Common Reflection Surface (CRS) paraxial traveltime approximation. This is a model based strategy that is an important tool for identifying multiple reflections, being helpful for interpreting and providing informations about possible attenuation of these undesirable events.

Introdução

A sísmica de reflexão tem como principal objetivo obter uma imagem da estrutura geológica em subsuperfície. Com este intuito, os dados são submetidos a uma série de operações as quais levam à obtenção de uma seção sísmica final que será interpretada. Uma das etapas aplicadas com esse objetivo simula uma seção de afastamento nulo (AN) a partir de dados de reflexão sísmica de múltipla cobertura para meios 2D, o que permite a redução na quantidade de dados e a melhoria na razão sinal/ruído.

Os métodos utilizados para simular uma seção AN baseados na teoria do Imageamento Homeomórfico (Berkovitch et al, 1997), são: Empilhamento de Superfície de Reflexão Comum (Hubral et all,1998; Muller, 1999) e Multifocos (Gelchinsky et al.,1997; Chira, 2000), os quais não necessitam a priori do conhecimento explícito do modelo de velocidade e se baseiam no trio de parâmetros: (1) ângulo de emergência β_o, (2) raio de curvatura R_N ; e (3) raio de curvatura R_{NIP} , introduzidos por Hubral & Krey (1980) e obtidos através das ondas fictícias chamadas Onda Ponto de Incidência Normal (NIP) e onda Normal (N).

Neste artigo aplicamos o método de empilhamento Superfície de Reflexão Comum mostrado por Müller (1999). Empilhamos dados sísmicos contendo eventos de reflexões múltiplas de primeira ordem com o objetivo de simular a seção afastamento nulo realçando os referidos eventos de forma a facilitar a interpretação.

Metodologia

Tempo de Trânsito para Reflexões Primárias:- O método SRC apresentado por Müller (1999) tem sido aplicado com êxito na simulação de eventos de reflexões primárias mostrado por Chira, 2000. Está baseado no método do raio que descreve o tempo de trânsito para um raio paraxial arbitrário na vizinhança do conhecido raio central. Utiliza a aproximação hiperbólica do tempo de trânsito mostrada abaixo considerando o meio com variações suaves de velocidade.

$$t^2{}_{hyp}(x_m,h) = [t_0 + (2sin\beta_0 / v_0)(x_m - x_0)]^2 + (2t_0 \cos^2 \beta_0 / v_0)(K_n(x_m - x_0)^2 + K_{NIP}h^2) \quad (1)$$

Onde t_0 é o tempo de trânsito afastamento nulo, v_0 é a velocidade local no ponto X_0 definido pela coordenada x_0. x_m e h denotam o ponto médio e o meio-afastamento de um par fonte-geofone, respectivamente. Os demais parâmetros são o ângulo de emergência do raio normal β_o , a curvatura da onda NIP (K_{NIP}) e a curvatura da onda N (K_N), ambas observadas em X_0.

Observa-se na equação (1) que este método independe do macro modelo de velocidades, sendo necessário apenas: a velocidade próxima da superfície v_0 e o trio de parâmetros β_o , K_N e K_{NIP} , os quais definem a superfície de empilhamento com o respectivo tempo de trânsito do raio de reflexão normal.

A Onda NIP e a Onda N são ondas fictícias relacionadas ao experimento com afastamento nulo, a partir das quais torna-se possível a obtenção do trio de parâmetros. Ambas são geradas hipoteticamente. Para a Onda NIP consideramos que a fonte esteja em profundidade no refletor escolhido, coincidindo com um ponto NIP de incidência normal ao refletor e se propagando em direção a superfície. Já a Onda Normal é considerada o envelope de todas as ondas NIP uma vez que se propaga, por definição, perpendicularmente a todos os raios normais ao refletor. As curvaturas das ondas N e NIP são calculadas em função dos respectivos raios de curvatura R_N e R_{NIP} , assim representadas:

$$K_N = \frac{1}{R_N} \text{ e } K_{NIP} = \frac{1}{R_{NIP}} \quad (2)$$

Segundo Hubral & Krey (1980) os raios de curvatura podem ser calculados através do procedimento recursivo mostrado na equação (3), o qual foi obtido com base nas leis de transmissão (reflexão e refração)

para o caso de três camadas sobre um semi-espaço infinito e meio 2D.

$$R_0 = \frac{1}{v_1}\left[s_1 v_1 + \left(\frac{\rho_1}{v_1 \cos^2 \alpha_1} \frac{1}{R_{F,1}} + \left\{ s_2 v_2 \frac{\cos^2 \alpha_1}{\cos^2 \beta_1} + \left[\frac{\rho_2 \cos^2 \beta_1}{v_2 \cos^2 \alpha_1 \cos^2 \alpha_{21}} \frac{1}{R_{F,2}} + \left(s_3 v_3 \frac{\cos^2 \alpha_1 \cos^2 \alpha_2}{\cos^2 \beta_1 \cos^2 \beta_2} \right)^{-1} \right]^{-1} \right\}^{-1} \right)^{-1} \right] \quad (3)$$

Onde R_0 é o raio da onda emergindo na superfície da terra, s_i é o comprimento do raio, v_N velocidade do meio, β_i.é o ângulo de reflexão ou refração, α_i é o ângulo de incidência, ρ_N é a densidade do meio e $R_{F,i}$ é o raio de curvatura da interface.

Tempo de Trânsito para Múltiplas Reflexões:- As equações (1), (2) e (3) também são válidas para o cálculo dos tempos de trânsito dos eventos de reflexões múltiplas de primeira ordem conforme trajetória descrita na Figura 1. Contudo tornam-se necessários alguns ajustes na equação (3), de forma a considerar dentro do processo recursivo uma trajetória de reflexão. Dessa forma substituímos a parcela que se refere à transmissão do raio na terceira camada por outra que considera a trajetória do raio de reflexão na segunda camada $R_{R,2}$ aplicando a lei de reflexão equação (4). Dessa forma $v_2 = v_3$ e $\alpha_2 = \beta_2$.

$$R_{R,2} = \frac{1}{\frac{1}{R_{I,2}} + \frac{2}{\cos\alpha_2} \cdot \frac{1}{R_{F,2}}} \quad (4)$$

Onde $R_{R,2}$ é o raio refletido na interface 2, $R_{I,2}$ é o raio incidente na interface 2 e $R_{F,2}$ é o raio de curvatura da interface.

Superfície de Empilhamento:- O método SRC empilha dados sísmicos ao longo de uma superfície que se sobrepõe aos tempos de trânsito t_0 do raio de reflexão normal. A definição desta superfície é feita a través do trio de parâmetros supramencionados. Nesta superfície é efetuada a somatória de todas as amplitudes dos traços contidos na mesma, para cada raio central. O mesmo princípio é válido para as múltiplas.

Exemplo

Na parte inferior da Figura 2 mostramos o modelo, o qual é constituído de duas camadas sobre um semi-espaço infinito com velocidades: v_1 =2.5, v_2 = 3.5 e v_3 = 4.5 m/s. E na parte superior a seção fonte comum correspondente gerada para compor os dados a serem empilhados. Foi utilizado o pulso fonte Gabor com freqüência dominante igual a 50Hz. A primeira fonte foi posicionada em x_s=1.00km e o primeiro geofone em x_g =1.10km, sendo distribuídos 48 geofones com distância de 0.025km entre eles, sendo disparados 81 tiros com intervalo de 0.025km.

A seção afastamento nulo a ser simulada é mostrada na Figura 3 e consta de 81 traços com intervalos de 0.025 Km.

Ao aplicarmos o método proposto obtemos seção simulada visualizada na Figura 4. Onde podemos observar a presença das reflexões primárias e múltiplas. Pra reforçar os resultados obtidos exibimos nas Figuras 5 e 6 em detalhe o trecho das seções AN e simulada referente somente às reflexões múltiplas.

Conclusões

Ao aplicar a técnica proposta constatamos que a seção AN foi simulada satisfatoriamente. Conforme resultados obtidos podemos observar o bom posicionamento dos tempos de trânsito e a boa visualização dos eventos de reflexões primárias e múltiplas.

Referências

Berkovitch, A, Keydar,S.,Landa, E, Trachtman, P. 1998. Multifocusing in Pratice. In: Annual Int. MTG., 68. Expanded Abstracts. Soc. Expl. Geophys.

Cervený. V & Psencik, I. 1988. SEIS88, Ray Tracing Program Package .

Chira, P. Imageamento Multifocos de Refletores Sísmicos: tese de Mestrado, CPGF – UFPa., Brasil.

Gelchisnky, B., Berkovitch, A, Keydar, S. 1997. Multifocusing Homeomorphic Imaging: Parts I and II. Course Notes. Special Course on Homeomorphic Imaging, Seeheim, Germany.

Hubral, P. 1980. Wave fronts Curvatures in 3D Laterally Inhomogeneos Media With Curved Interfaces. Geophysics, v 45, p 905-913.

Müller, T. 1999. Seismic Imaging Without Explicit Knowledge of Velocity Model: Ph.D. thesis Karlsruhe University, Germany.

Agradecimentos

Agradecemos ao apoio financeiro investido através das bolsas de pesquisas concedidas pelo CNPQ e ANP (Agência nacional de Petróleo). E ainda ao grupo de Geofísica do Instituto Universitário Charles em Praga, Czechoslovakia, por fazer a avaliação do traçamento do raio no pacote SEIS88.

Empilhamento SCR Considerando Reflexões Múltiplas

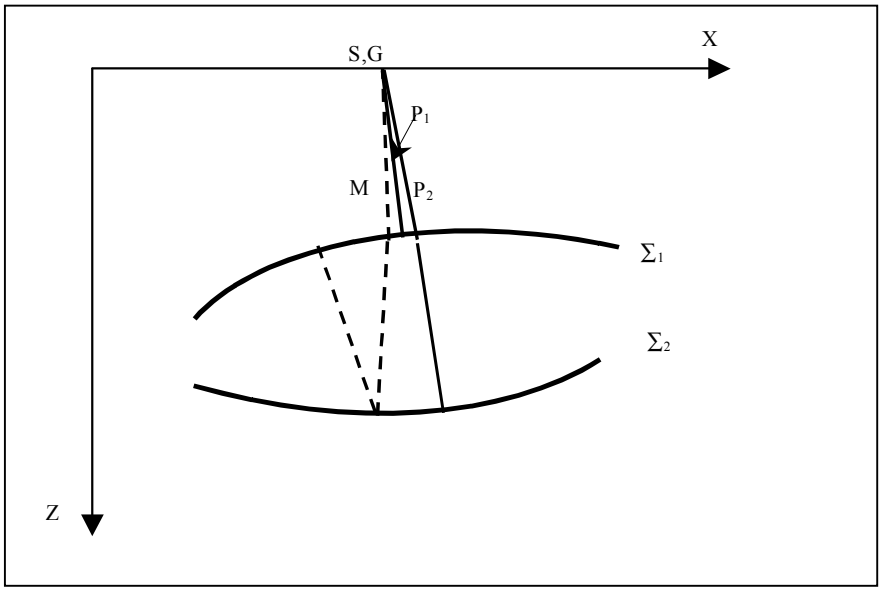

Figura1:Trajetória dos Raios Normais considerada para o cálculo do trio de Parâmetros β_o, R_N e R_{NIP}, onde P_1 e P_2 são os raios de reflexão primária na primeira e segunda interfaces respectivamente e M é a múltipla de afastamento nulo.

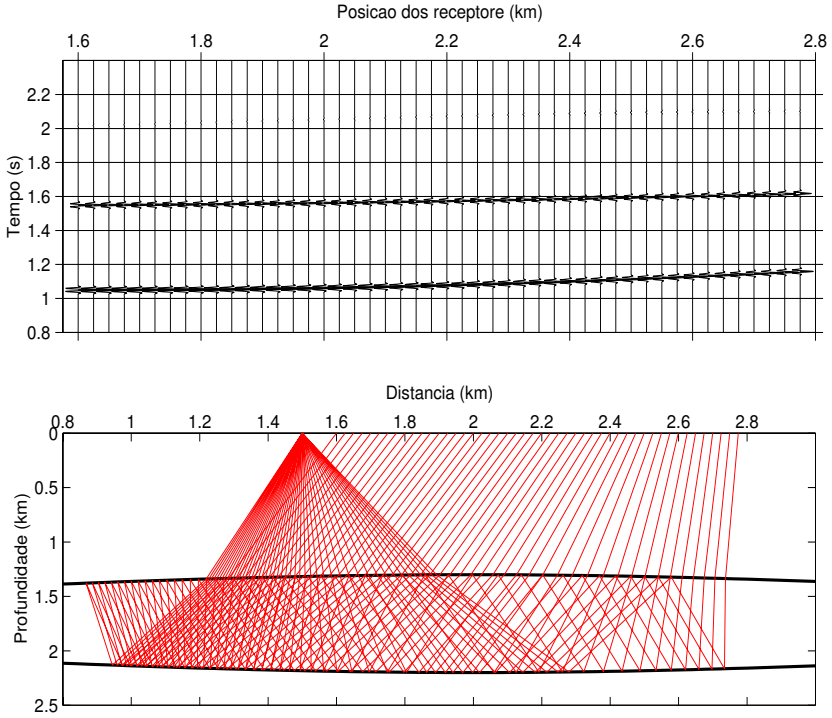

Figura 2 – Uma das seções Fonte Comum que compõe o cubo de dados a ser empilhado. Na parte superior da figura vê-se o sismograma e na parte inferior o modelo mostrando o traçamento dos raios somente para reflexões múltiplas, de forma que sejam bem visualizadas.

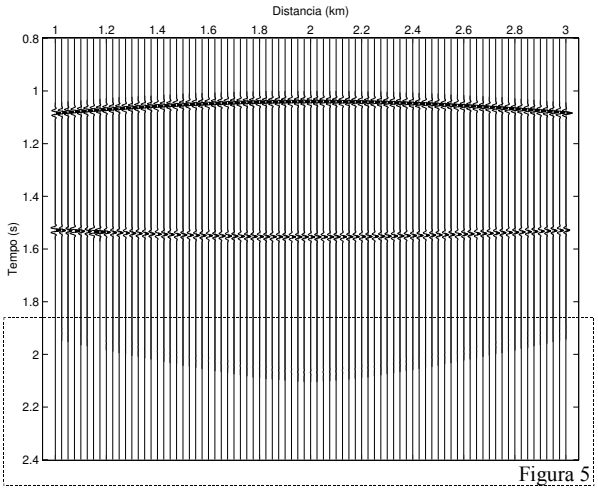

Figura 3 – Seção AN – obtida através do traçamento de raios no pacote SEIS88.

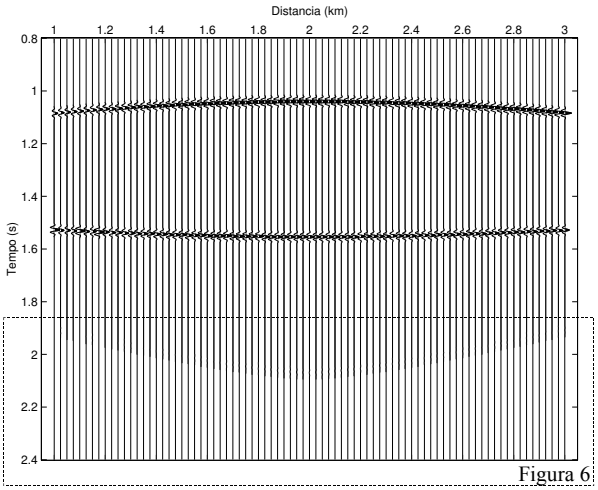

Figura 4 – Seção empilhada pelo método SRC.

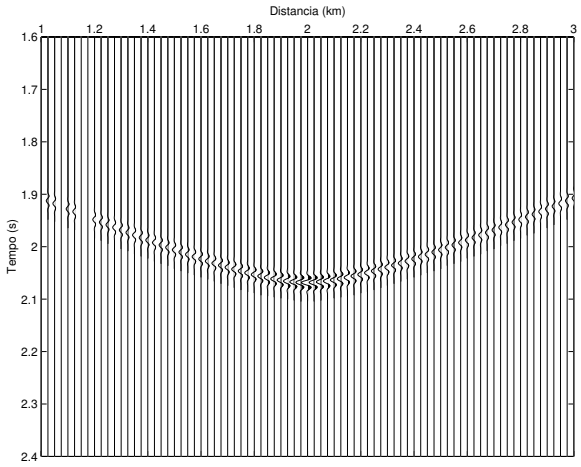

Figura 5 – Detalhe na seção AN visualizando apenas o trecho referente aos eventos de reflexões múltiplas da Figura 3.

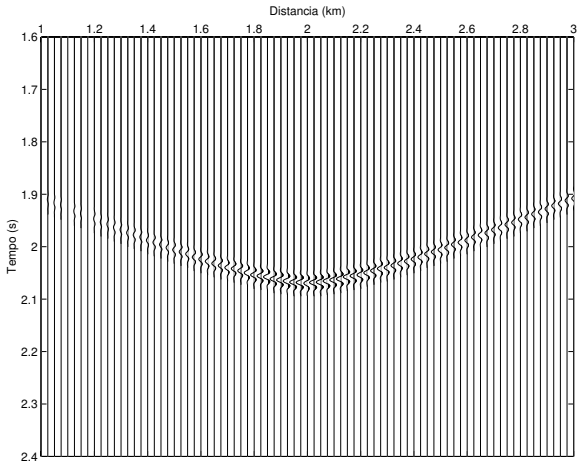

Figura 6 - Detalhe na seção Simulada visualizando apenas o trecho referente aos eventos de reflexões múltiplas da Figura 4.

Extrapolation of seismic data to small offsets

Carlos E. Theodoro[†] *and Ken Larner*[‡]

Abstract

Recorded data starting from offset-zero are required for surface-related multiple-attenuation methods that use the data themselves to develop the multiple prediction operator. Traces close to the source are not usually recorded in the field, so they have to be extrapolated from the recorded field data. Multi-valued moveout (e.g., reflections at about the same recording time, but with different moveout) is a problem for extrapolation methods presently in use in industry. We present an offset-continuation method, based on Hale's dip-moveout approach for constant-velocity background, for extrapolating data from one offset to a smaller offset, and compare the quality of predicted traces with that of those predicted using a conventional approach. Tests with synthetic data show better prediction of smaller-offsets when compared with predictions by the conventional method.

Introduction

A difficulty for modern methods of surface-related multiple attenuation (Carvalho et al., 1992; Verschuur et al., 1992; Dragoset and MacKay, 1993; and Borselen et al., 1996) is that these methods require a continuous spatial sampling of the wavefield over a large range of offsets, starting with zero-offset. The absence of data recorded at offsets close to the source results in an error in the prediction of the multiples; because this error propagates along the record during the process of multiple prediction and subtraction, strong residuals will be present in the data after the multiple-suppression process. A way of minimizing the problem is to extrapolate data from the shorter recorded offsets in order to model the missing close-to-the-source traces.

To extrapolate the short-offset traces in marine seismic data, a split-spread record is first simulated, in the common-midpoint (CMP) domain, by the symmetric repetition of traces from one side of the source to the other, obeying the offset distribution. The data are then NMO corrected, the missing traces are laterally interpolated, and finally inverse NMO correction is applied. We use results of this procedure, split-spread simulation and interpolation (SSSI), to compare with those of the offset-continuation (OC) extrapolation presented here.

Problems may occur with this conventional approach: (a) for reflections at about the same recording time but with different moveout, proper NMO correction for one of these events will leave residual NMO for the other event, degrading the extrapolation; (b) random noise may introduce spurious events and incorrect interpolated amplitudes; and (c) where the water bottom is shallow, the information recorded at early times, even close to the source, may be post-critical, so amplitude and phase corrections are necessary for the extrapolation. The method for extrapolation of near-offset data proposed here addresses primarily the first, and, to some extent, the second of these problems.

Dip-moveout (DMO) is a technique for correction of distortions in CMP data due to the dip of reflectors. If we could apply DMO before the multiple-attenuation process, we would overcome the problem of multi-valued moveout. Unfortunately, in applying DMO to the data, the spatial and temporal relationship between primaries and multiples is distorted, thus harming the result of the multiple-attenuation process.

The method

For reflections from the dipping base of a homogeneous medium, the dip-dependent relationship between nonzero-offset recording time t and zero-offset time t_0 is given by

$$t^2 = t_0^2 + (2h)^2 \cos^2\theta / v^2, \qquad (1)$$

where h is the half-offset, v is the velocity, and θ is the reflector dip.

Following Hale (1984), equation (1) can be expanded as

$$t^2 = t_0^2 + (2h)^2 / v^2 - (2h)^2 \sin^2\theta / v^2. \qquad (2)$$

Considering the NMO corrected time t_n,

$$t_n^2 = t^2 - (2h)^2 / v^2,$$

equation (2) can be rewritten as

$$\begin{aligned} t_n^2 &= t_0^2 - (2h)^2 \sin^2\theta / v^2 \\ &= t_0^2 - h^2 k^2 / \omega^2, \end{aligned}$$

[†]EP-Corp, Petrobras, email: ctheo@petrobras.com.br
[‡]Center for Wave Phenomena, Dept. of Geophysics, Colorado School of Mines

where k and ω are the spatial and temporal frequencies, respectively.

Consider two half-offsets, a recorded one, h_I, and a desired one, h_O (where the subscripts I and O refer to input and output, respectively), so

$$t_{n_I}^2 = t_0^2 - h_I^2 k_I^2/\omega_I^2 \text{ , and}$$
$$t_{n_O}^2 = t_0^2 - h_O^2 k_O^2/\omega_O^2,$$

giving the relationship between t_{n_I} and t_{n_O},

$$t_{n_O}^2 \overline{=}_{n_I} t^2 + (h_I^2 k_I^2)/\omega_I^2 - (h_O^2 k_O^2)/\omega_O^2. \quad (3)$$

Let us assume that

$$k_I/\omega_I \cong k_O/\omega_O \cong k/\omega, \quad (4)$$

which means that the slopes in the NMO-corrected common-offset sections, for the offsets of interest, are approximately the same.

Under assumption (4), equation (3) reduces to

$$t_{n_O} = A t_{n_I}, \quad (5)$$

where

$$A = \sqrt{\quad 1 + (h_I^2 - h_O^2)k^2/(\omega^2 t_{n_I}^2)}.$$

Since the extrapolation is from larger to smaller offsets, $h_I > h_O$ making A real.

We want to compute the wavefield $p_O(t_{n_O}, x, h_O)$, given the NMO-corrected recorded data $p_I(t_{n_I}, x, h_I)$. Under the small-offset approximation one can assume

$$p_O(t_{n_O}, x, h_O) = p_O(t_{n_O}, x, h_I),$$

then the double Fourier transform of $p_O(t_{n_O}, x, h_O)$ can be written as

$$P_O(\omega_{n_O}, k, h_O) = \int dt_{n_O} e^{i\omega_{n_O} t_{n_O}} \int dx e^{-ikx} p_O(t_{n_O}, x, h_I). \quad (6)$$

From equation (5), recalling that A also is a function of t_{n_I}, one gets

$$dt_{n_O} = A^{-1} dt_{n_I}. \quad (7)$$

Changing variables, from t_{n_O} to t_{n_I} in equation (6), using equations (5) and (7), and observing that

$$p_O(A t_{n_I}, x, h_I) = p_I(t_{n_I}, x, h_I),$$

which is exactly the DMO correction, one gets

$$P_O(\omega_{n_O}, k, h_O) = \int dt_{n_I} A^{-1} e^{i\omega_{n_O} t_{n_I} A} \int dx e^{-ikx} p_I(t_{n_I}, x, h_I). \quad (8)$$

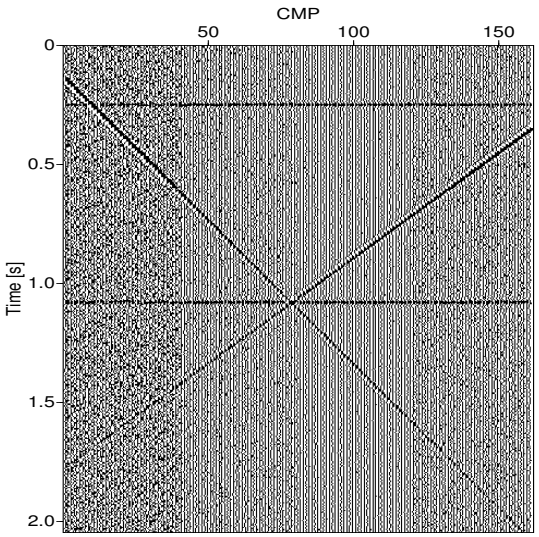

Figure 1: Zero-offset data for the first model, contaminated with random noise having spatially varying amplitude.

Now, to get $p(t_{n_O}, x, h_O)$ is just a matter of double inverse Fourier transformation of equation (8),

$$p_O(t_{n_O}, x, h_O) = 1/(2\pi)^2 \int d\omega e^{-i\omega_{n_O} t_{n_O}} \int dk e^{ikx} P_O(\omega_{n_O}, k, h_O). \quad (9)$$

Bleistein et al. (1997) suggested a correction to the amplitude treatment in Hale's (1984) DMO process to make it a true-amplitude one. With their correction, the factor A^{-1} in the integrand of integral (8) is replaced by

$$(1 + 2[hk/(t\omega)]^2)A^{-1}. \quad (10)$$

For the OC extrapolation we modified the factor that multiplies A^{-1} in expressions (8) and (10) to

$$1 + 2(h_I^2 - h_O^2)[k/(\omega t)]^2.$$

Application to Synthetic Data

The model has two horizontal reflectors and two plane reflectors, with dip of 45 and 75 degrees. A Ricker pulse with 25-Hz peak-frequency was used as the source wavelet. The velocity field is constant, equal to 2000 m/s. Use of this velocity for NMO correction for both conventional SSSI and

OC extrapolation causes residual moveout for the dipping events. To make the test more interesting, we added to the signal temporally bandlimited random noise, with Gaussian amplitude distribution, over the frequency range from 8 to 60 Hz. The noise is uncorrelated spatially, and has a root-mean-square amplitude that varies along the line. The noise-contaminated, zero-offset section (generated with the SUSYNLV and SUADDNOISE programs, within the Seismic Unix system) is shown in Figure 1. The data consist of 161 CMP gathers, with 12.5 m between midpoints, each gather with a trace every 25 m, from offset 0 to 800 m. Offsets from 0 to 175 m, which were excluded from the data that were used for the extrapolation, were generated only for comparison with the extrapolated data.

For the conventional SSSI method, we used as input NMO-corrected data over the offset range 200 to 800 m. With these data, we simulated split-spread data for use in interpolating offsets from 0 to 175 m. To assess the quality of the extrapolation we will look at *difference* sections - the difference between the result of the extrapolation for a given offset and a noiseless version of the modeled synthetic data for that same offset. Figure 2 shows the difference section, for the 25-m common-offset dataset, displayed at the same amplitude scaling as that in Figure 1. As expected, in Figure 2 the horizontal events are well predicted (i.e., extrapolated) because the SSSI process should predict well those events that are enhanced by the NMO correction. The dipping events, in contrast, are poorly extrapolated, leaving a strong residual.

The difference section for the OC extrapolation of the 25-m offset is shown in Figure 3. The input data used for the extrapolation were common-offset at an offset of 200 m, again contaminated with noise having the same amplitude variation with CMP as before. Except for the steepest event at early time, all reflections have been well extrapolated, independent of dip. The residual signal present in Figure 3 is a mixed result of edge-effect, violation of the assumption of small-offset, and erroneous amplitude prediction for the shallow, dipping extrapolated data.

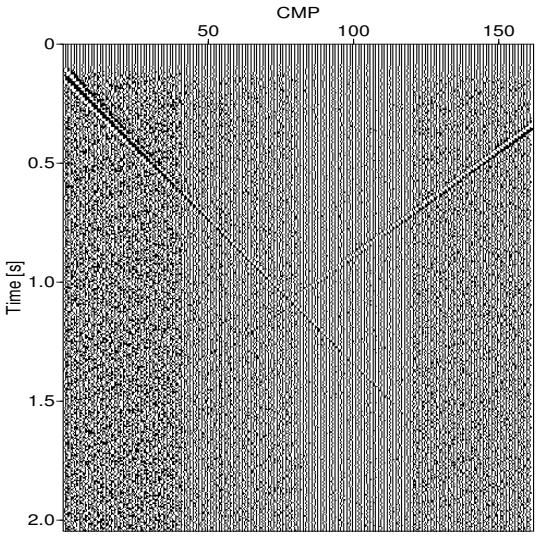

Figure 2: Common-offset difference section for an extrapolated offset of 25 m, obtained using the conventional SSSI method.

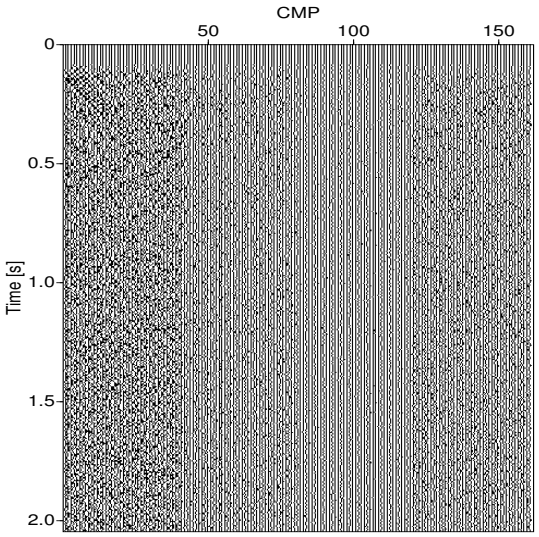

Figure 3: Common-offset difference section for an extrapolated offset of 25 m, obtained using offset-continuation extrapolation from 200 m, common-offset data.

Discussion and Conclusion

OC extrapolation, like the conventional method in use in industry (split-spread simulation of CMP gathers and interpolation of the missing offsets), does not correct for reflection amplitude and phase

variation with offset (or incidence angle) between input and output data. While including the amplitude correction term given by Bleistein et al. (1997) in the OC extrapolation improved the amplitude prediction, mostly for shallow dipping events, like any other method in use nowadays, OC extrapolation cannot properly extrapolate smaller-offset data from post-critical recorded data.

Although the larger difference between the results of the SSSI and OC extrapolations is in the prediction of the primaries, we also observed improvement in the extrapolation of multiple events to shorter offsets in areas with low structural complexity (not illustrated in this expanded abstract). Good prediction of the smaller offsets by SSSI requires perfect NMO correction (using $v/\cos\theta$, where v is the velocity and θ is the dip). OC extrapolation also requires a good approximation of velocity for NMO correction (here NMO is corrected using v, only), but that requirement is less stringent. Since primaries are better NMO-corrected than are multiples, OC results in better extrapolation of primaries than of multiples. However OC still yields a better extrapolation of multiples than does the SSSI method in areas of low structural complexity.

In presence of dip, using v for the NMO correction yields reflections with residual moveout in CMP gathers, violating the assumption of equation (4). Departure from this assumption is a function of dip, recording time, and difference between input and output offsets; the steeper the reflector, the earlier the time, or the bigger the difference in offsets, the weaker is the assumption of equation (4). As illustrated in Figure 3, however, even for steep features (75 degrees) and a difference of 175 m between input and output offsets, the methodology presented here resulted in a good prediction of shorter-offset data.

OC extrapolation, like migration, spreads amplitudes from one trace to its surrounding traces, and since random noise does not have lateral consistency it tends to attenuate. Also, it is possible to perform as many extrapolations as desired (or as are consistent with the small-offset approximation) to the target offset, using data with different common-offsets as input, and then stack the results of each extrapolation at each CMP.

Extrapolation by SSSI is of course less costly since the interpolation is simply done laterally over the input traces. The number of computations for the OC approach is basically that of two double Fourier transformations (one direct and one inverse transform) and $2n$ multiplications (where n is the number of time samples per trace), n multiplications for the amplitude term and another n for the phase term.

Tests using synthetic data showed better extrapolation for the OC method as compared with the conventional SSSI. For data from areas with low structural complexity, whether contaminated or not by random noise, and whether velocity is constant or depth-dependent, OC extrapolation results in better prediction of events (primaries, multiples, and diffractions) than does SSSI. Only for noiseless data from horizontal reflectors both results are equivalent. For data from areas of complex subsurface structure, with curved and truncated reflectors, diffractions, and velocity varying both vertically and laterally, although the result of the extrapolation is better for the OC extrapolation than for the conventional SSSI, the error in the prediction is substantial and will likely degrade the quality of any subsequent multiple-attenuation process. How much OC helps or fails to help for multiple suppression must await application of multiple suppression to field data having short offsets predicted by conventional SSSI and OC extrapolation.

References

- Bleistein, N., Cohen, J. K., and Jaramillo, H., 1999, *True amplitude transformation to zero offset of data from curved reflectors*: Geophysics, 64, 112-129.
- Borselen, R. G. van, Fokkema, J. T., and van den Berg, P. M., 1996, *Removal of surface-related wave phenomena - The marine case*: Geophysics, 61, 202-210.
- Carvalho, P. M., Weglein, A. B., and Stolt, R. H., 1992, *Nonlinear inverse scattering for multiple suppression: application to real data*: 62nd Ann. Internat. Mtg., Soc. Expl. Geophys., Extended Abstracts, 1093-1095.
- Dragoset, B., and MacKay, S., 1993, *Surface multiple attenuation and subsalt imaging*: 63rd Ann. Internat. Mtg., Soc. Expl. Geophys., Extended Abstracts, 1099-1102.
- Hale, D., 1984, *Dip-moveout by Fourier transform*: Geophysics, 49, 741-757.
- Verschuur, D. J., Berkhout, A. J., and Wapenaar, C. P. A., 1992, *Adaptive surface-related multiple elimination*: Geophysics, 57, 1166-1177.

Implementations and applications of the Sparse Radon transform.

*Daniel T rad† and T adeuszUlrych**

Abstract

The Radon transform (RT) is currently implemented in the time-offset, frequency-offset or frequency-wavenumber domains, with linear, parabolic or hyperbolic basis functions. Problems appear as a result of discrete sampling in offset and time, discrete velocity parameterization, finite aperture in offset and velocities, and missing data in particular due to low fold. As a consequence of all these practical issues, that could be referred in general as limited information, the RT suffers of low resolution, artifacts, aliasing and a non trivial null space. Even though none of these problems can be completely solved because they arise from the character of discrete signals, fortunately it happens that many of them can be attenuated by the sparse RT. The price to pay is however higher computational complexity. This complexity is sometimes related to the numerical algorithms, and sometimes to the design of the operators that perform the transformation. And most of the time, the complexity is required by the very limited time available per CDP for routine seismic processing.

In this paper we present different implementations of the sparse RT, in frequency and time domain, and explore new applications, elliptical and hybrid RT. We discuss also how the typical problems of low resolution and aliasing are attenuated in some measure by this method.

Introduction

In contrast to other common transformations, like the Fourier and many wavelet transforms, the RT operator is not orthogonal. As a consequence the problem of applying the forward and inverse transform without lost of data is not trivial. Many different methods have been developed for obtaining the RT, but the most commonly used is inversion. The misfit between observed and predicted data is minimized subject to a constraint of obtaining the smallest model, an approach usually leading to what is known as zero order regularization. This procedure leads to the standard RT, often used with linear or parabolic basis functions (Beylkin, 1987; Hampson, 1986).

The decreasing of resolution as a consequence of limited aperture is somewhat attenuated by the substitution of zero order regularization with stochastic inversion, originally proposed by Thorson and Claerbout (1985), leading to the high resolution time domain RT. Sacchi and Ulrych (1995) applied a similar idea to the frequency domain RT, which is much more utilized for seismic processing. Since then, some other variants of the sparse RT have been developed. Peter Cary (1997) noted the superiority of the time domain algorithms because of their ability to enforce simultaneously time and Radon parameter sparseness. We can add also as an advantage the ability of time domain methods to deal with time variant problems in the data and model by using time variant model and data weights. Cary also proposed to use frequency domain operators in the time domain algorithms to obtain a better waveform conservation.

Nemeth and Marfurt (paper in review process) and Trad and Ulrych (1999), noted the capability of time domain algorithms to deal with aliasing. Herrmann et al (1999) developed the dealiased RT, that prevents aliasing by carrying model weights from low (non aliased) frequencies to high (potentially aliased) frequencies. The algorithm also improves efficiency as a result of avoiding iterations. All these papers showed that not only resolution but also aliasing problems can be attenuated in some measure by the use of sparseness criteria.

Enforcing sparseness brings new problems and new possibilities. The problems are the increase in computation time, the introduction of artifacts, the difficulty to set inversion parameters, etc. The possibilities arise because a sparse RT can be used for other purposes that are not feasible with the standard smooth RT, for example

- Improving the continuity of events in incomplete data, provided that we can parsimoniously decompose these events in sets of curves.
- Separating overlapping events with different geometry, provided that we can find basis functions that approximate those geometries and create a different operator for each one.
- Removing some artifacts like aliasing that require a high degree of dispersion in the model space.

†University of British Columbia, Vancouver, Canada (UBC).

We have explored some of these possibilities in previous papers. In Trad et al. (2001), we tested the sparse time domain RT as an interpolation tool, and worked in improving efficiency by working with sparse matrices loaded into RAM memory, an irregular time variant Radon grid, and using a fast preconditioned CG algorithm. In the same paper we developed an elliptical RT to improve continuity in the slant stack of hyperbolic reflections. In Trad et al. (2001) we developed a hybrid sparse RT that allows the use of linear and hyperbolic basis functions simultaneously to separate ground roll and other linear events from reflections, and at the same time to reduce the null space of the transformation. All of these applications were possible only because of the sparseness imposed on the RT. In this presentation, we will discuss some of the implementations and applications that we have tried, and comment about why and how problems created by sampling and limited information can be attenuated by the addition of a sparse criteria for the RT.

Implementations

Given any transformation $\mathbf{m}$ on some data $\mathbf{d}$, for example the RT, we can set the problem as the inversion for the model that generates the data under the action of the operator $\mathbf{L}$

$$\mathbf{d} = \mathbf{L}\mathbf{m}. \tag{1}$$

To invert operators we define a cost or objective function, that is a mathematical expression that measures the undesired characteristics of the model. There are many possibilities, but most often we pursue a model that honors the data and has a minimum of information not required by the data. This statement of goals is commonly presented as

$$\begin{aligned} &\text{minimize } \|\mathbf{W}_m\mathbf{m}\|_p^p \\ &\text{subject to } \|\mathbf{W}_d(\mathbf{d}-\mathbf{L}\mathbf{m})\|_q^q = \phi_d \end{aligned} \tag{2}$$

where ϕ_d is some estimation of the noise level in the data plus failure of the proposed model to explain the data. $\mathbf{W}_d$ is a matrix of data weights, often a diagonal containing the inverse of the standard deviation of the data, and $\mathbf{W}_m$ is a matrix of model weights that we can design in order to enhance our preference in the model, for example resolution or smoothness. $\|.\|_p^p$ indicates that different norms can be applied to measure the size of vectors. A sparse model can be obtained by simply choosing a norm that does not penalize very strongly large elements on it. Conversely, a norm that penalizes large elements leads to smooth models. These model and data weights can be easily related to model and data covariances matrices, producing a statistical foundation for the choice.

A common approach is to transform the mixed norm problem to a $\ell_2 - \ell_2$ problem by using model dependent model weight matrices. With this previous step, setting these two anti-goals in a cost function and minimizing it, the model that fulfills our mathematical appetite can be found by solving the system of equations

$$(\lambda\mathbf{W}_m^T\mathbf{W}_m + \mathbf{L}^T\mathbf{W}_d^T\mathbf{W}_d\mathbf{L})\mathbf{m} = \mathbf{L}^T\mathbf{W}_d^T\mathbf{W}_d\mathbf{d}. \tag{3}$$

where λ is a tradeoff hyperparameter that will allow a different weight to be assigned to the misfit and model constraints.

Most variants of the sparse RT share the same basic system of equations (3). However, different methods are used to solve it. One of the favorites for its simplicity and efficacy is the Iteratively Re-weighted Least Squares (IRLS) algorithm (Scales and Smith, 1997), where the non linear system of equations is solved by fixing the model weights to some previous estimation and applying a linear minimization at every external iteration. The system of equations (3) is equivalent to the following extended system of equations

$$\begin{bmatrix} \mathbf{L} \\ \lambda\mathbf{W}_m \end{bmatrix} \mathbf{m} = \begin{bmatrix} \mathbf{d} \\ \mathbf{0} \end{bmatrix}, \tag{4}$$

or after a transformation of variables $\tilde{\mathbf{L}} = \mathbf{L}\mathbf{W}_m^{-1}$ and $\tilde{\mathbf{m}} = \mathbf{W}_m\mathbf{m}$,

$$\begin{bmatrix} \widetilde{\mathbf{L}} \\ \lambda\mathbf{I} \end{bmatrix} \tilde{\mathbf{m}} = \begin{bmatrix} \mathbf{d} \\ \mathbf{0} \end{bmatrix}. \tag{5}$$

This last system can be solved very efficiently by setting $\lambda = 0$ (no regularization) and letting the number of internal iterations in the CG algorithm play the roll of regularizer. The resulting linear problem can be solved by a subspace method, in this case a conjugate gradient algorithm. The inner problem is partially solved because the conjugate gradient algorithm is stopped before completing the solution.

None of the variants mentioned above require the transformation operator in matrix form. For time invariant (linear, parabolic and pseudo-hyperbolic) RTs this operator can work in the frequency domain, and then it is small but also non sparse. Time variant RTs (hyperbolic, elliptical, and other variants) require very large (and sparse) operators in the time domain. The design of the

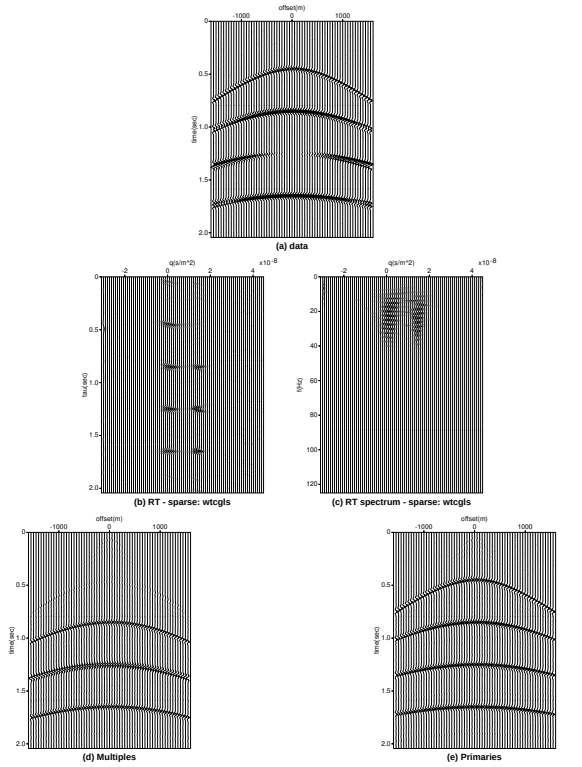

Figure 1: (a) Synthetic gather. (b) Sparse RT. (c) Spectrum of (b). (d) Recovered multiples after muting in (b). (e) Primaries obtained by substraction between (d) and (a).

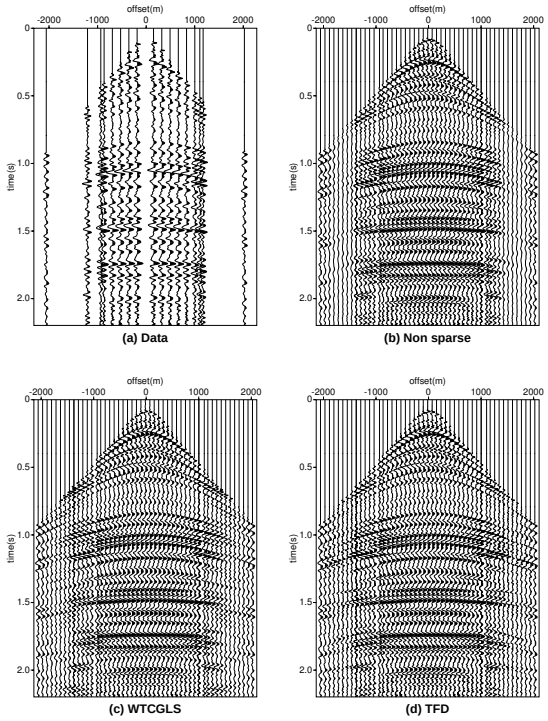

Figure 2: (a) CMP from land data. (b-c-d) Interpolation by using b) non sparse RT. c) Sparse RT in the frequency domain. d) Sparse RT obtained with a time domain method with frequency domain operators.

operators makes a large difference in time domain methods because of their complexity and flexibility. Very briefly, the fastest methods are those in the frequency domain where the multiplication inside the CG algorithm is performed by means of circular convolutions in the Fourier domain (Sacchi and Porsani, 1999). Time domain methods produce the most sparse results, and when they are implemented with time invariant RTs, the operator can be applied in the frequency domain, avoiding the need for interpolation during the summation inside the most inner loop of a time domain operator. Unfortunately, all time domain methods are slow. We have applied other method based on the weighted conjugate gradient least squares algorithm that produces very sparse results with excellent stability, thanks to a stopping criteria based in Generalized Cross Validation for subspaces (Haber, 1997).

Applications and examples

The achievement of high resolution in the RT has different applications. Multiple removal is immediately facilitated by the high localization of events (Figure 1). Interpolation is promoted because events with slow amplitude variation between data and gaps give optimal models for the sparse inversion. On the other hand, non sparse RTs produce interpolation mainly because of symmetry in the data space, but fail to do so when there is missing information at both sides of a gather (Figure 2). The flexibility of the Radon transform to separate events with different shape can be extended by creating hybrid transforms with more than one operator (Figure 3).

Conclusions

The Radon transform suffers from the typical problems of loss of resolution and aliasing that arise as a consequence of incomplete information, including

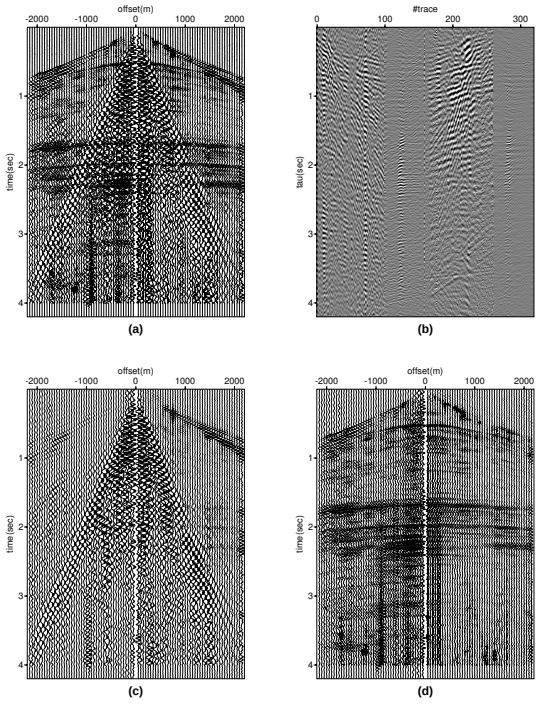

Figure 3: (a) Shot gather. (b) Combined Linear + Pseudo Hyperbolic Radon domain, for negative and positive offsets. (c) Recovered gather from linear space only. (d) Signal obtained by difference between (a) and (b).

limited aperture and discretization. Sparseness in the Radon domain is a valid and useful criterion for supplying this missing information, equivalent somehow to assuming smooth amplitude variation in the transition between data and gaps. Applying this constraint while honoring the data can become a serious challenge for routine seismic processing because of the very limited processing time available in general per CDP. To develop methods which are robust, easy to use and flexible to adapt to different problems we have to pay attention to varieties of algorithms and operator design. Frequency domain RTs provide a robust fast tool for interpolation and separation of events. Iterative subspace algorithms produce usually good results, but robust stopping criteria are required. Often the main weakness of these implementations is the introduction of artifacts, a problem that is efficiently addressed by time domain methods. Time domain kernels have extra flexibility to use more complicated curves. By using closer approximations to the events in the data the parsimony of the representation is increased, leading to better separability. However, they are slow and often difficult to implement. Their main weakness resides in their non trivial null space as a result of applying too few iterations, as is often required by processing time constraints.

References

Beylkin Gregory, 1987, Discrete Radon Transform: IEEE transactions on acoustics, speech, and signal processing, **35**, 162–172.

Cary P., The simplest discrete Radon transform, 1998: 68th Ann. Internat. Mtg Soc. Explo.Geophys., Expanded Abstracts, 1527–1530.

Haber, E., 1997, Numerical strategies for the solution of inverse problems. Ph.D. thesis, University of British Columbia.

Hampson, D., 1986, Inverse velocity stacking for multiple elimination: Journal of the Canadian SEG, **22**, 44–55.

Herrmann P., Mojesky T, and Magesan M., 1999, Amplitude prserving Radon demultiple: beyond sampling and aperture limitations: CSEG 1999 National Convention, Abstracts, 73-74.

Marfurt, K. and Nemeth, T., Antialias discrete Radon transforms: Geophysics

Sacchi, M., Fast high resolution parabolic RT, 1999: 69th Ann. Internat. Mtg Soc. Explo. Geophys., Expanded Abstracts, 1477–1480.

Sacchi, M. and Ulrych, T., 1995, High-resolution velocity gathers and offset space reconstruction: Geophysics, **60**, 4, 1169–1177.

Scales, J. and Smith, M., 1997, Introductory Geophysical Inverse Theory: Samizdat Press.

Thorson, R. and Claerbout, J., 1985, Velocity-stack and slant-stack stochastic inversion: Geophysics, **50**, 4, 2727-2741.

Trad D., Ulrych T., and Sacchi M (paper in preprint). Geophysics, Accurate interpolation with high resolution time variant Radon transforms

Trad D., Sacchi M., and Ulrych M (paper in preprint). Journal of Seismic Exploration, A hybrid linear-hyperbolic Radon transform.

Trad, D. and Ulrych, T., 1999,Beyond aliasing in the Radon transform: SBGf, Rio'99 Conference.

Método bidimensional de atenuação de múltiplas de superfície no domínio das ondas planas através de um filtro modelador

Erica Dantas P. Gama e Reynam Pestana (CPGG/UFBA) e Paul L. Stoffa (IG-UTEXAS)

Abstract

In this paper we discuss and apply a method for predicting and attenuating multiples in unstack seismic data. For horizontally stratified media, multiples are periodic with respect to the intercept time in the tau-p domain. Thus, multiples can be estimated and removed within each single trace. But, this is not the case in 2-D media. For 2-D media, we implemented the method in the 2-D plane wave domain, where the lateral variation of the structure is taken in account by the coupling of diferent ray parameters. The multiples are estimated from the primaries from the shallow part of the data by convolving the primaries with the data followed by the least-square filter to better match the mutiples present in the data. The application of the method is illustrated on synthetic and real data and the results demonstrate its effectiveness in attenuating multiples.

Introduçao

O aparecimento de múltiplas numa seção final prejudica a interpretação dos dados, modificando o car´ater do pulso sísmico, acarretando com isso interpreta¸cões falsas posi as múltiplas podem ser interpretadas, de uma forma errada, como eventos primários e, devido a alta energia das suas repetições, podem ainda simplesmente mascarar a energia da maioria das reflexões primárias de interesse, dificultando assim sua identifica¸cão.

A identifica¸cão e a remoção dessas múltiplas é de grande importância na etapa do processamento sísmico. As várias técnicas de elimina¸cão desses eventos múltiplos estão baseadas no reconhecimento de diferentes características capazes de descrimin´a-las das primárias. Basicamente, o que diferencia as múltiplas das primárias é a diferen¸ca de sobre-tempo normal (*normal moveout* (NMO)) e a periodicidade desses eventos múltiplos no domínio x-t, periodicidade esta, que só é observada em modelos de refletores aproximadamente horizontais (1-D), mesmo assim, apenas nos afastamentos curtos.

O método bidimensional de atenuação de múltiplas, aqui apresentado, é uma extensão para o caso 2-D dos operadores 1-D de elimina¸cão de múltiplas formulados por Sen et al. (1998), aplicados por Pestana et al. (1999) e Santos (2000) e também desenvolvido e aplicado mais recentemente por Liu et al. (2000), baseado na simula¸cão de eventos repetitivos utilizando-se a equação acústica da onda. O método 2-D utiliza-se da mesma metodologia usada por Sen et al. (1998) e Lokshtanov (1993), na qual o dado sísmico com melhor resultado na atenuação de múltiplas seria aquele obtido atrav´es de uma sol¸cãootima, correspondendo assim ao de menor energia. Os principais métodos existentes na literatura necessitam de uma boa estimativa da refletividade (Wiggins (1988) e Lokshtanov (1993)) ou da função fonte (Verschuur et al. (1992) e Fokkema and Van den Berg (1994)). Em meios 2-D, os eventos múltiplos, no domínio $(\tau - p)$, n˜ao serão periódicos em todos os parâmetros de raio, e com isso os mesmos não poderão ser estimados e removidos em cada traço. A varia¸cão lateral da estrutura causa a jun¸cão de diferentes par^ametros de raio, no domínio $(\tau - p)$, tornando-se necessário o uso de operadores com forma matricial para elimina¸cão desses eventos múltiplos. A partir de uma estimativa desses eventos múltiplos e, posteriormente, de uma correção na forma (amplitude e fase) dessas repetições, feita através de filtro modelador, obtido por meio de um processo de otimiza¸cão, pode-se finalmente então subtrair as múltiplas estimadas do registro sísmico original de entrada.

Teoria geral

Aplicando a formula¸cão matricial, (Kennett (1984)), para propagação sísmica no domínio w-p de meios compostos de camadas planas inclinadas, e fazendo-se uso do conceito de partição de matrizes na formula¸cão dos operadores de reflexão e transmissão em função das propriedades do meio e do sentido da propagação (ascendente e descendente) da onda, chega-se a uma forma matricial simples de representação completa do dado originalmente registrado no domínio (w-p), contendo primárias, múltiplas e ondas convertidas, que é dado pela seguinte equação (Liu et al. (2000)):

$$\bar{\mathbf{U}} = (\mathbf{I} + \mathbf{R})^{-1}\mathbf{R}\mathbf{S}, \qquad (1)$$

onde $\bar{\mathbf{U}}$ é o dado registrado sem as ondas diretas, $\mathbf{R}$ é a refletividade, e $\mathbf{S}$ é o espectro da função fonte.

Como se trata de um meio 2-D, $\bar{\mathbf{U}}$ e $\mathbf{R}$ são matrizes de ordem $\mathbf{N}$ x $\mathbf{N}$ o que diferem do caso para meio 1-D onde os mesmos são funções que dependem da frequência (w) e do parâmetro de raio (p). $\mathbf{S}$ é uma matriz diagonal onde seus elementos consistem no espectro do pulso da fonte e do fator de obliquidade do meio e $\mathbf{I}$ é matriz identidade.

As matrizes $\bar{\mathbf{U}}$ e $\mathbf{R}$, da Eq.(1), possuem basicamente a mesma forma. Cada coluna da matriz de dados $\bar{\mathbf{U}}$ corresponde a uma família de parâmetros de raio $\mathbf{p_d}$ comum, ou seja, é um supervetor de dados registrados devido a uma única onda plana incidente no sentido descendente, enquanto que cada linha corresponde a uma família de $\mathbf{p_0}$ comum, isto é, é o dado registrado devido a uma única onda plana refletida, mas devido a N ondas planas incidentes.

Liu et al. (2000) também mostrou que a partir da Eq. (1), pode-se chegar a duas expressões para os dados livres de múltiplas, após a remoção das chegadas diretas. Uma expressão em função apenas da refletividade e a outra a partir da função fonte. A expressão que representa os dados livres de múltiplas, que requer o conhecimento da refletividade do meio, é dada por:

$$\mathbf{U_0} = \mathbf{RS} = \bar{\mathbf{U}} + \mathbf{R}\bar{\mathbf{U}}. \qquad (2)$$

Para a expressão que representa os dados livres de múltiplas, utilizando a função fonte, pode-se ainda reescrever a própria Eq. (2) através de uma aproximação por uma expansão em série de Taylor de forma que, desprezando-se os termos a partir da 3^a ordem, obtém-se:

$$\mathbf{U_0} \approx \bar{\mathbf{U}} + (\bar{\mathbf{U}}\mathbf{S}^{-1})\bar{\mathbf{U}} + (\bar{\mathbf{U}}\mathbf{S}^{-1})^2\bar{\mathbf{U}} \qquad (3)$$

Filtro modelador para correção de amplitude e fase

Para se atenuar as múltiplas do fundo do mar, correspondentes as $\mathbf{k}$ primeiras reflexões do registro sísmico, é necessário uma boa estimativa da refletividade das $\mathbf{k}$ interfaces referentes as essas múltiplas que se deseja atenuar (Sen et al. (1998), Liu et al. (2000)). Dessa forma a Eq. (1) pode ser adaptada, para o caso de $\mathbf{k}$ interfaces, ficando da seguinte forma:

$$\mathbf{U_{0k}} = \bar{\mathbf{U}} + \mathbf{R_k}\mathbf{S}\mathbf{S}^{-1}\bar{\mathbf{U}} \qquad (4)$$

fazendo $\mathbf{P_k} = \mathbf{R_k}\mathbf{S}$ e $\mathbf{A} = \mathbf{S}^{-1}$, a Eq. (4), torna-se:

$$\mathbf{U_{0k}} = \bar{\mathbf{U}} + \mathbf{P_k}\mathbf{A}\bar{\mathbf{U}}, \qquad (5)$$

onde $\mathbf{P_k}$ é uma matriz que consiste nas primárias das $\mathbf{k}$ primeiras camadas e $\mathbf{A}$ é uma matriz diagonal que corresponde ao inverso da fonte. Então, o registro livre das múltiplas provinientes de $\mathbf{k}$ interfaces, depende tão somente de uma boa estimativa do tempo de ocorrência e da forma das múltiplas.

A estimativa do filtro $\mathbf{A}$, que corresponde ao filtro modelador, pode ser obtida através de um processo de otimização em que, os dado livres de múltiplas são aqueles em que a energia é mínima, ou seja:

$$E(\mathbf{A}) = \|\bar{\mathbf{U}} + \mathbf{P_k}\mathbf{A}\bar{\mathbf{U}}\|^2 = \text{mínimo} \qquad (6)$$

Para uma implementação numérica, basta fixar $\mathbf{A} = \mathrm{I}$, filtro inicial igual a matriz identidade, tal que:

$$\bar{\mathbf{U}}_\mathbf{k} = \mathbf{P_k}\bar{\mathbf{U}}, \qquad (7)$$

onde $\bar{\mathbf{U}}_\mathbf{k}$ é uma estimativa inicial das múltiplas, relacionadas às $\mathbf{k}$ primeiras camadas, obtidas através da convolução entre $\mathbf{P_k}$ e $\bar{\mathbf{U}}$, no domínio (tau-p), ou, como mostrado na Eq. (7), através da operação de multiplicação no domínio (w - p).

Essas múltiplas modeladas se equivalerão com as múltiplas observadas nos dados em tempo de trânsito, mas não em amplitude fazendo-se então necessário a aplicação do filtro modelador $\mathbf{A}$, para corrigir a amplitude e fase dessas múltiplas estimadas, e em seguida subtraí-las do dado de entrada.

Para aplicar o algoritmo 2-D de atenuação de múltiplas, os dados de entrada estão inicialmente no domínio da fonte, afastamento e frequência, $d(\mathbf{x_s}, \mathbf{x_0}, \mathbf{w})$. Aplicando-se uma transformada (τ - p) 2-D ao longo do afastamento e da fonte, obtém-se os dados no domínio $D(p_s, p_0, w)$, ou seja:

$$D(\mathbf{p_s}, \mathbf{p_0}, \mathbf{w}) = \sum_{x_s}\sum_{x_0} d(\mathbf{x_s}, \mathbf{x_0}, \mathbf{w}) e^{-\mathbf{iw}(\mathbf{p_0}\mathbf{x_0} + \mathbf{p_s}\mathbf{x_s})}$$

Porém, esse domínio ainda não é o mais adequado para a aplicação do operador 2-D de atenuação de múltiplas. Precisa-se aplicá-lo no domínio D$(\mathbf{p_d}, \mathbf{p_0}, \mathbf{w})$, pois este é o domínio correto para estimar as múltiplas.

Então, fazendo-se $\mathbf{p_d} = \mathbf{p_0} - \mathbf{p_s}$, e com isso, $\mathbf{p_s} = \mathbf{p_0} - \mathbf{p_d}$, tem-se:

$$D_{\tau p}(\mathbf{p_d}, \mathbf{p_0}, \mathbf{w}) = \sum_{x_s}\sum_{x_0} d(\mathbf{x_s}, \mathbf{x_0}, \mathbf{w})\ e^{-\mathbf{iw}\mathbf{p_0}\mathbf{x_0}} e^{-\mathbf{iw}(\mathbf{p_0} - \mathbf{p_d})\mathbf{x_s}} \qquad (8)$$

A modelagem dos dados 2-D nas coordenadas da fonte e afastamento, $d(\mathbf{x_s}, \mathbf{p_0}, \mathbf{w})$, é dada pela superposição de ondas planas, de acordo com Lokshtanov (1995), por:

$$d(\mathbf{x_s}, \mathbf{x_0}, \mathbf{w}) = \frac{w^2}{4\pi^2}\int_{-\infty}^{+\infty}\int_{-\infty}^{+\infty} D_{pl}(\mathbf{p_d}, \mathbf{p_0}, \mathbf{w})\, e^{\mathbf{iw}\mathbf{p_0}\mathbf{x_0}} e^{\mathbf{iw}(\mathbf{p_0} - \mathbf{p_d})\mathbf{x_s}} dp_0\, dp_d \qquad (9)$$

Aplicando-se, agora, uma transformada $(\tau - p)$ 2D inversa em (9), obtém-se:

$$d(\mathbf{x_s}, \mathbf{x_0}, \mathbf{w}) = \frac{w^2}{4\pi^2} \int_{-\infty}^{+\infty} \int_{-\infty}^{+\infty} D_{\tau p}(\mathbf{p_s}, \mathbf{p_0}, \mathbf{w}) e^{\mathbf{iwp_0x_0}} e^{\mathbf{iwp_sx_s}} dp_0 dp_s \qquad (10)$$

Comparando-se as equações (9) e (10), concluí-se que:

$$D_{pl}(\mathbf{p_d}, \mathbf{p_0}, \mathbf{w}) = D_{\tau p}(\mathbf{p_0} - \mathbf{p_s}, \mathbf{p_0}, \mathbf{w}), \qquad (11)$$

onde, $D_{pl}(\mathbf{p_d}, \mathbf{p_0}, \mathbf{w})$ é o dado depois da decomposição 2-D em ondas planas, enquanto que $D_{\tau p}(\mathbf{p_0} - \mathbf{p_s}, \mathbf{p_0}, \mathbf{w})$ é a transformada $(\tau - p)$ 2-D dos dados.

Como citado anteriormente, a variação lateral da estrutura é levada em conta pela junção de diferentes parâmetros de raios. Nas situações onde a variação lateral é pequena, os dados são bem comprimidos no domínio de ondas planas, o que produz uma estrutura banda limitada da matriz, relacionada na Eq.(5), que reduzirá significativamente o tempo de computação.

Aplicação em Dados Sintéticos e Reais

A aplicação em dados sintéticos é utiliza para demonstrar como se comporta o método de atenuação de múltiplas 2-D em situações em que o refletor primário, simulando o fundo do mar possui uma certa inclinação. A figura (1a) mostra um sismograma contendo primárias e multiplas, gerado no domínio tau-p a partir do modelo de uma camada com inclinação de 10 graus. Este dado é usado para ilustrar a aplicação do método de atenuação de múltiplas descrito anteriormente. O registro gerado tem um total de 60 parâmetros de raio ($\mathbf{p}$), variando de 0.0 até 0.6 s/km, com intervalos de 0.01 s/km. A figura (1b) mostra as múltiplas simuladas, após a aplição do filtro modelador, e na figura (1c) tem-se o resultado da subtração das múltiplas estimadas dos dados (figura 1a). Como podemos notar, o processo de estimativa e filtragem das múltiplas foram bastantes efetivos e as duas múltiplas presentes nos dados foram completamente atenuadas.

O método de atenuação de múltiplas também foi aplicado a um trecho de uma linha sísmica da Noruega. Ao final do processo de atenuação 2-D de múltiplas, obtivemos o processamento dos dados. Para efeito de comparação usamos os dados empilhados sem filtragem (figura 2a), ou seja, com todas as múltiplas e também o resultado obtido pelo método de atenuação 1-D (figura 2b). O resultado obtido com o método 2-D é mostrado na figura 2c. Os resultados apresentados pelos métodos 1-D e 2-D são bastantes parecidos para esses dados, que apresenta o refletor do fundo do mar com pouca inclinação.

Conclusões

O método de atenuação de múltiplas, aqui descrito, obteve resultados bastante satisfatórios no dado sintético, que apresenta uma não periodicidade entre as múltiplas e a reflexão primária em cada parâmetro de raio. Durante o processo de atenuação as mútiplas foram estimadas, corrigidas de amplitude e fase, através do filtro modelador, e completamente eliminadas do sismograma de entrada. Nos dados reais, que apresenta várias múltiplas associadas com a superfície livre, utilizamos para efeito de comparação os dados antes e após o processo de atenuação de múltiplas. Verificou-se que grande parte da energia associada com as múltiplas foram bastante removidas pelo método bidimensional de atenuação, descrito neste trabalho.

Agradecimentos

E. D. P. Gama agradece à ANP pela bolsa de Mestrado. Reynam Pestana agradece ao CNPq (projeto no. 300312/81) e a PGS do Brasil (projeto UFBA/CPGG/PGS).

Referências

Fokkema, J., and Van den Berg, P., 1994, Removal of surface related multiple phenomena; the marine case: Removal of surface related multiple phenomena; the marine case:, 64th Ann. Internat. Mtg., SEG, Expanded Abstracts, Los Angeles, 1689–1692.

Kennett, B., 1984, Reflection operator methods for elastic waves ii-composite regions and source problems: Reflection operator methods for elastic waves ii-composite regions and source problems:, Wave Motion, 419–429.

Liu, F., Sen, M., and Stoffa, P., 2000, Dip selective 2-d multiple attenuation in plane wave domain: Geophysics, **65**, 264–274.

Lokshtanov, D., 1993, Adaptive multiple suppression in tau-p domain: Adaptive multiple suppression in tau-p domain:, 63rd Ann. Internat. Mtg., SEG, Expanded Abstracts, 1086–1089.

Lokshtanov, D., 1995, Multiples suppression by single channel and multichannel deconvolution in

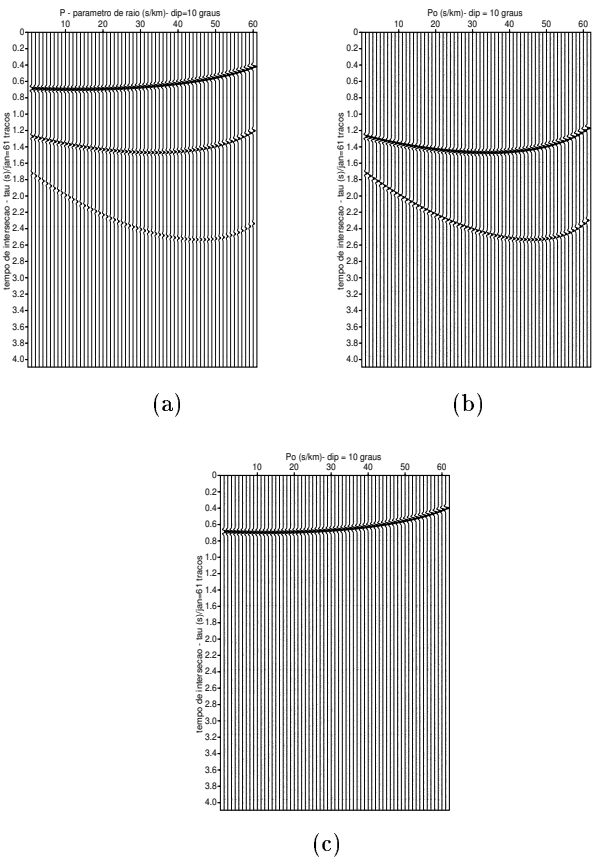

Figura 1: (a) Sismograma sintético no domínio (tau-p) com primárias e suas múltiplas - refletor com inclinação de 10 graus; (b) Múltiplas estimadas a partir da primária e corrigidas de amplitude e fase pelo filtro modelador e (c) resultado do processo da atenuação de múltiplas obtido através da subtração das múltiplas estimadas (figura 1(b)) com o dado de entrada (figura 1(a)).

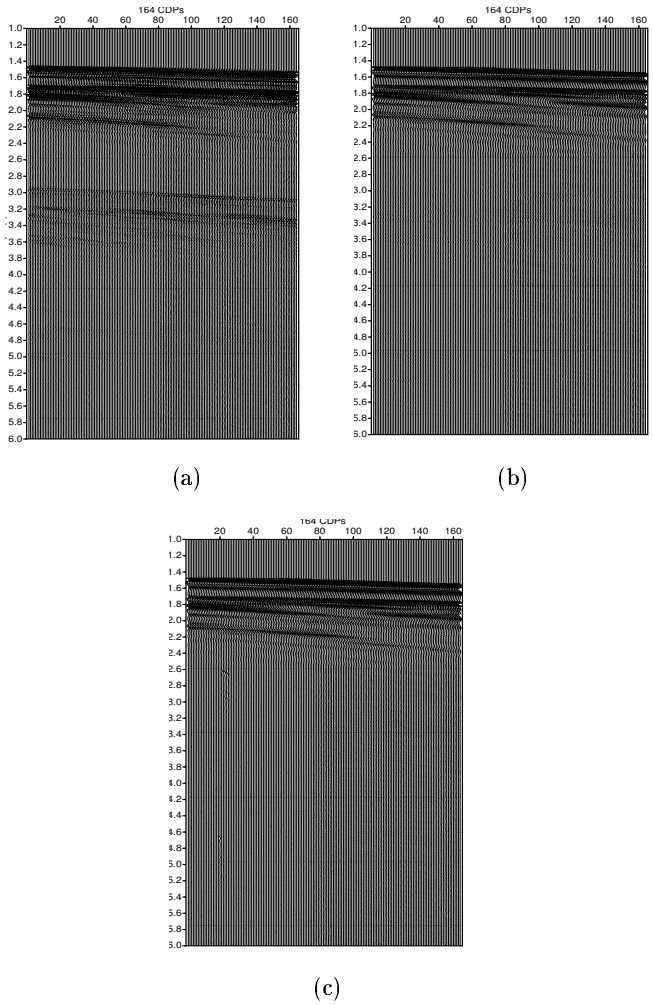

Figura 2: Atenuação de múltiplas do fundo do mar no domínio das ondas planas. Comparação entre as seções empilhadas sem AGC, de um trecho de 164 CDPs de uma linha sísmica da Noruega. (a) Seção empilhada com múltipla, (b) resultado do método de atenuação 1-D (Santos (2000)) e (c) com o método 2-D proposto aqui.

the tau-p domain: Multiples suppression by single channel and multichannel deconvolution in the tau-p domain:, 65rd Ann. Internat. Mtg., SEG, Expanded Abstracts, 1482–1485.

Pestana, R., Stoffa, P., and Sen, M., 1999, Multiple attenuation in the plane wave domain by match filtering: Multiple attenuation in the plane wave domain by match filtering:, Anais do VI Congresso Internacional da SBGF, Brasil.

Santos, J. R. S. B., abril 2000, Atenuação de Múltiplas do Fundo do Mar e Migração Pré empilhamento no Domínio das Ondas Planas: Master's thesis, Universidade Federal da Bahia, Salvador, Brasil.

Sen, M., Liu, F., Stoffa, P., and Fokkema, J., 1998, An unified treatment to free surface multiple elimination methods: J. Seismic Explor., pages 129–143.

Verschuur, D., Berkhout, A., and Wapenaar, C., 1992, Adaptive surface-related multiple elimination: Geophysics, **57**, 1166–1177.

Wiggins, J., 1988, Attenuation of complex water-bottom multiples by wave equation-based prediction and subtraction: Geophysics, **53**, 1527–1539.

Multiple Approaches to Deep Water Multiples

Raymond A. Ergas, Chevron Petroleum Technology Company, rae@Chevron.com

Abstract

Despite the tremendous progress that has recently been made in the development and evolution of algorithms for deep water multiple suppression, no one method seems able to solve all problems. Among the commercially available techniques, some combination will probably be needed to adequately remove all types and orders of multiples. Factors that can influence the best solution include acquisition style, noise environment, water depth, geologic complexity, and reservoir type. Finding the optimal solution for each situation will remain a challenge as both the business and technical opportunities change with time.

Introduction

There is a very long history of attempting to remove multiples from deepwater data. A recent compilation of significant papers by Weglein (1999) is already out of date, as many new contributions have appeared (see also Yilmaz, 2001). Yet, we are still unable to adequately improve the interpretive quality of images in certain kinds of geologic environments. In this paper, we will consider why no single algorithmic approach is likely to provide the complete solution to the problem of multiples in complex geology and deep water, particularly with the seismic data most commonly available. For clarity, we are restricting the discussion to suppression of multiple reflections, not using multiples for imaging, or treatment of other source-generated energy such as converted energy or multipaths. These are topics worthy of separate treatment. Also, we will consider primarily techniques that can be applied to multi-streamer marine acquisition, which are usually the first and only seismic data available for a given prospect.

Four Biggest Problems

There are (at least) four significant challenges which must be addressed in removing deep water multiples. The first is that complex velocity structures, such as allochthonous salt bodies in tertiary sediments, produce truly three-dimensional multiples. Some of the most successful multiple suppression methods now available (*e.g.* SRME, Berkhout and Verschuur, 1997) probably would work very well if we could record with shots and receivers at all possible locations. Since this is impractical, we are often forced into making assumptions about multiple generation that rely on the narrow azimuthal distribution of multi-streamer data.

The second difficulty is that the multiple generating surfaces can change rapidly in position, dip, and reflectivity. There are excellent methods of attacking multiples if the generators are smooth on the order of a cable length (*e.g.* Radon Filtering, Foster and Mosher, 1992), but this assumption breaks down and the methods either fail to remove multiples or attack primary energy.

Often a significant, but overlooked problem is caused by the presence of a number of strong reflectors, so that internal multiples are a major source of contamination. Internal multiples (as opposed to surface-related multiples) are often more complex, because all of the reflection surfaces are rugose, or possibly because the "surfaces" are actually a composite of many closely spaced interfaces. Higher order multiples can be generated within the recording time, which is often not as significant for surface multiples in deep water. Additionally, the recurrence period can be short enough to begin to overlap the source wavelet length, so that the multiples take on the character of a shallow-water multiple train.

Finally, there is the ever-present danger of modification of the primary energy. In particular, systematic changes in prestack amplitude caused by aggressive multiple suppression can give rise to incorrect interpretations of potential reservoirs. Ensuring effective multiple energy reduction while trying to image subtle prestack features requires great care.

Data and Models, Prediction and Subtraction

Multiple suppression approaches have usually been divided between the direct filtering methods (*e.g.* deconvolution and Radon in various domains) and prediction/subtraction techniques (SRME, wave equation extrapolation, *etc*.). As these techniques have evolved, the distinction has become somewhat arbitrary. Many of the direct filtering methods are now used as predictors, with adaptivity used to improve the suppression. The traditional filtering approaches can be considered to use adaptive subtraction with no degrees of freedom.

Perhaps a more fundamental division is between the earth-model driven methods, and the data driven

methods. The development of data driven convolutional predictors, such as are used in SRME, has been a major improvement in our prediction ability for complex areas. However, the data acquisition limitations of normal field practice introduce significant errors in the accuracy of the predictions, due to lack of complete 3D coverage, source and receiver imperfections, and near surface complexity.

Modern imaging practices result in the development of earth models that can be used to guide demultiple techniques. These models can be used with forward seismic techniques such as ray tracing or finite difference wave equations to predict multiples. In deep water, often we only require the water bottom and upper part of the overburden. And hybrid schemes, which take advantage of both data and model results are being used. There is a range of solutions that practitioners must consider to obtain optimal results on any specific dataset.

The subtraction step is also undergoing an evolution from the minimum energy methods used with SRME in the past to more model driven techniques. Frequently, aggressive adaptive subtraction attacks primary energy or is unable to handle more than one event at a time. Progress in the development of new subtraction schemes potentially will improve multiple removal by all of the prediction techniques, so there is a significant challenge in learning how to match the two steps.

Examples

Many of the issues associated with suppressing multiples in complex, deep water data have been addressed by my colleagues and me as part of the SMAART Joint Venture, a group of petroleum companies who came together in 1998 to try to improve the quality of subsalt images in the Gulf of Mexico through better multiple suppression. As part of that effort, we have created a series of realistic synthetic datasets designed to test and improve the industry's capabilities. One of those datasets, called Pluto 1.5, was designed to test improvements in our ability to remove multiples from deep water subsalt targets. Details of the model construction are given by Stoughton *et al*. (2001). The elastic 2D finite-difference seismic response was used to provide a standard test for modern demultiple methods where the results could be validated without uncertainties introduced by lack of knowledge of the structure or geophysical issues such as velocity estimation or acquisition noise. This data has been released for use by other investigators, and more information can be obtained at `www.smaartjv.com`.

The prestack seismic data was sent to a number of commercial processing firms, who applied their production multiple removal techniques. The data were then returned to SMAART to undergo a standard processing flow including prestack depth migration using the exact velocities. Our methodology is described in Bishop, *et. al*. (2001). A total of 22 implementations were tested and evaluated.

While the SRME method was generally the best, there was a large range of variation in quality. Use of SRME on data of this complexity can require careful pre-processing and parameter selection (Miley *et al*., 2001).

Figure 1 shows a window of prestack-migrated data with the strong base salt reflector dipping to the right in the upper right corner. This data has had no specific demultiple algorithm applied, although the imaging procedure will reduce the amplitude of multiples compared to prestack data.

Figure 2 shows the same window, where we have used a dataset produced without a reflecting free surface, representing the air-water interface. It has been replaced with an absorbing boundary, so that free surface multiples will not be produced. Energy propagating upward in the water column will not return downward, and hence these multiples will not be generated. The difference in data quality is remarkable, as the stratigraphy, fault planes, and artificial point reflectors are now apparent. Some internal multiple energy can be seen.

Figure 3 presents what we judged to be the best of the SRME algorithm results. Clearly, a large percentage of the free surface multiple energy has been removed, with a significant improvement in interpretability compared to figure 1. Some events are only partly removed, and our investigations of the reasons are discussed by Miley, *et al*. (2001).

Figure 4 is the best of a number of attempts to Radon filter the multiples prior to depth migration. While some energy has been removed, it is not very effective at most of the free surface multiples. The reasons include the difficulty of correctly selecting filter parameters in noisy data, and the rapidity with which the multiple generators change spatially. Radon filtering is used frequently in less complex areas, but is very difficult to use effectively when the

moveout curves of both multiples and primaries are unpredictable without ray tracing or other expensive modeling techniques.

A significant observation from these examples is that none of the currently available techniques are capable of completely removing multiples, even under essentially ideal conditions. The Pluto 1.5 data contains no out of plane energy, little random noise, has perfect acquisition geometry, and the velocity is known. Thus it seems important to consider whether there is some combination of techniques that are needed to provide the best result. Due to the rapid progress recently on individual techniques, and the cost and time required to experiment on 3D data, little information seems to be available about how best to combine techniques.

Conclusions

While great progress is being made in removing deep water multiples in complex geologic environments, no single technique appears to attack all of the elements of the problem. Higher order and internal multiples, three-dimensionality in multiple generation, and interference among events during subtraction are remaining challenges. Methods that using data driven convolution to predict surface and some internal multiples have success in moderately complex areas. Increased use of earth models estimated as part of normal imaging for both prediction and subtraction would seem a useful direction to overcome some the difficulties.

Direct filtering methods, such as Radon domain filtering or deconvolution, still have a role to play, as they are inexpensive, or can be useful in cases where other methods are insufficient. These techniques have the advantages of attacking both surface and internal multiples of all orders. However, they can be difficult to parameterize when the reflectors change rapidly and are very sensitive to aliasing.

In the end, it appears that no single method will work for all multiples. For a given combination of acquisition style, water depth, overburden, and target type, we will need to predict how to best remove multiples without exhaustive testing. From the ever-growing toolbox of methods available, certain key combinations are likely to represent the "best practice" at any time. Discovering which set will be an enduring challenge.

References

Berkhout, A. and Verschuur, D., 1997, Estimation of multiple scattering by iterative inversion, Part 1: Theoretical Considerations, **Geophysics 62,** p. 1586.

Bishop, K., Keliher, J., Paffenholz, J. Stoughton, D., Michell, S., Ergas, R., and Hadidi, M., 2001, Investigation of Vendor Demultiple Technology for Complex Subsalt Geology: submitted to SEG Ann. Int'l. Meeting.

Foster, D. and Mosher, C., 1992, Suppression of multiple reflections using the Radon transform, **Geophysics 57,** p. 386-395.

Miley, M., Paffenholz, J., and Hall, K. and Michell, S., 2001, Optimizing surface-related multiple elimination on a synthetic subsalt dataset: submitted to SEG Ann. Int'l. Meeting.

Stoughton, D., Stefani, J., and Michell, S., 2001, Pluto 1.5 2D elastic model for wavefield investigation of subsalt objectives, deep water Gulf of Mexico: EAGE Ann. Meeting Expanded Abstracts.

Weglein, A., 1999, Multiple attenuation: an overview of recent advances and the road ahead, **The Leading Edge 18**, p. 40.

Yilmaz, O., 2001, **Seismic Data Analysis: processing, inversion and interpretation of seismic data, 2nd edition**, SEG Investigations in Geophysics No. 10, Chapter 6.

Acknowledgements

I would like to thank my colleagues in the SMAART JV (from BP, BHP Petroleum, Texaco, Chevron, and (previously) Mobil) for their many discussions and ideas, and whose contributions form the major part of this paper. Also, my gratitude to the many distinguished scientists from the service companies and universities who participated in SMAART's activities. My thanks also, to the management of Chevron for permission to present this paper. The opinions expressed are my own.

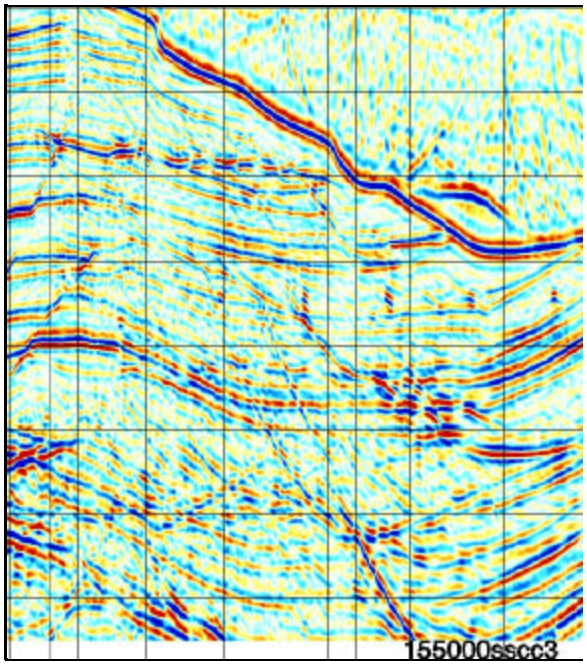

Figure 1 – Prestack migrated and stacked data from the subsalt target window without any specific multiple suppression applied.

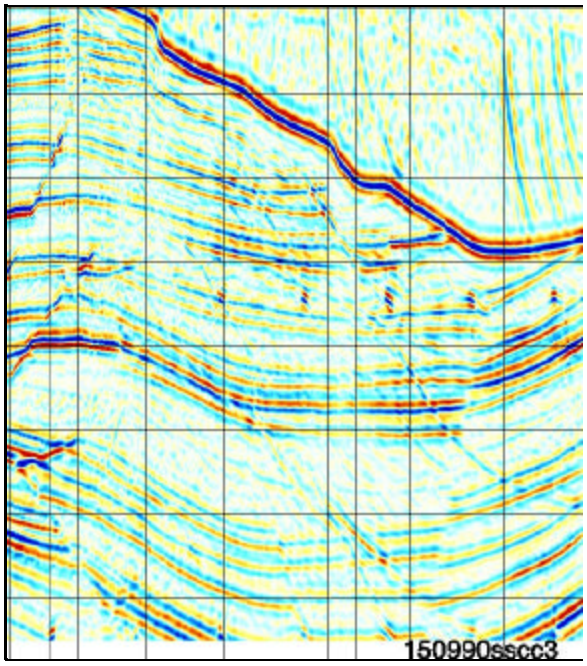

Figure 2 – Prestack migrated and stacked data with no free surface, and therefore, no free surface multiples. Internal multiples and converted energy are still present.

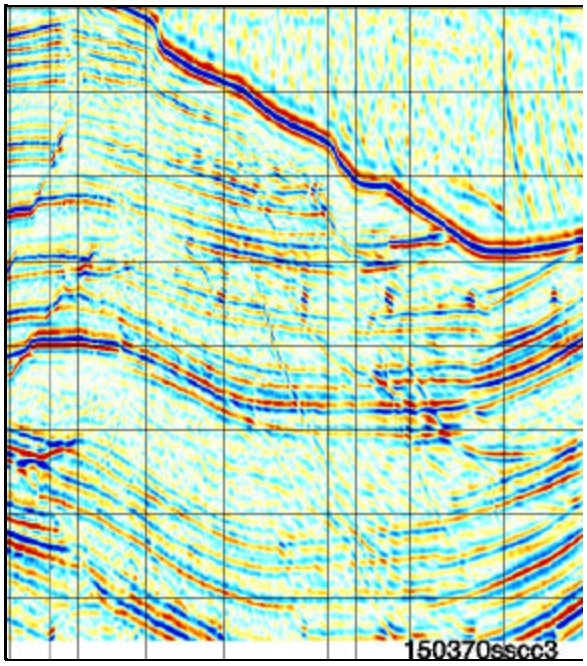

Figure 3 – Prestack migrated and stacked data with the best SRME application.

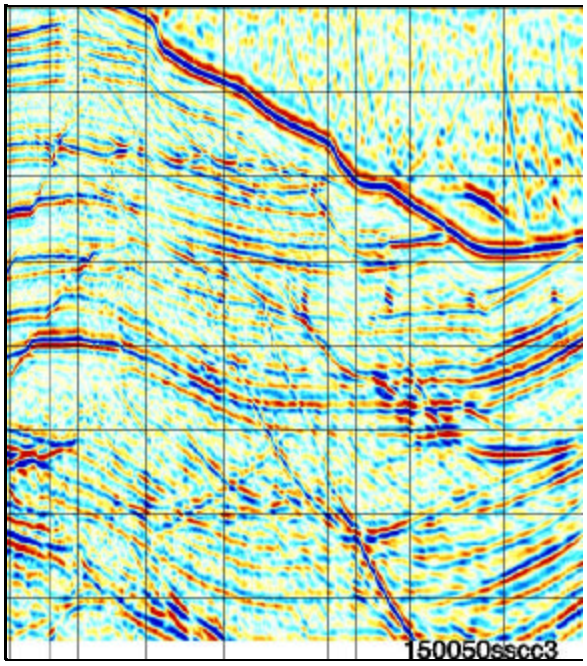

Figure 4 – Prestack migrated and stacked data with the best Radon filtering applied.

Operator Details in Demultiple by Prediction

Fábio J. C. Alves and Lourenildo W. B. Leite
UFPa - Curso de Pós–graduação em Geofísica. *fjca@ufpa.br. lwbleite@ufpa.br.*

Summary
This paper presents details of the mechanics of multiple suppression by time moving windows, for time variant operators in 1D extended to 2D. This method is based on the theory named as Wiener-Hopf-Levinson (WHLP).

Introduction
Desired solution for suppression of symmetric and asymmetric multiples depends on the type and amount of a priori information available.
The WHL equation in parametric form for prediction is initially organized for single-channel (1D) time-invariant as:

$$\sum_{k=1}^{N} h(k)[\phi_{ss}(k-l)+\sigma_n^2\,\delta(k-l)]=\phi_{gg}(l+T)\,.$$

The input, $g(k)$, has a message, $m(k)$, under convolution, and a noise component, $n(k)$, expressed as: $g(k)=s(k)*\varepsilon(k)+n(k)$, where $\varepsilon(k)$ is the white reflectivity series, and $s(k)$ is the primary source-pulse. The desired output is: $d(k)=g(k+T)$, where $T\neq T(x;\bar{v})$ is the prediction distance, and $\phi_{gg}(k)$ is the autocorrelation. For the multichannel (2D) time-variant, the solution is organized as:

$$\sum_{k=1}^{N} h_2(k,x)\phi_{gg}[l-k;x]=W(l_2-l_1;x)\phi_{gg}[l+T(x;\bar{v})]\,,$$

where the prediction distance has the expression $T(x;\bar{v})=\left[T_0^2+(x/\bar{v})^2\right]^{1/2}$, with $\bar{v}^2=\sum_{i=1}^{N+M} v_i^2 t_i \Big/ \sum_{i=1}^{N+M} t_i$, the root-mean square velocity, and it implies on the staking velocity for this case. (Leite & Alves, 2001; Taner & Koehler,1969). The signal/noise ratio (S/R) is here defined by the statistical variance in the form:

$$\left(\frac{S}{R}\right)^2=\frac{\frac{1}{P}\sum_{i=1}^{P}[g_i-\bar{g}]^2}{\frac{1}{P}\sum_{i=1}^{P}[n_i-\bar{n}]^2}\,,\quad \bar{n}=\frac{1}{P}\sum_{i=1}^{P} n_i\,,\quad \bar{g}=\frac{1}{P}\sum_{i=1}^{P} g_i\,.$$

Where g_i is the signal without noise, P is the number of samples, $\bar{g}$ and $\bar{n}$ are averages.

Examples and Conclusions
The examples are constructed in 2 convenient models. Model-1 is formed by 1 layer over a half-space (Figure 1 to 4). Model-2 is formed by 202 layers over a half-space (Figure 5 to 9). Layer thickness vary between 1 and 20 meters. Transmissivity effects are included as based on ray theory. Noise was built in for 5 different $(S/R)^2$ levels (0.5, 3, 5, 10 e 20).
The deconvolved time section make the information from interfaces below the sill layers more evident.
The form of the operator becomes more complex with the increase of the quantity of events within the pass-window. The WHLP operator removes the multiple one by one, and also gives good results in the presence of contamination by additive noise.

References
Leite, L. W. B. & Alves, F. J. C. (2001). *Basis for moving pass-windows for multiple suppression.* Submitted to VII CISBGF, Salvador, Bahia.
Taner, M. T. and Koehler, F. (1969). Velocity spectra-digital computer derivation and application of velocity functions. Geophysics, 34, 859-881.

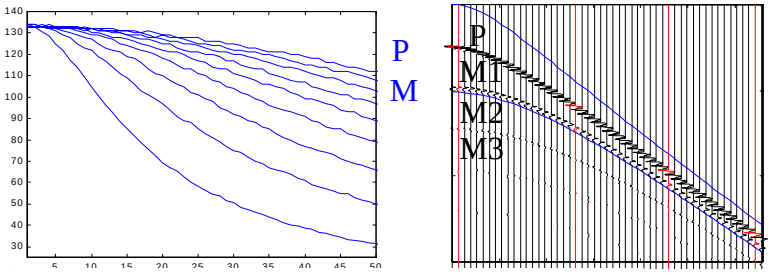

Figure 1. (left) Time-distance curves for the time difference between primary and first multiple, and time difference between successive multiples. (Right) Seismic section, where P inform the primary, and M1, M2 and M3 the multiples. The blue lines are the upper and lower limits of the pass-window. The red lines are the selected trace.

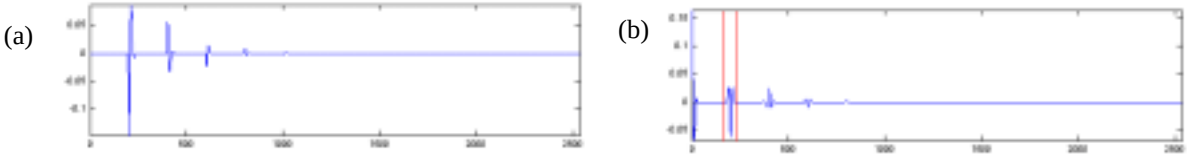

Figure 2. (a) Selective trace nearer zero-offset taken from Figure 1 (right). (b) The autocorrelation of trace in (a), and the red lines are the limits of the pass-window. The selected event corresponds to the multiple to be suppressed.

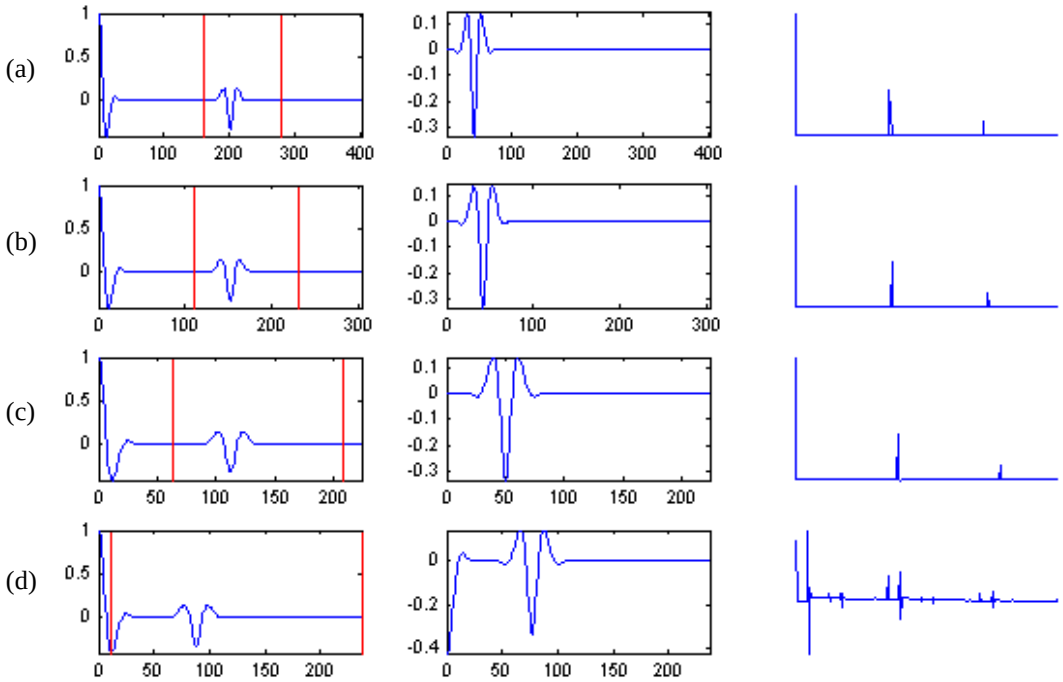

Figure 3. (Left) Autocorrelation of windowed traces of Figure 4-left. The red vertical lines are the borders of the pass-windows. (Center) Crosscorrelations obtained from windowed parts of the autocorrelations. (Right) Complete prediction-error operators. The sequence corresponds to the one of Figure 4.

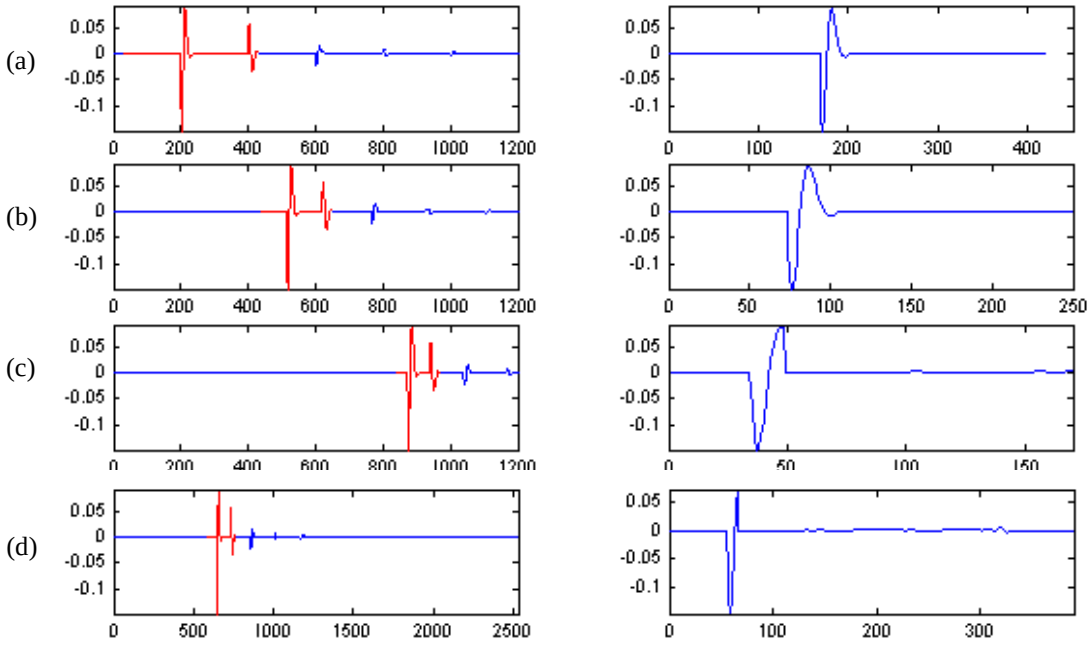

Figure 4. (Left) Selected traces 1, 20, 35 and 50 of time section in Figure 1. In red are the extracted information to be deconvolved that contains the primary and its first multiple. (Right) Output of deconvolution of windowed information, where we observe the multiple suppression inside the moving window. The number of points in the filter input is the same as of the output.

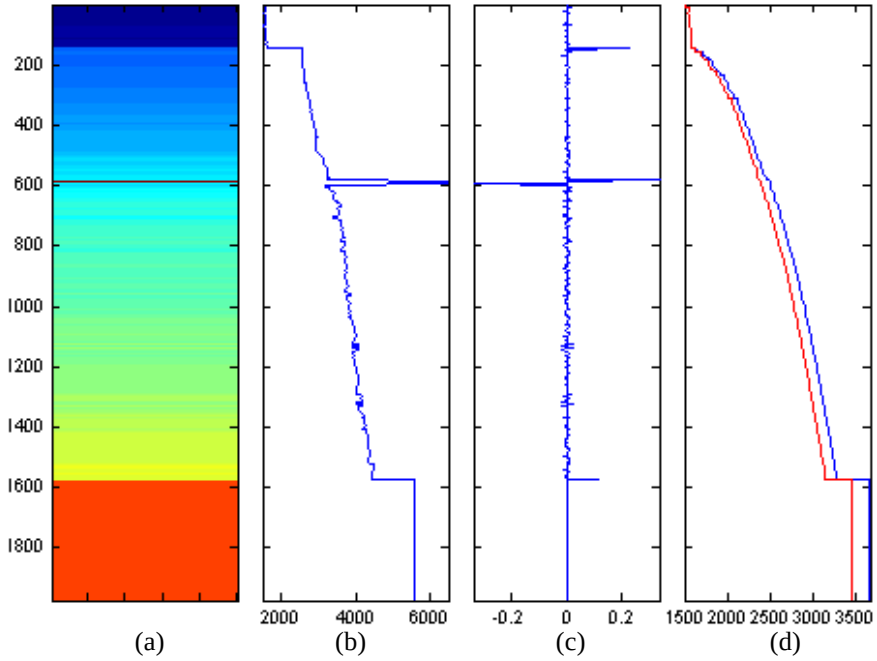

Figure 5. Model 2 (202 layers) for operator analyses. Sedimentary basin. Layer thickness vary from 1 to 20 meters.
(a) Geological Section.
(b) Velocity Log.
(c) Distribution of Reflection Coefficients.
(d) RMS and Average Velocities.
The model should present undesirable effects from diabase sills that haze the information from lower interfaces of low impedance.

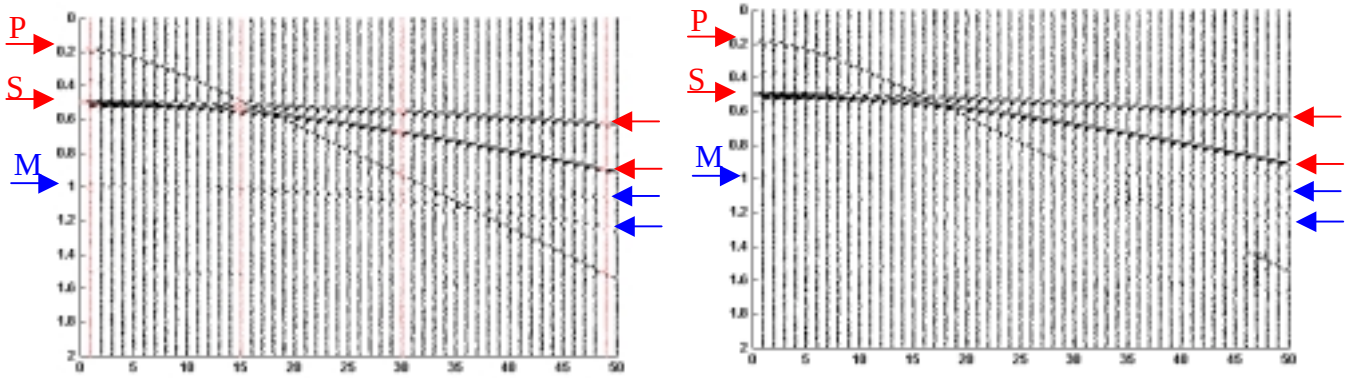

Figure 6. (Left) Input section common source with $(S/R)^2 = 10$ (model of Figure 5). The red traces are detailed in Figures 7 to 9. (Right) Output of filter. Primaries are P (low velocity) and S (diabase sill), and multiple is M (diabase sill). It is clear the suppression of the selected multiple.

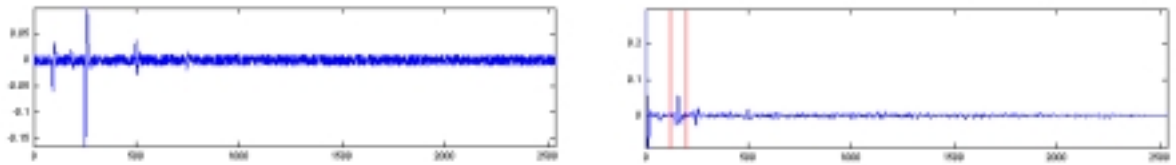

Figure 7. (Left) Selected trace nearer zero-offset from Figure 6-left. (Right) Autocorrelation of trace in left, and red vertical lines show the borders of the pass-window.

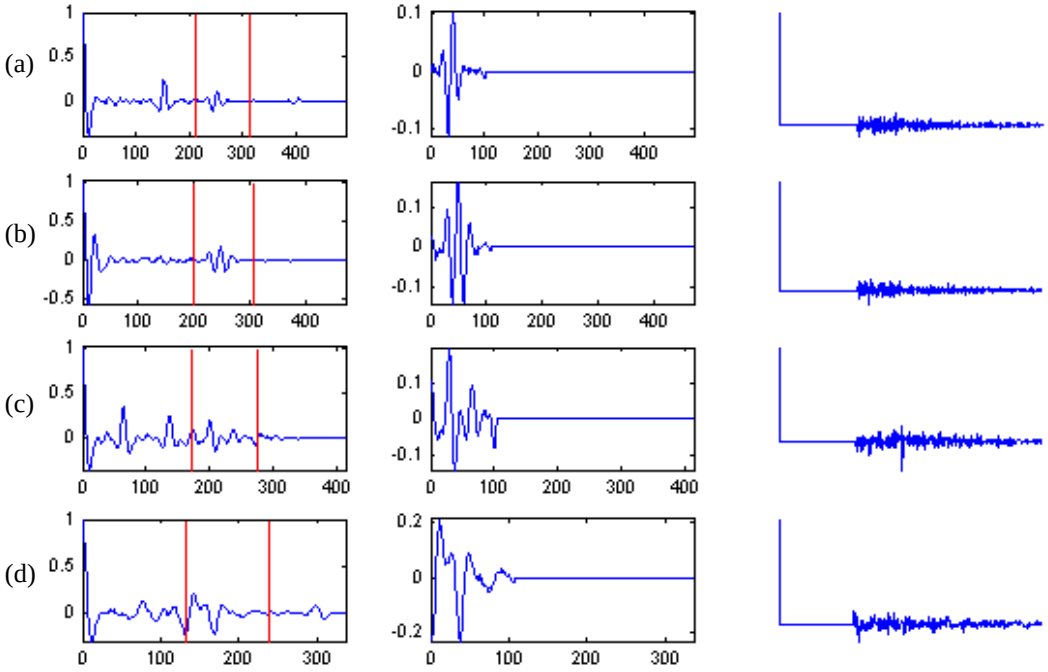

Figure 8. (Left) Autocorrelation of windowed traces of Figure 9-left. The red vertical lines are the borders of the pass-windows. (Center) Crosscorrelations obtained from windowed parts of the autocorrelations. (Right) Complete prediction-error operators. The sequence corresponds to the one of Figure 9.

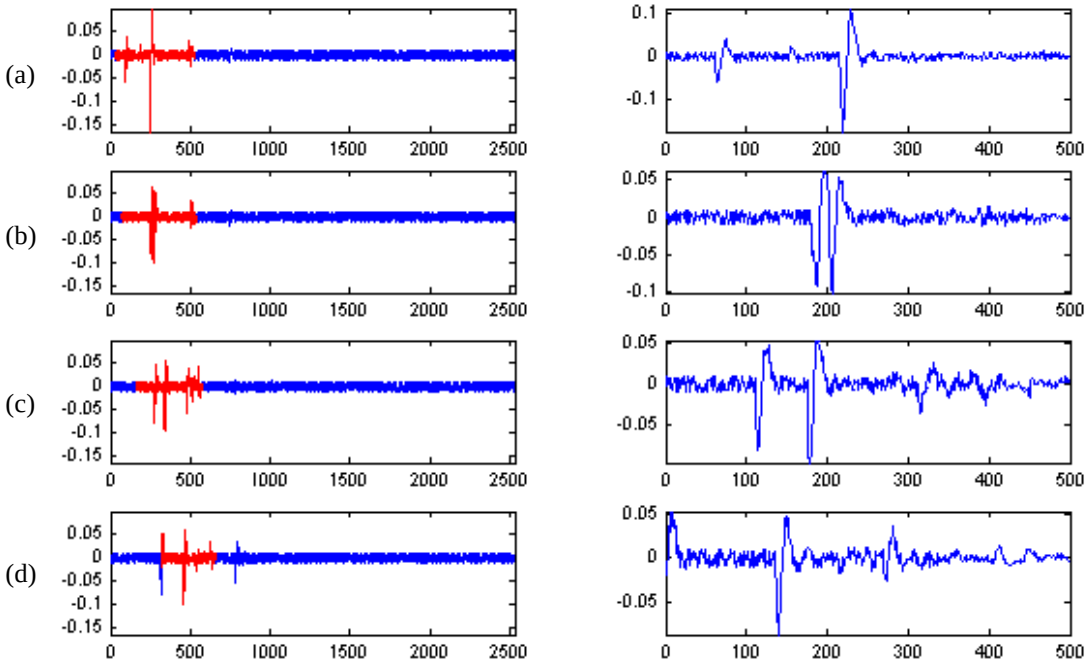

Figure 9. (Left) Selected traces 1, 15, 30 and 50 of time section in Figure 6. In red are the extracted information to be deconvolved that contains the primary and its first multiple. (Right) Output of deconvolution windowed information, where we observe the multiple suppression inside of the moving window. The number of points in the filter input is the same as of the output.

Results of a Proposed WHL Operator for Multiple Suppression

Fábio J. C. Alves and Lourenildo W. B. Leite
UFPa - Curso de Pós–graduação em Geofísica. *fjca@ufpa.br. lwbleite@ufpa.br*

Abstract
We submit examples of 1D and 2D synthetic seismic sections of a WHLP operator designed on the basis of a deterministic moving window applied to the time section, and on a time moving window applied to the autocorrelation function to select events to be suppressed. Non-zero off-set results are systematically compared to zero off-set for performance.

Introduction
This paper presents results of a strategy for the Wiener-Hopf-Levinson prediction (WHLP) for the suppression of symmetric and asymmetric multiples. The synthetic traces are generated by thin layer Goupillaud´s solution, and by ray theory under plane waves. (Silvia & Robinson, 1979).
The period of the multiples is at least twice the length of the effective source-pulse. The interpretation of the presence of multiples is made on the seismic traces, and on their autocorrelation functions.
We generate traces, $g(k)$, based on the convolutional model, with dependency on the horizontal ray parameter, *p*, expressed as: $g(k) = m(k) + n(k) = s(k) * \varepsilon(k) + n(k)$. Here $s(k)$ represents the effective source-pulse, $\varepsilon(k)$ the reflectivity function, $m(k)$ the signal-message, and $n(k)$ the additive signal-noise not accounted for in $\varepsilon(n)$, or in $s(k)$. The effective source-pulse, $s(k)$, can be described by several components along its trajectory. These effects are the original source-pulse (source signature), the multiples not accounted for in the reflectivity, the inelastic attenuation, the recording instrument, the spherical divergence, and the effects of porosity could also be contemplated.
Our eternal temptative to describe noise involves a local random and a local coherent part, and by a component related to the seismic source with a random and a coherent part. They may be submitted to a convolution with filtering functions. For our control in designing pulses, the most effective filter component is the instrument (sensor).

The modified WHLP method
A convenient model consider time sections as stationary. The filter , $h(t)$, is an unknown time-invariant operator that is constrained to satisfy a desired output, $d(t)$, through the WHLP 1D operator, now expressed as:

$$\sum_{k=1}^{N} h_1(k)\phi_{gg}(l-k) = W(l_2 - l_1)\phi_{gg}(l+T).$$

The solution defines the coefficients $h(k)$, which depend on the operation that is intended for, and organized by a priori conditions. $\phi_{gg}(.)$ represents the theoretical stochastic autocorrelation of the input, and $W(l_2 - l_1)$ is the rectangular pass-window that limits the information that lie in between l_2 and l_1.
For the 2D case, the modified solution is:

$$\sum_{k=1}^{N} h_2(k,x)\phi_{gg}[l-k;x] = W(l_2 - l_1;x)\phi_{gg}[l+T(x)],$$

where the prediction distance has the expression $T(x) = \left[T_0^2 + (x/\bar{v})^2\right]^{1/2}$, with $\bar{v}$ the root-mean square velocity. (Leite & Alves, 2001; Taner & Koehler,1969).

Numerical results
The synthetic model is formed by 250 layers over a half-space, and it simulates the estratigraphy of the Amazon sedimentary basin. Layer thickness vary from 1 to 20 meters. (Figure 1)
The analyses of the contents of the autocorrelation of the seismic trace is illustrated in Figure 2, where it is also shown the pass-window used to select the event to be treated, and the correspondent operator.
We organized and selected 3 situations to illustrate the performance of the modified WHLP operators for the suppression of symmetric and asymmetric multiples, and in particular the undesirable effects from diabase sills that haze the information from lower interfaces of low impedance. The first situation has the sill at the middle part (Figure 3); the second has one sill in the middle and one in the bottom (Figure 4); and the third has one at the upper part, one in the middle, and one at the bottom (Figure 5). Figures 6, 7 and 8 are the multi-channel correspondent to the single-channels of Figures 3, 4 and 5 (zero off-set).
For presentation, we introduced in the same time sections white gaussian noise added with different signal/noise ratios. The results are that the modified WHLP operator shows good performance in the suppression of multiples under the moving windows. When the density of events becomes large the deconvolution operator presents many oscillations, and the performance decreases in resolution. The attenuation of the operator oscillations by a convenient exponential window placed around its maximum makes it possible to improve the results.

Conclusions

The proposed WHLP operators are efficient in the suppression of coherent noise of zero-offset data. The performance is specially good for the suppression of symmetric multiples and peg-legs.

The deconvolved traces by prediction make evident the information from interfaces underneath the sill layers making their interpretation easier.

The form of the operator becomes more complex as a function of the density of events on the trace.

The results of multiple suppression is also directly related to the pass-window on the event on the autocorrelation function. If the window does not entirely contain the event to be suppressed, the filter output is very much different from desired results.

The high density of events on the seismic trace makes the operation for selecting multiples difficult.

Acknowledgments

The authors are to grateful to the project sponsors FINEP and PRH-ANP/MME/MCT-UFPa.

Bibliography

Leite, L. W. B. & Alves, F. J. C. (2001). *Basis for moving pass-windows for multiple suppression.* Submitted to VII CISBGF, Salvador, Bahia.

Silvia, M. T. & Robinson, E. A. (1979). *Deconvolution of Geophysical Time Series in the Exploration for Oil and Natural Gas.* Elsevier Scientific Publishing Co. Amsterdam.

Taner, M. T. & Koehler, F. (1969). *Velocity spectra-digital computer derivation and application of velocity functions.* Geophysics, 34, 859-881.

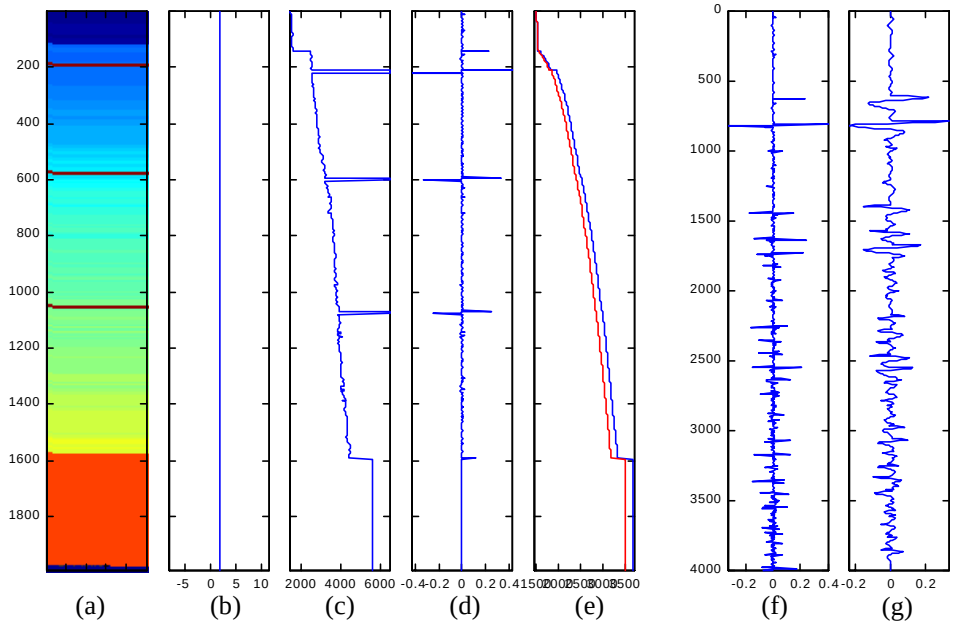

Figure 1. The model of 250 layers for operator analyses. (a) Geological Section. (b) Density Log. (c) Velocity Log. (d) Distribution of Reflection Coefficients. (e) Log of RMS and Average Velocities. (f) Reflectivity Function. (g) Seismic trace obtained by convolution of the medium impulse response (calculated by the Goupillaud solution) with an effective source pulse (Berlage function).

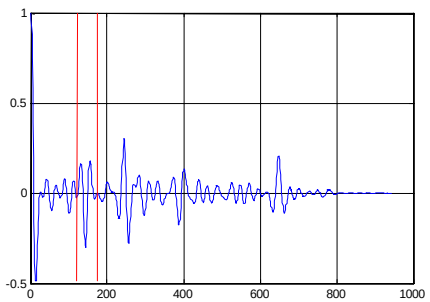

Figure 2. Example of the unilateral autocorrelation function of the first seismic trace of Figure 3, showing the limits of the rectangular pass-window (red lines).

Results of the Proposed WHL Operator for Suppression of Multiples

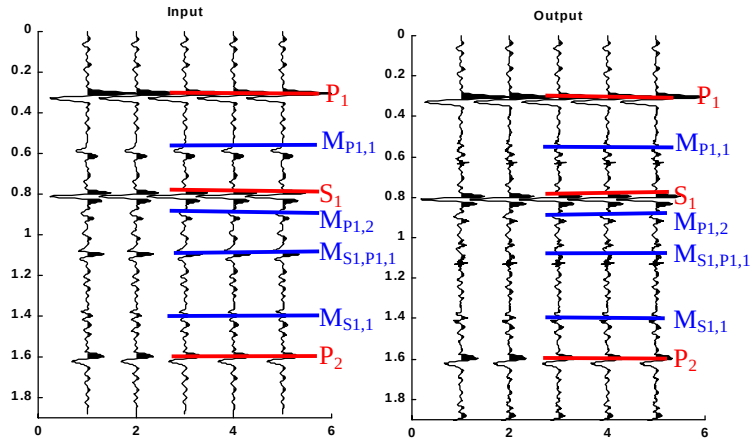

Figure 3. The model corresponds to the one of Figure 6. Left: input. The red lines indicate the primaries, and the blue lines the multiples. P_1 is the event from the interface that separates the low from high velocity layers. P_2 is the event from the basement. S_1 is the event from the middle sill. $M_{P1,1}$, $M_{P1,2}$ and $M_{S1,1}$ are multiples. $M_{S1,P1,1}$ and $M_{S1,1}$ are the peg-legs. Right: output. The performance on suppression of multiples and peg-legs is clear and good. Zero off-set

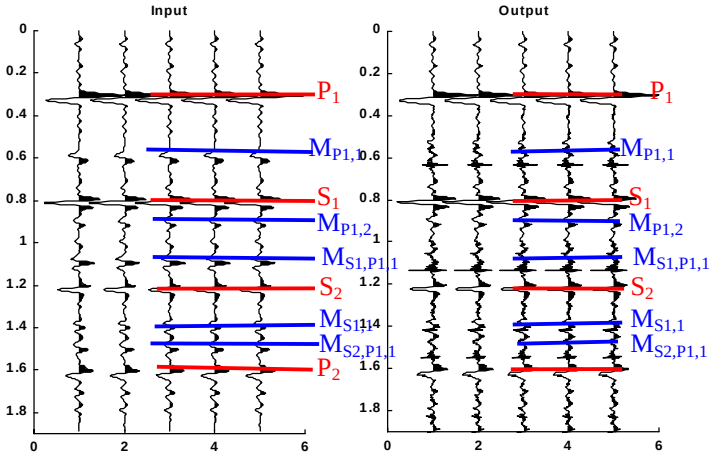

Figure 4. The model corresponds to the one of Figure 7. Left: input. The red lines indicate the primaries, and the blue lines the multiples. P_1 is event from the interface that separates the low from high velocity layers. P_2 is the event from the basement. S_1 and S_2 are events from the sills. $M_{P1,1}$, $M_{P1,2}$ and $M_{S1,1}$ are multiples. $M_{S1,P1,1}$, $M_{S1,1}$ and $M_{S2,P1,1}$ are peg-legs. Right: output. The performance on suppression of multiples and peg-legs is good. Zero Off-set

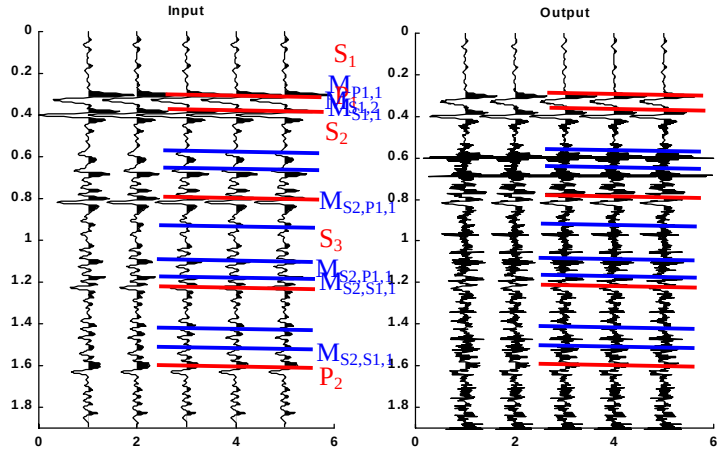

Figure 5. The model corresponds to the one of Figure 8. Left: input. P_1 is the event from the interface that separates the low from high velocity layers. P_2 is the event from the basement. S_1 and S_2 are events from the sills. $M_{P1,1}$, $M_{S1,2}$, $M_{S1,2}$ and $M_{S2,S1,1}$ are multiples. $M_{S2,P1,1}$, $M_{S2,S1,1}$ and $M_{S2,P1,1}$ are peg-legs. The performance is complicated by the density of events. Zero off-set

Results of the Proposed WHL Operator for Suppression of Multiples

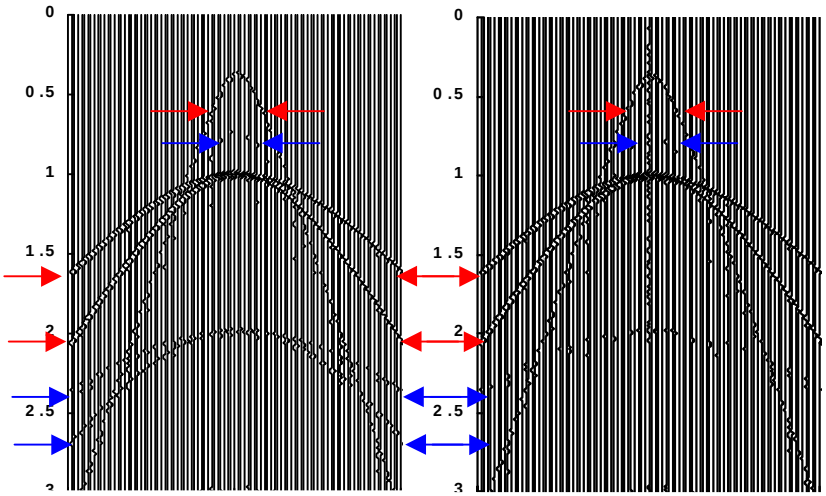

Figure 6. The model corresponds to the one of Figure 3. Left: input. The time section shows the primaries (red arrow) and multiples (blue arrow). Right: output. The deconvolved time section shows good performance of the modified prediction operator.

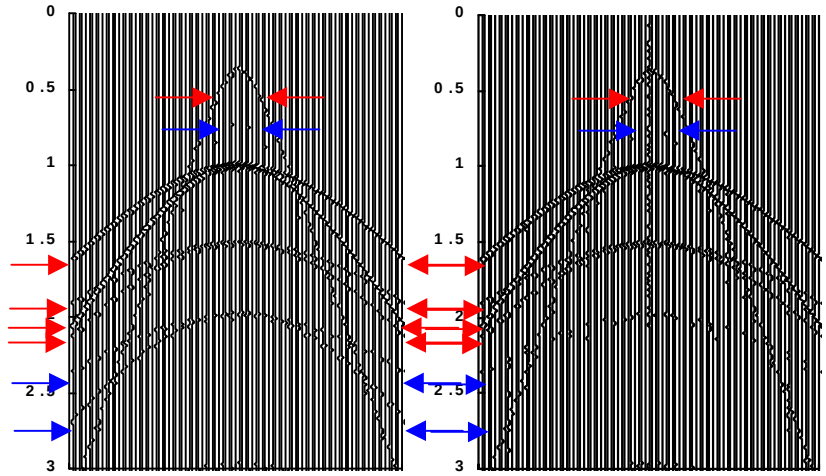

Figure 7. The model corresponds to the one of Figure 4. Left: input. The time section shows the primaries (red arrow) and multiples (blue arrow). Right: output. The deconvolved time section shows good performance of the modified prediction operator.

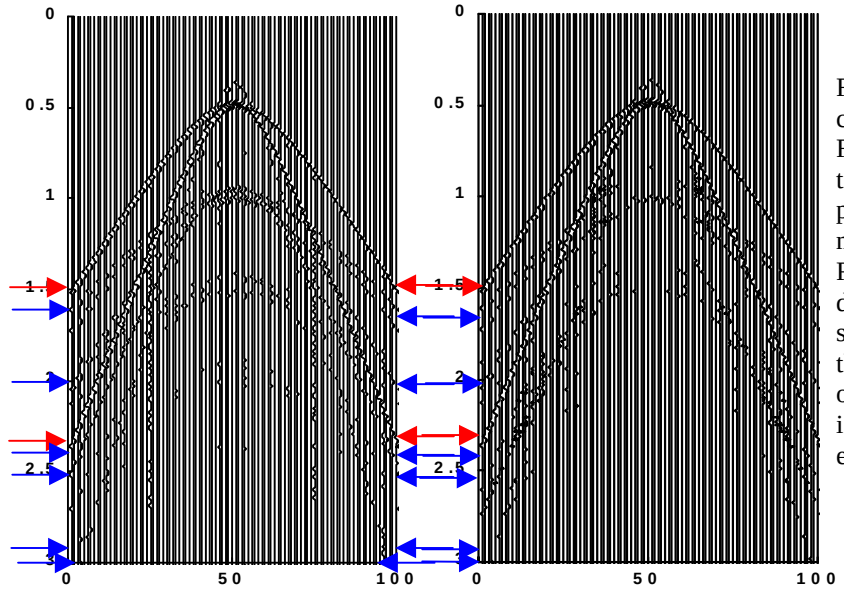

Figure 8. The model corresponds to the one of Figure 5. Left: input. The time section shows the primaries (red arrow) and multiples (blue arrow). Right: output. The deconvolved time section shows good performance of the modified prediction operator. The performance is affected by the density of events.

Results of Suppression of Multiples the KBC Method

Marcus P. C. Rocha and Lourenildo W. B.. Leite
UFPa - Curso de Pós–graduação em Geofísica. mrocha@ufpa.br. lwbleite@ufpa.br.

Abstract
New results are presented based on the Kalman-Bucy-Crump (KBC) theory, here adapted for prediction (KBCP), and applied to the suppression of symmetrical and of nonsymmetrical multiples. These multiples are related to upper low velocity layers (weathering zone) and to deeper high velocity layers (diabase sills). The method is to be compared to the Wiener-Hopf-Levenberg (WHL) classical solution for prediction in reflection seismics. The cases studied are for (1D) zero off-set, and for (2D) time sections.

Introduction
The problem under study is the multiple suppression related to an upper low velocity layer (weathering zone), and peg-legs related to the same low velocity layer and to a deeper high velocity layer (diabase sills). This situation is considered as encountered in the Amazon sedimentary basin to where our goals are aimed at. The amount of existing seismic data is rather large, and as they deserve more attention as processing and interpretation problems are submitted, and plausible solutions analyzed on synthetic models.
We look at extending the application to true amplitude studies where the suppression of multiples from the time sections represent an important task. This challenge is mathematically related to the general representation of inverse problems.

Forward Model
We construct the reflection trace by the convolution model. The physics of propagation is governed by the equation of particle motion in 1-D acoustic form: $\rho(x)\partial_t^2 g(x,t)=\partial_x[E(x)\partial_x g(x,t)]$, where $\rho(x)$ is the density, and $E(x)$ is an elastic constant. The phenomenon is of a incident vertical plane wave on a medium formed by horizontal, homogeneous and isotropic layers. The boundary conditions of displacement (or pressure) and of continuity of stress result in defining the reflection, r_k, and the transmission, t_k, coefficients for the interface k between the layers k and k+1 in terms of impedance: $r_k=(I_k-I_{k+1})/(I_k+I_{k+1})$, $t_k=2I_k/(I_k+I_{k+1})$. The propagation is now transformed to a physics of interfaces, and the events making the seismic trace are considered as primary and secondary reflections (multiples). The relation between the descendent, $D(z)$, and the ascendent, $U(z)$, waves, and between the top, $k=0$, and the bottom, $k=K+1$, is expressed by the matricial propagator:

$$\begin{bmatrix} D_{K+1}(z) \\ U_{K+1}(z) \end{bmatrix} = \frac{z^{-K/2}}{(1-r_K)(1-r_{k-1})..(1-r_2)(1-r_1)} N_K..N_1 N_0 \begin{bmatrix} D_0(z) \\ U_0(Z) \end{bmatrix}$$

The reflection transfer function for a system of K layers is given by:

$$R(z) = R_K(z) = \frac{U_0(z)}{D_0(z)} = \frac{r_0 P_k(z) - Q_k(z)}{P_k(z) - r_0 Q_k(z)}.$$

The denominator $P_k(z) - r_0 Q_k(z)$ has the property of being of minimum-phase. The numerator $r_0 P_k(z) - Q_k(z)$ is not necessarily of minimum-phase, what makes $R(z)$ be or not to be of minimum-phase. The polynomial division is ilimited, but numerically made to correspond to the number of layers K.
In special conditions for analysis we can admit $\varepsilon(n) \approx r(n)$, or yet that $\varepsilon(n) = r(n)$. The total response in the examples show that the secondary field can gradually have the same importance as that of the primary field along the trace.
The source time history is represented by the Berlage function: $f(t) = Au(t)t^n e^{-\gamma t}\cos(2\pi f_0 t + \phi_0)$.
Control parameters are as: $A=1$, $n=1$, $f_0 = 32{,}5$ Hz, $\phi_0 = 30$ rd, and $u(t)$ is the step function.

Governing Equations
This problem, with respect to the non-stationarity and to the data window, does not satisfy the conditions required by the convolution integral. For this reason, it is rewritten in the form of a moving average according to the commonly referred to as the Wiener-Kolmolgorov integral equation, and the generalization is expressed by the matrix integral equation:

$$\underline{\underline{\phi}}_{dg}(t,\sigma) = \int_{t_0}^{t} \underline{\underline{h}}(t,\tau)\underline{\underline{\phi}}_{gg}(\tau,\sigma)d\tau,$$

and $\underline{\underline{h}}(t,\tau)$ is the corresponding desired optimum time-variant operator. The real output is:

$$\underline{\hat{g}}(t) = \int_{t_0}^{t} \underline{\underline{h}}(t,\tau)\underline{g}(\tau)d\tau,$$

The criterion used is the minimization of the residue variance: $I(h) = E[\{\underline{\hat{g}}(t) - \underline{d}(t)\}^2]$.
The formulation has for basis expressing the response of any linear system by an ordinary differential equation of order $N-1$:

$$\sum_{n=0}^{N-1} a_n(t)\frac{d^n y(t)}{dt^n} = w(t).$$

The transformation to the state variable $x_n(t)$ and $\dot{x}_n(t)$ is by substituting the higher derivatives of $y(t)$. The resulting dynamic state equations in the general (continuous, time-variant) compact form are:

$$\underline{\dot{x}}(t) = \underline{\underline{F}}(t)\underline{x}(t) + \underline{\underline{G}}(t)\underline{w}(t), \quad \text{(system)},$$

$$\underline{z}(t) = \underline{y}(t) + \underline{v}(t) = \underline{\underline{H}}(t)\underline{x}(t) + \underline{v}(t), \quad \text{(output)}$$

$\underline{\underline{F}}(t)$, $\underline{\underline{G}}(t)$ and $\underline{\underline{H}}(t)$ are matrices with variable elements in *t*; $\underline{w}(t)$ is the forcing function that generates the state; $\underline{z}(t)$ is the selected form for the output given by the structure of the matrix $\underline{\underline{H}}(t)$; $\underline{v}(t)$ is the additive noise present.

The continuous form solution is given by a system of three coupled equations:

$$\frac{d\underline{\hat{x}}(t)}{dt} = [\underline{\underline{F}}(t) - \underline{\underline{K}}(t)\underline{\underline{H}}(t)]\underline{\hat{x}}(t) + \underline{\underline{K}}(t)\underline{z}(t),$$

$$\underline{\underline{K}}(t) = \underline{\underline{P}}(t)\underline{\underline{H}}(t)\underline{\underline{V}}^{-1}(t),$$

$$\dot{\underline{\underline{P}}}(t) = \underline{\underline{F}}(t)\underline{\underline{P}}(t) + \underline{\underline{P}}(t)\underline{\underline{F}}^{T} - \underline{\underline{K}}(t)\underline{\underline{H}}^{T}(t)\underline{\underline{P}}(t) + \\ + \underline{\underline{G}}(t)\underline{\underline{Q}}(t)\underline{\underline{G}}^{T}(t).$$

Method

The numerical algorithm is based on a discretized process according to $x_n(t) = x_n(k\Delta t)$, where $k\Delta t \le t \le (k+1)\Delta t$, and from Euler's rule:

$$\frac{\underline{x}(k+1) - \underline{x}(k)}{\Delta t} = \underline{\underline{F}}(t)\underline{x}(t) + \underline{\underline{G}}(t)\underline{w}(t),$$

to give

$$\underline{x}_{k+1} = \underline{\underline{\Phi}}_k \underline{x}_k + \underline{w}_k, \quad \text{(system)}$$

$$\underline{z}_{k+1} = \underline{\underline{H}}_{k+1}\underline{x}_{k+1} + \underline{v}_{k+1} \quad \text{(output)}.$$

We start identifying the variable with the non-stationary model and rewrite the system-output pair. First, the time variant pulse is contained in the matrix: $H_{ji} = s_j(i)$. Second, the selection of the state vector is nonunique, and it is defined as: $\underline{x}(k) = [g(k) \quad g(k-1) \quad \cdots \quad g(k-L+1)]$. The dynamic equation to establish the recursive process of generation of the state vector is completed by the following model:

$$g(k) = \sum_{i=1}^{L} b_i(k-1)g(k-1) + u(k-1), \quad \text{(system)},$$

where $u(k)$ is theoretically considered as a white stochastic process. The 2D functions $b_i(k)$ are defined by a chosen model and experimentation; in the present case it is a smooth decreasing function. The transition state equation is

$$\underline{x}(k) = \underline{\underline{\Phi}}(k, k-1)\underline{x}(k-1) + \underline{s}u(k-1), \quad \text{(system)}.$$

A window of gate given by the primary and its multiple is established for each operation, where the convolution length is limited to the pulse length.. Other details of the theoretical basis for this method are presented in Leite & Rocha (2001).

Results

We constructed 1 basic model and 3 cases to show the performance of the KBC operator for multiple suppression. The basic model is formed by 100 layers over a half-space. In the first case a sill layer is placed in the upper part of the model (Figures 1 and 2); in the second, the sill layer is placed in the middle (Figure 3); and in the third the sill layer is placed in the bottom (Figure 4). The layer thicknesses vary from 1 to 20 meters. This model serves to simulate the estratigraphy of the Amazon sedimentary basin.

Conclusions

Figures 2b, 3b and 4b shows the results of the KBC, where we observe the good performance of (KBC) operator in suppressing the surface related symmetric multiples.

The analysis of the outputs indicate clearly that the undesirable effects from sills and upper layers of low velocities are diminished, and information from lowers target layers (low acoustic impedance) are better visualized.

The same strategy can be applied to other multiples (internal, asymmetric), as long as a deterministic law is established.

Acknowledgments

The authors are grateful to project sponsors FINEP/CTPETRO and PRH-ANP/MME/MCT-UFPa, Brazil.

Bibliography

Crump, N. (1974). *A Kalman filter approach to the deconvolution of seismic signals.* Geophysics, v. 39, n. 1, p. 1-13.

Leite, L.W. B. & Rocha, M. P. C. *Basis for Non-stationary Suppression of Multiples by KBC.* Submitted to VII CISBGf. Salvador - Bahia

Mendel, J.M. (1983). *Optimal Seismic Deconvolution. An Estimation-Based Approach.* Academic press. New York, USA.

Silvia, M.T. & Robinson, E.A. (1979). *Deconvolution of Geophysical Time Series in the Exploration for Oil and Natural Gas.* Elsevier Scientific Publishing Co. Amsterdam, Netherlands.

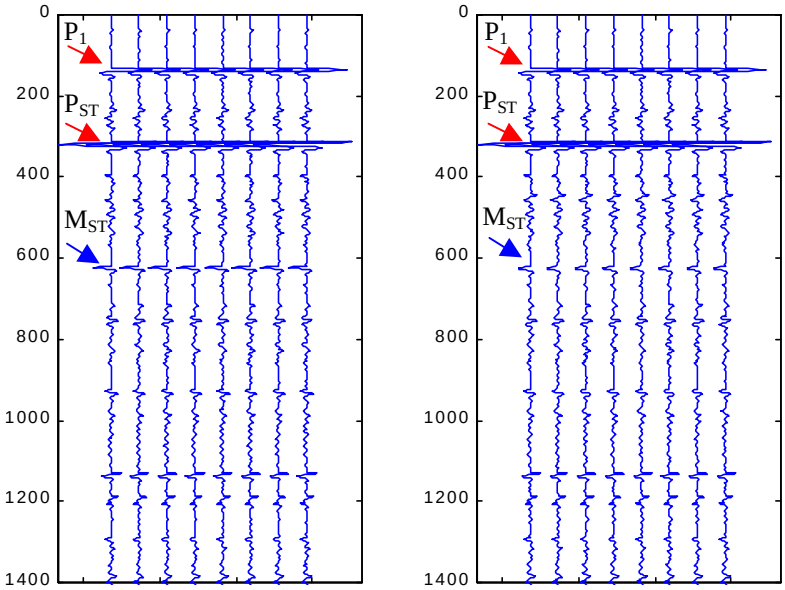

Figure 1. Zero offset time section (1D) corresponding to Figure 2. Model of 100 layers over a half-space, with a sill layer placed at the upper part (P_{ST}) of the sedimentary package. Red arrows are primaries (P), and blue arrows are multiples (M).

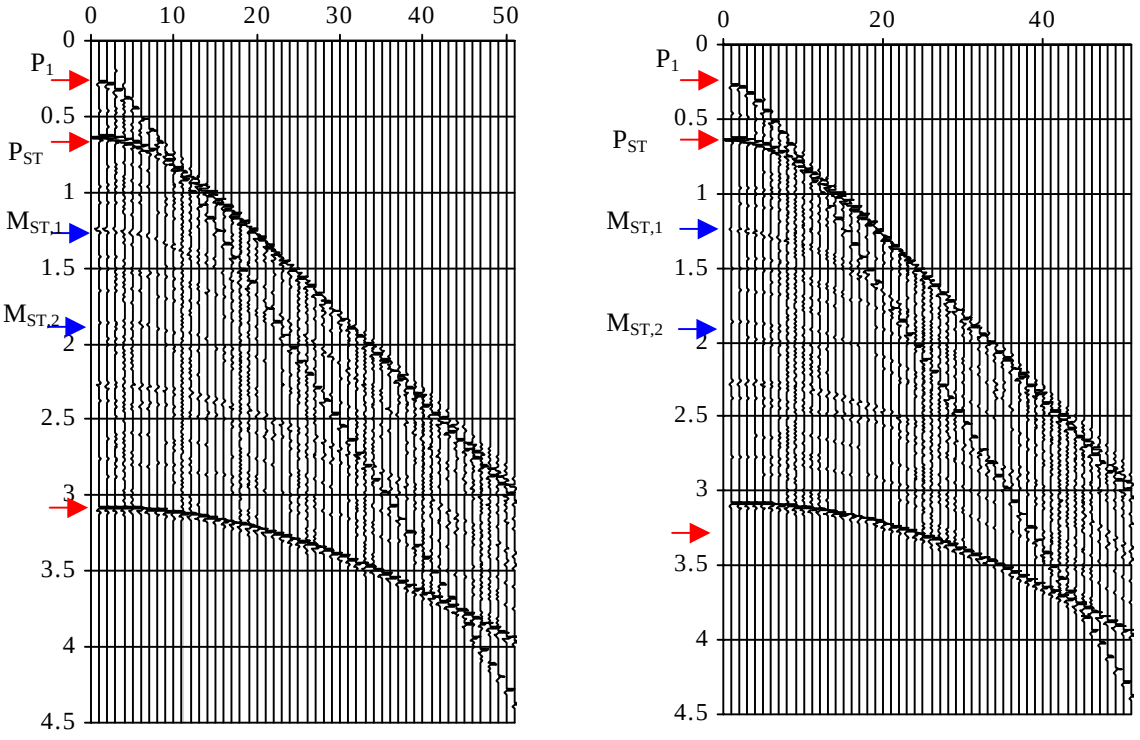

Figure 2. 2D time section corresponding to Figure 1. (a) Model of 100 layers over a half-space, with a sill layer placed at the upper part (P_{ST}) of the sedimentary package. Red arrows are primaries (P), and blue arrows are multiples (M). (b) Result of the prediction deconvolution where the surface related multiples are suppressed.

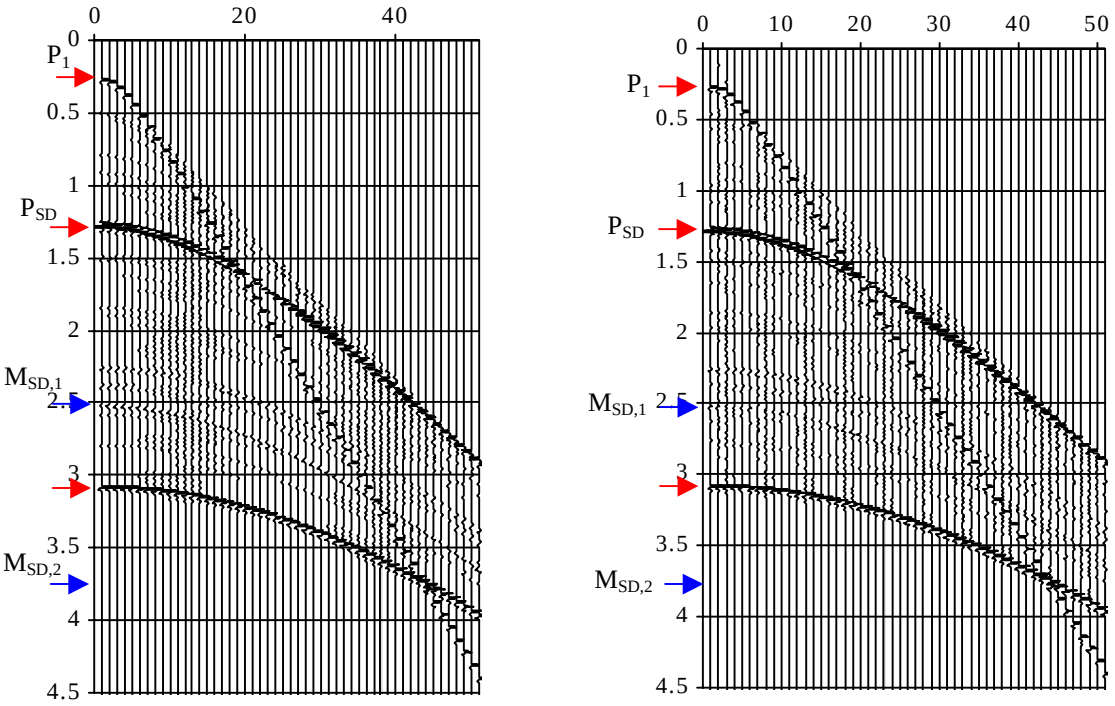

Figure 3. 2D time section. (a) Model of 100 layers over a half-space with a sill layer placed at the middle-part (P_{SD}) of the sedimentary package. Red arrows are primaries (P), and blue arrows are multiples (M). (b) Result of the prediction deconvolution where the surface related multiples are suppressed.

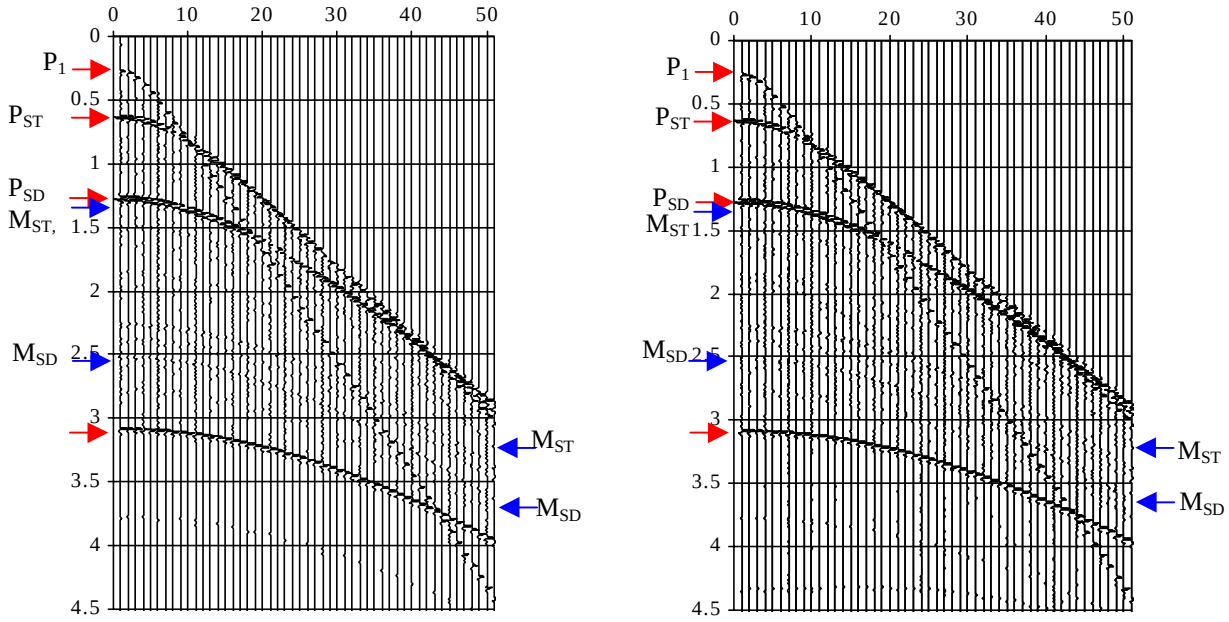

Figure 4. 2D time section. (a) Model of 100 layers over a half-space with 2 sill layers placed at the upper (P_{ST}) and at the middle (P_{SD}) parts of the sedimentary package. The red arrows are primaries (P), and the blue arrows are multiples (M). (b) Result of the prediction deconvolution where the surface related multiples are suppressed. The operation takes care of one multiple at a time.

The inverse-scattering sub-series for the removal of free-surface and internal multiples: Status, open issues and plans

A. B. Weglein (University of Houston, aweglein@uh.edu)

Introduction

The industry trend to deepwater has raised the bar on seismic effectiveness due to a confluence of higher cost and technical challenges. Imaging beneath complex overburdens, e.g., salt, basalt, or karsted sediments, are high economic priority for hydrocarbon exploration and production and represent technical challenges without an immediately available effective response.

A prerequisite for the imaging of primaries is the removal of multiples. Traditional multiple elimination techniques typically assume a 1-D earth, or periodicity of multiples, or move-out differences, or they require: velocity analysis, or interpretive intervention, or event picking. However, the level of technical challenge represented by the types of plays described above cause traditional methods to bump-up hard against their assumptions with a concomitant degradation or cessation of effectiveness.

A response to the challenge

The inverse-scattering multiple attenuating sub-series for free-surface and internal multiples is a direct response to this tough and important challenge. The sub-series for attenuating free-surface and internal multiples (Weglein et al. 1997, Carvalho et al. 1992, Araujo et al. 1994, Matson and Weglein 1996, Coates and Weglein 1996) were described and exemplified for towed streamer and multi-component ocean bottom and on-shore data. These multiple attenuation sub-series have excellent convergence properties, assume absolutely no information concerning the subsurface, require no velocity analysis, no event picking, nor interpretive intervention, and they have demonstrated effectiveness on field data (Carvalho et al 1992, Carvalho and Weglein 1994, Matson et al. 1999).

Imagine predicting and subtracting all the multiples from a salt body, while preserving all primaries, with no information about the salt structure, nor what is above the salt, i.e., no velocity, nor any other cause or influence on these multiples. Many considered this absolutely impossible in 1990, considered it somewhat understandable by 1997, and today it is considered eminently reasonable, when production strength codes routinely apply those algorithms and fulfill that promise. Another wave-theoretical technique, the feedback method, was pioneered by Berkhout (1982) and developed by Verschuur et al. (1992) and these two methodologies were compared (e.g., Berkhout et al., 2000 and Weglein et al., 2000). The inverse-scattering methods were the first and remain the only comprehensive method for eliminating all multiples from a heterogeneous earth with absolutely no subsurface information or user intervention of any kind.

A useful method for attenuating internal multiples was developed independently by E.Landa et al. (1999). Although it requires event picking, it shares the timing prediction apparatus for the selected multiples whose primaries it has picked with the more complete and general inverse scattering internal multiple procedure. As we mentioned, the inverse scattering internal multiple method predicts the timing and amplitude of all internal multiples, at all depths at once, with absolutely no need for event picking nor interpretive interference. The Landa method is a cost-effective solution when the primaries from the reflectors generating the internal multiples are identifiable. This is also true for the feedback approach to internal multiples. However, under highly complex conditions, e.g., with hard to identify and/or interfering events, highly heterogeneous media, diffractive or corrugated reflectors, or small amplitude salt internal multiples proximal to small amplitude subsalt primaries, the wave-theoretical generality and power of the inverse scattering free-surface and internal multiple prediction methods stand alone.

All inverse-series applications require a good estimate of the source signature in the water, which is achievable under many circumstances (Verschuur et al. 1992, Carvalho et al. 1992, Carvalho and Weglein 1994, Matson, 2000) and new techniques are being investigated and developed (e.g., Weglein et al. 2000, Manin and Spitz, 1995). The latter direct wavelet prediction and pattern recognition subtraction techniques are motivated by the need to go beyond the current energy minimization standard for complex and subtle free-surface and internal multiple subtraction and the problems presented by 3-D out of plane multiples to 2-D algorithms, respectively. The near future will see closer to true 3-D data acquisition and 3-D implementation of the algorithms, mitigating some of the impediments to reaching the full potential of these demultiple concepts.

Money and influence: Assumptions move from the subsurface to the measurement surface.

No amount of money can impress, induce or influence a 1-D algorithm to understand a diffraction or to sympathize with a complicated multidimensional wavefield. However, money can affect the completeness of seismic acquisition and thereby allow multidimensional algorithms, designed to address a complex and largely unknown subsurface (albeit with greater demands on a complete and sampled wavefield on the measurement surface) to reach their inherent capability for providing added value. The development of more complete, realistic and costly demultiple and imaging algorithms empower the petroleum industry to allow those interested in spending more to achieve greater reliability and reduced risk, to have a new choice with a better chance at getting more. More realism and completeness are aligned with greater reliability and reduced risk.

The industry trend is to develop new methods with fewer unrealistic assumptions about the subsurface and replace them with greater demands on the definition and completeness of the seismic experiment.

Summary

In this talk, we will briefly trace the evolution of the inverse scattering demultiple concepts and algorithms and exemplify them with synthetic and field-data examples. We will discuss their relationship to the important feedback methods, and describe issues that need to be addressed or that require further attention. The recent application of the feedback method to land data by Kelamis and Verschuur is noteworthy. Among the outstanding issues that will be discussed are: 3-D, wavelet estimation, near trace and cross-line interpolation and extrapolation, and deghosting. Candidate methods for addressing several of these impediments to effective multiple removal will be described.

Acknowledgements

It is a pleasure to recognize the following contributors to the development and application of inverse scattering multiple attenuation: P. M. Carvalho, F.A. Gasparotto, R. H. Stolt, R. T.Coates, K.H.Matson, D.Corrigan, L.Ikelle, L. Amundsen, S.A.Shaw, G.Roberts, and D. Miller.

A. J. Berkhout and D. Verschuur are thanked for a positive, constructive and expansive research collaboration.

ARCO, Petrobras, BP, Schlumberger, and Phillips managements are recognized for encouragement and support. The M-OSRP sponsors and the Margaret S. and Robert E. Sheriff Faculty Endowment are thanked for strong and constant support.

Andre Romanelli Rosa, Dodd DeCamp, J. O'Connell, H.J. Al-Hakeem, Craig Cooper, M. Porsani, J.Schmidt, V. Oliveira, T. Ulrych, J. Robertson, B. Barley, D. Foster, R.A.Ergas, P. A. F. Christie, Reid Smith , A.C. Vailas, J. Bear, and J. van Sant are thanked for both technical advice and support.

References

Amundsen, L., Ikelle, L, and Martin, J. (1998) "Multiple attenuation and P/S splitting of OBC data at a heterogeneous sea floor", 60th EAGE Abstracts PO44.

Araujo, F.V., Weglein, A.B., Carvalho, P.M., and Stolt, R.H. (1994) "Inverse scattering series for multiple attenuation: an example with surface and internal multiples": 64th Ann. Internat. Mtg., Soc. Expl. Geophys., Exp. Abstracts, 1039–1041.

Bannagi, M.S., Kelamis, P.G., and Verschuur, D.J. (2001), "Land multiple elimination applicable for low-relief structures" Poster presented to 63rd EAGE Conference, Amsterdam.

Berkhout, A.J., (1982): Seismic migration, imaging of acoustic energy by wavefield extrapolation, A: Theoretical Aspects, Elsevier.

Berkhout, A.J., Weglein, A.B., Verschuur, D.J. (2000) "Wave theoretic multiple attenuation Part I" Invited paper to Offshore Technology Conference, OTC Houston, Texas.

Carvalho, P.M., Weglein, A.B., and Stolt, R.H., (1992) "Nonlinear inverse scattering for multiple suppression: application to real data pt.1" SEG Expanded Abstracts, 1093-1095.

Carvalho, P. M., and Weglein, A. B. (1994) "Wavelet estimation for surface multiple attenuation using a simulated annealing algorithm." SEG Expanded Abstracts, Los Angeles, CA.

Carvalho, P.M., Weglein, A.B., and Stolt, R.H. (1992)

"Non-linear inverse scattering for multiple attenuation: Applications to real data, Part I": Society of Exploration Geophysicists International Exposition and 62nd Annual Meeting, 1093–1095.

Coates, R. T., and Weglein, A. B. (1996) "Internal multiple attenuation using inverse scattering: results from prestack 1D and 2D acoustic and elastic synthetics." SEG Expanded Abstracts, PR 4.2, pp. 1522–1525.

Fokkema, J.T. and Van den Burg, P.M. (1990), "Removal of surface related phenomena: the marine case" SEG Abstracts, 1689-1692.

Kelamis, P.G., Chiburis, E.F., and Shahryar, S.,1990, Radon Multiple multiple elimination , a practical methodology for land data:SEG Expanded Abstracts, 1611-1614.

Landa, E., Belfer, I., and Keydar, S., (1999) "Multiple prediction and attenuation using wavefront characteristics of multiple-generating primaries" The Leading Edge, 18(1), 60-66.

Manin, M., and Spitz, S. (1995) "3-D attenuation of targeted multiples with a pattern recognition technique", 57th EAGE Paper BO46, Glasgow, 29 May – 2 June.

Matson, K.H. (2000) "An overview of wavelet estimation using free-surface multiple removal." Leading Edge, January, Vol. 19, No. 1, pp. 50–55.

Matson, K.H., and Weglein, A. B. (1996) "Removal of elastic interface multiples from land and ocean bottom data using inverse scattering." SEG Expanded Abstracts, PR 4.3, pp. 1526–1529.

Matson, K.H., Paschal, D., and Weglein, A.B. (1999) "A comparison of three multiple attenuation methods applied to a hard water-bottom data set", The Leading Edge, January, p. 120–126.

Verschuur, D.J., Berkhout, A.J., and Wapenaar, C.P.A. (1992) "Adaptive surface-related multiple elimination": Geophysics, 57, 1166–1177.

Weglein, A.B., Gasparotto, F.A., Carvalho, P.M., and Stolt, R.H. (1997) "An inverse scattering series method for attenuating multiples in seismic reflection data": Geophysics, 62, pp. 1975–1989.

Weglein, A.B., Matson, K.H., Berkhout, A.J. (2000) "Wave theoretic multiple attenuation Part II" Invited paper to Offshore Technology Conference, Houston, Texas.

Weglein, A.B., Tan, T.H., Shaw, S.A., Matson, K.H., Foster, D.J., (2000) "Prediction of the wavefield anywhere above an ordinary towed streamer" 70th Annual Meeting of the Society of Exploration Geophysicists, Calgary, Canada.

Weglein, A. B., (1999a) "Multiple attenuation: an overview of recent advances and the road ahead (1999)", The Leading Edge, p.40–44.

Weglein, A. B., (1999b) "How can the inverse-scattering methods really predict and subtract all multiples from a multidimensional earth with absolutely no subsurface information?" The Leading Edge, p.132–136.